FACULTY OF SCIENCES

Characterisation of Colacosomes, a curious fungal interaction mechanism involved in mycoparasitism.

Arno Leroy
Student number: 01601520

Supervisors: Prof. dr. Annemieke Verbeken, Prof. dr. Bart Devreese
Counsellors: Prof. dr. Bart Devreese, Nathan Schoutteten

Master's dissertation submitted in order to obtain the academic degree of
Master of Science in Biology

Academic year 2021-2022

GHENT UNIVERSITY

Introduction

When it comes to diversity in lifestyle and morphology, fungicolous fungi (i.e. fungi associated with other fungi) are amongst the most diverse groups of organisms within the kingdom of the Fungi (Sun et al. 2019; Bauer 2004, Bauer et al. 2006). This group comprises a variety of ecological niches, varying from mutualism, commensalism, saprotrophism, and also parasitism (Sun et al. 2019; Bauer et al. 2006). The latter lifestyle, where a parasitic fungus (mycoparasite) derives its nutrients from another living fungus (host) is referred to as mycoparasitism. Such mycoparasites can affect their hosts in a variety of ways (biotrophic and necrotrophic), and infect their hosts through a variety of specific mechanisms. Examples of these mechanisms can be fusional, where the parasite's and the host's cytoplasm make contact through the development of nanopores and micropores, through the usage of haustoria, (a specialized intrusive hyphal branch formed by the parasite to attach or penetrate the host), by secretion of antifungal compounds, or even by entering the host completely and living intracellularly (Sun et al. 2019; Naranjo-Ortiz and Gabaldón 2019). These mechanisms are in place for the mycoparasite to take up necessary nutritional compounds from the host. Like many other parasites, mycoparasites often have a rather small genome due to the loss of genes associated with (sometimes vital) metabolic pathways, thus making them rely on the host for provision of essential nutrients (Naranjo-Ortiz and Gabaldón 2019).

Based on the effect mycoparasites have on their fungal host species, two main categories can be discriminated: biotrophic and necrotrophic mycoparasites. The former are detrimental to the host but do not aim to kill the host, while those belonging to the latter group aggressively attack their host and consume their damaged, necrotic tissues. Mycoparasites can potentially kill their host by outcompeting them for nutrients or by secreting enzymes and antibiotics, reducing their hosts fitness (Sun et al. 2019). Since parasitism in general is a prime example of the Red Queen hypothesis, it should be noted that the hosts too, can develop defense mechanisms to deter or counteract potential parasites, such as the usage of toxic secondary metabolites and reactive oxygen species (Naranjo-Ortiz and Gabaldón 2019).

Research on mycoparasitism has mainly focussed on the usage of ascomycetous mycoparasitic fungi as a means of biological pest control. A few examples of this are the usage of *Sphaerellopsis filum* (Biv.) B. Sutton as a biocontrol agent against the rust diseases caused by *Puccinia sp.* in agriculture (Sun et al. 2019). Other examples are the application of the mycoparasites *Chaetomium globosum* (Kunze), *Clonostachys rosea* ((Link) Schroers), and *Penicillium oxalicum* (Currie & Thom), which have also proven to be effective at lowering the incidence of white rot disease caused by *Stromatinia cepivora* (Berk.) Whetzel (Elshahawy et al. 2017).

Mycoparasitism is found in multiple lineages within the kingdom of Fungi, with documented occurences in at least eight different phyla (Naranjo-Ortiz and Gabaldón 2019). The largest diversity and best studied examples belong to Ascomycota, comprising several well-known genera such as *Hypocrea* Fr. and *Trichoderma* Pers. Also among Basidiomycota, mycoparasitic taxa are found within two out of three subphyla: Pucciniomycotina and Agaricomycotina. Within Pucciniomycotina, mycoparasites are found in at least six different classes: Agaricostilbomycetes, Classiculomycetes,Cryptomycocolacomycetes, Cystobasidiomycetes, Microbotryomycetes, Pucciniomycetes and Spiculogloeomycetes. Within Agaricomycomycotina, mycoparasites are mainly to be found within the Tremellomycetes. These mycoparasites generally display special characters such as septated basidia and secondary spore production, based on which they were formerly classified within the heterobasidiomycetes.

Pucciniomycotina has been suggested to be the earliest diverging subphylum in Basidiomycota (Aime et al. 2014, Prasanna et al. 2019), which led to the suggestion that mycoparasitism may have been their ancestral lifestyle (Weiss et al. 2004, ; Naranjo-Ortiz and Gabaldón 2019). This subphylum

displays a remarkable diversity in species morphology, nutritional strategies, life cycle complexity and habitats (Bauer et al. 2006, Aime et al. 2014). The largest number of species in this subphylum belongs to the phytoparasitic Pucciniales (Rusts) and Microbotryales (Anther smuts). Other lineages in this subphylum mainly comprise species isolated as yeasts (often assumed to be saprotrophs) and mycoparasites (He et al. 2019). Only a few examples of mutualism have been found within this subphylum (e.g., Kottke et al. 2010). Many species in Pucciniomycotina have a dimorphic lifecycle, alternating between an asexual ontogenetic yeast stage and a sexual hyphal stage. This seems to be specifically true for mycoparasitic species in this group (Oberwinkler 2017).

Interaction mechanisms of basidiomycetous mycoparasites can roughly be divided in two categories: haustorium- and colacosome-forming parasites (Bauer 2004). Haustoria-forming mycoparasites can be found in Pucciniomycotina (Agaricostilbomycetes, Classiculomycetes, Cryptomycocolacomycetes, Cystobasidiomycetes, and Spiculogloeomycetes) and Agaricomycotina (Tremellomycetes). Colacosome-forming fungi are only to be found in Pucciniomycotina, more specific in Cryptomycocolacomycetes and Microbotryomycetes.

The Microbotryomycetes is a class of fungi characterised by a large degree of heterogeneity. Whereas most species belong to the phytoparasitic Microbotryales, the other clades within this group comprise fungi isolated as yeasts from most diverse habitats and colacosome-forming mycoparasites (mostly in Heterogastridiales). It should be noted that colacosomes have also been identified from several hyphae-forming yeast species belonging to Leucosporidiales and Sporidiobolales.

Colacosomes are subcellular structures found in hyphae, that were described as lenticular bodies by Kreger-van Rij & Veenhuis (1971a). Later, Bauer and Oberwinkler (1991) observed similar structures in the filamentous state of *Colacogloea effusa* (J. Schröt.) V. Malysheva, Schoutteten & Spirin, a mycoparasite of *Peniophorella praetermissa* (P. Karst.) K.H. Larss., and described these as colacosomes. A list of all known species that contain colacosomes can be seen in table 1 in the annexes.

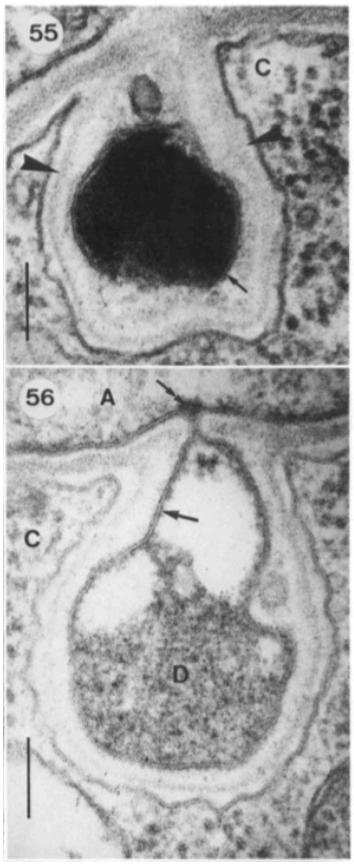

Figure 1: Transmission electron micrographs of the mycoparasite Cryptomycocolax abnorme. The upper micrograph (55) shows a type 1 colacosome. The lower micrograph (56) shows a type 2 colacosome. The pore is indicated with the double arrow.

C = Cryptomycocolax abnorme

A = Ascomycetous host

(Oberwinkler and Bauer 1990).

There has been made a distinction between two types of colacosomes as seen in figure 1. The *Type 1-colacosome* is very electron-dense, and forms a connection through the host and parasite cell wall but doesn't enter the plasmalemma of the host. *Type 2-colacosomes* are less electron-dense, also pass through the cell walls of parasite and host, but in this case the membrane surrounding the colacosome is fused with the host's plasmalemma, forming a nanopore connection (Oberwinkler and Bauer 1990). Type 2-colacosomes have only been reported in *Cryptomycocolax abnorme* (Oberw. & R. Bauer), where it co-occurs with Type 1-colacosomes. The other representative of the Cryptomycocolacomycetes, *Colacosiphon filiformis* (R. Kirschner), only has type 1-colacosomes. Type 1-colacosomes are known from both Cryptomycocolacomycetes and Microbotryomycetes (Bauer et al. 2006; Oberwinkler 2017). Since this thesis will focus on species within Microbotryomycetes only, type 2-colacosomes will not be discussed further. The diameter of colacosomes are estimated to be around 0,5-0,6 µm, including the electron transparent sheath surrounding them (Bauer et al. 2006; Oberwinkler and Bauer 1990; Oberwinkler 2017).

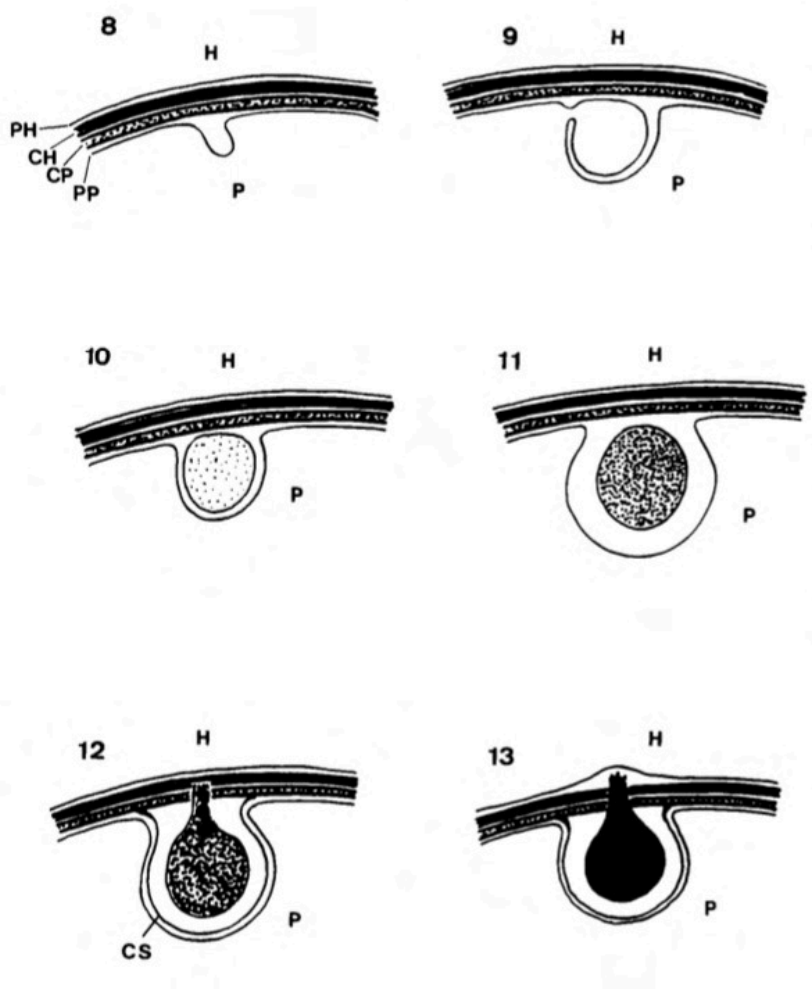

Figure 2: Development of the type 1 colacosome in Colacogloea effusa (J. Schröt.) V. Malysheva as proposed by Bauer and Oberwinkler (1991).

H = host,

P = Parasite,

PH = Plasmalemma of host cell,

CH = Cell wall of host cell,

CP = Plasmalemma of parasite,

PP = Plasmalemma of parasite,

CS = Secondary cell wall.

Colacosomes are thought to be very rapidly developing cell structures. Formation of the type 1-colacosomes in *Colacogloea effusa* (J. Schröt.) V. Malysheva, Schoutteten & Spirin, a mycoparasite belonging to Microbotryomycetes, has been investigated by Bauer & Oberwinkler (1991). Based on their observations, the authors proposed a schematic development of type 1 colacosomes (Figure 2). As reported by these authors, it is hard to find early developmental stages of colacosomes. This is mainly due to the incapabilities of creating dynamic transmission electron microscopy footage. The formation of colacosomes is fast and occurs at contact points with a fungal host. However, a host is not always required as the structures have been found in monocultures too. This could be interpreted as a form of self-parasitism (Bauer et al. 2006).

The initial formation stages are assumed to be found near a close hyphal interaction of the host and parasite. The formation of these structures is thought to start at the plasmalemma of the parasite's hyphae. It is postulated that the plasmalemma is folded inwards to the cytoplasm and subsequently fuses with itself, thus forming a spherical compartment. Due to the suggested method of formation, a small space in between the newly generated compartment and the plasmalemma is created. The core of this newly found vesicle becomes more and more electron dense. This electron dense core will subsequently begin to penetrate the cell wall of the parasite, followed by penetration of the host's cell wall. However, it does not enter the plasmalemma of the host. Another peculiar thing can be seen: a secondary cell wall is formed around the colacosome by the mycoparasite (Bauer and Oberwinkler 1991). This is expected to be made of the same components as the parasite's cell wall. It has been reported that the main sugar components are mannose chains, leading to the presence of mannan in the cell wall (Prillinger et al. 1993).

As of today, the exact function of colacosomes remains unclear. It has been suggested that these could work as anchoring organs, making sure that the parasite stays connected to the host (Bauer and Oberwinkler 1991; Bauer and Oberwinkler

2008). However, due to the change in electron density and the undistorted nature of the cell wall at the penetration site, a difference in contents between the colacosome and the cytosol is to be expected. This could potentially point towards enzymes that are capable of precisely breaking down the cell wall of the host. This is supported by the undistorted appearance of the cell wall at the penetration site (Bauer and Oberwinkler 2008). It is not yet clear as to what degree the contents within the colacosomes play a role in the parasite's metabolism (Bauer and Oberwinkler 1991).

Objectives

It is thus currently unknown what the exact contents of these curious structures are. The genes involved in the regulation of the formation of colacosomes are also unknown. Our main goal for this research is to unravel the mystery of the contents of the colacosomes by purifying the colacosomes and identifying the proteins within.

This can be divided into multiple sub-objectives:

1. *Identification of strains that form an abundance of colacosomes on a specific medium.*

First we need to identify strains that are capable of forming a large amount of colacosomes in monocultures. Since the environmental cues to activating colacosome formation are unknown, a variety of culture media will be screened.

2. *Purification of colacosome fraction.*

After the identification of suitable strains, a protocol needs to be developed to purify a colacosome fraction. This requires testing various lysis methods combined with rigorous screening.

3. *Identification of the colacosome content.*

Once an optimal lysis protocol or extraction protocol has been developed, the next step would be the identification of the contents within the colacosomes. For this, mass spectrometry will be utilized on the purified sample.

As such our research seeks to answer the following questions:

“What species and strains form colacosomes in a high density and on which medium?”

“Which protocol is het best to isolate colacosomes from the select number of strains?”

“What enzymes are residing within the colacosomes?”

Approach

To tackle these objectives, we need a concise and well-motivated approach. In this section, motivations in regards to the methodology will be provided.

Cultivation

First, we assessed the species and strains that were available to use for this research. A list of these species and strains will be provided in the annexes in table 2 and table 3. Since the environmental cues that activate or stimulate the formation of colacosomes are unknown, we took a closer look towards the origins of the available strains and, if possible, their hosts and their respective ecology.

The strains of *Colacogloea sp*. have been isolated from *Peniophorella praetermissa* as well as *Peniophorella pubera*. Both of these species are known to be saprotrophic species causing white rot (Eriksson and Ryvarden 1975; Korhonen et al. 2022).

Hyalopycnis blepharistoma belongs to the heterogastridiales, a group consisting solely of mycoparasites. The origins of the *H. blepharistoma* strains used in this research have a broad background. As was recorded by the Westerdijk Institute, the strains came from *Tricholoma populinum*, *Russula nigricans*, *Hypomyces lactifluorum*, decaying walnut skin (*Juglans ailanthifolia*) and a bulb of the *Iris hollandica*. *Tricholoma populinum* and *Russula nigricans* are both known to be ectomycorrhizal fungi (Gryta et al. 2006; Kumar and Atri 2019). There is a possibility that these fruiting bodies from which *H. blepharistoma* was collected, were affected by other fungal parasites. The latter of the two, *Russula nigricans*, is known to often fall prey to parasites such as *Asterophora parasitica*. This would make *H. blepharistoma* a hyperparasite. This is the case for the strain isolated from *Hypomyces lactifluorum*, as *H. lactifluorum* is a mycoparasite itself (Laperriere et al. 2018). The decaying skin of walnut could potentially contain other fungal saprobes or plant pathogenic fungi on which *H. blepharistoma* could grow. The same reasoning could be followed for the strain isolated from the *Iris hollandica* bulb, which is recorded to be prone to basal rot and blue mold infections (Skrzypczak 1988). The other species from table 3 have similar origins, where the prevalence of other fungi would be expected.

In general, it is safe to say that most of these environments from which the available selection of strains originated, were environments inhabited by either saprobes or mycoparasites. According to literature, saprotrophic species utilize enzymes such as hydrolytic enzymes and oxidases to degrade hemicelluloses as well as other cell wall compounds. These enzymes are most active at a pH of 4 - 5 (Highley 1979). Saprotrophic fungi have been found to have their growth optimum in culture media with a pH of 3,5 - 5,5. This leads us to suspect that our available fungal strains would also benefit from more acidic culture conditions.

GYPA medium is a nutrient rich medium which is preferred for fast growth of fungi. It is the most alkalic medium of our selection, with pH = ±7. MEA is also preferred, as this medium is very suited for yeast cultivation (Pitt and Hocking 2009). PDA medium is more preferred for stimulating sporulation as well as for long lived cultures of fungi. It has a pH = 5,6. X-agar is made from PEGS, cherry extract and oatmeal extract, which leads to a nutrient rich but more acidic culture medium (pH = 5,4). These factors might mimic the natural growth environments of the available fungi more. Since the exact environmental cues of colacosome formation are not clear yet, we also tried a nitrogen depleted medium. The base of this medium was yeast-peptone-dextrose agar (YPD). This base was modified in that it only contained half as much peptone and glucose (Yang et al. 2016). Recipes for the media are available in the annexes. As such, these 5 types of culture media were chosen for this thesis.

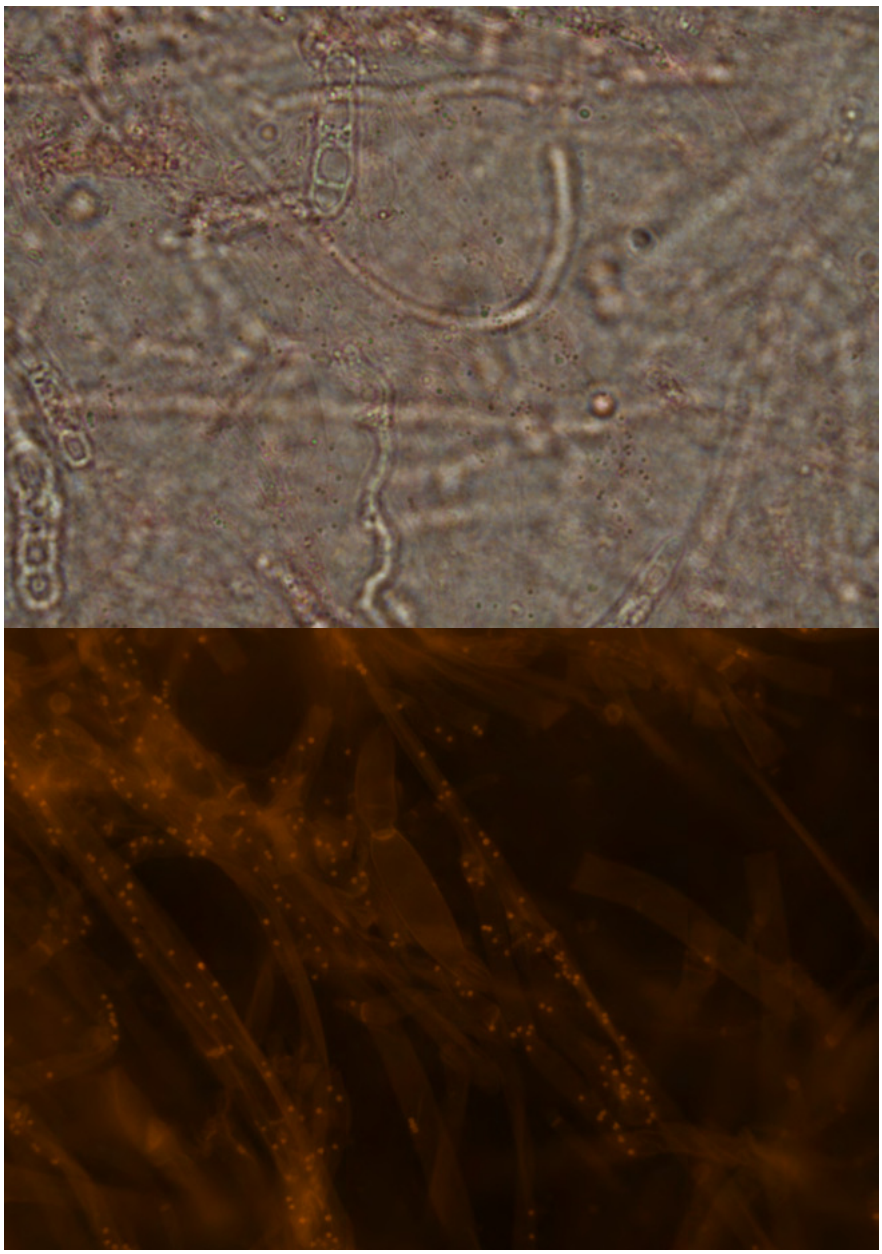

Figure 3: Microscopy photograph of Hyalopycnis blepharistoma (Berk.) Seeler, Farlowia (CBS 149.68) grown on solid GYPA medium.

The strain was stained with Congo red and the same section is viewed with regular light microscopy (picture above) with fluorescence enabled (picture below). Colacosomes are visible as minute black spheres but are more visible when using epifluorescence microscopy. Magnification of 1000x.

Naturally, the presence of colacosomes needs to be verified. Most aforementioned literature made use of transmission electron microscopy to visualize these structures, but due to the scope and amount of the available samples, this method isn't feasible. As an alternative, Congo red dye can be used. As Congo red stains the amyloid fibrils of the cell wall of fungi, the same is to be expected for the secondary cell wall formed around the colacosomes. In this way it would be possible to visually screen for the presence of colacosomes. However, light microscopy alone does not suffice for this method. Although colacosomes are visible as minute, dark intracellular spheres when stained with Congo red and viewed through light microscopy, they can still easily be missed, as can be seen in figure 3. To better visualize the colacosomes, epifluorescence microscopy can be used after Congo red staining.

Cell lysis and purification of colacosome fraction

For the isolation of the colacosomes, cell lysis is required. Cells have to be lysed to such an extent that the colacosomes itself aren't completely destroyed, but the majority of the cell walls are. Cell lysis can be achieved in a variety of ways, as chemical lysis but also physical force can be used to break the cells. The latter would be preferred as the former could potentially damage the colacosomes or their contents by rendering them more permeable which can lead to a possible loss of, or destruction of their contents (Borner 2020).

The next aspect, the purification or enrichment of the amount of colacosomes will be based on an organellar profiling technique: LOPIT-DC (Geladaki et al. 2019). This technique focuses on differential ultracentrifugation to separate organelles. Since there exists no specific protocol for this prior to this research, a series of protocols were created and experimentally tested and compared while also taking into account alternative options. A full list of the created protocols can be found within the annexes while the final protocol will be explained in detail in the materials and methods section while the differences will be discussed in the discussion section.

Materials and methods

Cultivation

The list of used strains available for cultivation, the master cultures, can be found in table 2 and table 3 which can be found in the annexes.

The 5 types of culture medium were prepared in accordance to the recipes provided in the annexes. After preparation of the medium, it was poured into plastic Peri dishes in a laminar flow cabinet. The poured agar plates were kept there for approximately an hour to completely solidify.

Inocculation took place at a sterile flame. A sterile inoculating loop was used to take a sample of tissue from the master culture and subsequently smeared out on the agar plates. After inoculation of a plate the loop was submerged in alcohol and thoroughly flamed. The plates were sealed off with parafilm and incubated at room temperature (21 ° C) for 4 weeks with daily check up for contamination. In case of contamination, the plates were discarded and new plates were inoculated.

Screening

After approximately 4 weeks of incubation, the cultures were ready to be screened for the presence of colacosomes. For this, a sample from the agar plate was taken and subsequently stained with Congo red. When present, both hyphal and yeast stages were evaluated.

To acquire a clear visual representation, fluorescence microscopy was used. For this, a Nikon Ni-U epifluorescence microscope with a TRITC filterset (excitation 543/22 nm, dichroic mirror 562 nm, emission 593/40 nm) was used. Photographs were taken with a DS-Fi3 Microscope Camera and by usage of the NIS-Elements software.

After completion of the screening process, test tube sized liquid cultures were be established for the strains that form an abundance of colacosomes. The medium will be made in accordance to the recipes provided in the annexes, save for the addition of agar. After inoculation with a small slice of the agar culture, these small volume cultures were incubated for 2 weeks at room temperature on an orbital shaker at 120 rpm. Afterwards, the cultures were sampled and screened using the aforementioned staining and fluorescence microscopy method.

Strains that formed colacosomes in these smaller liquid cultures were used to inoculate larger volume liquid cultures in erlenmeyer flasks. These were kept at room temperature on an orbital shaker at 120 rpm. These were suitable for use after approximately 6 weeks of incubation.

Colacosome isolation

1. *Cell lysis*

As stated before, a series of protocols have been made and tested prior to choosing the final, most ideal protocol for cell lysis. The best methodology follows the lysis procedure of protocol 6 and is described below.

For the preparation of a single sample, 0,2 g of tissue was taken from the large liquid culture. This sample was briefly put in an eppendorf with 0,5 ml TRIS buffer (0,375 M, pH = 8,8) for approximately 2 minutes. Next, the tissue was removed from the buffer, and put directly into liquid nitrogen until completely frozen. The frozen tissue was subsequently transferred into an eppendorf containing 0,5 g of zirconium beads with a 200 µm diameter. Mechanical cell lysation was achieved by using a Retsch Mixer Mill MM 400 at a frequency of 30Hz for 2 times 1 minute. 200 µl of TRIS buffer was added to the homogenized cells which were then vortexed for 1 minute.

2. *Enrichment of the colacosome fraction*

To ensure a high colacosome yield, separation from unlysed cells is in order. This was done through filtration by the usage of eppendorf filters (pluriStrainer Mini) with mesh size 100 µm, 40 µm, 20 µm and 10 µm. The beads and buffer were

Eppendorf	Volume of Diluent	Volume of BSA	Final BSA Concentration
A	0 µL	300 µL of Stock	2000 µg/mL
B	125 µL	375 µL of Stock	1500 µg/mL
C	325 µL	325 µL of Stock	1000 µg/mL
D	175 µL	175 µL of vial B dilution	750 µg/mL
E	325 µL	325 µL of vial C dilution	500 µg/mL
F	325 µL	325 µL of vial E dilution	250 µg/mL
G	325 µL	325 µL of vial F dilution	125 µg/mL
H	400 µL	100 µL of vial G dilution	25 µg/mL
I	400 µL	0 µL	0 µg/mL

Table 4: BSA dilution series.

transferred into an eppendorf filter which was placed into a new eppendorf. The samples were subsequently placed in a centrifuge and spun for 10 minutes at 8000 G after which the filter was removed and the pellet resuspended using a pipet. This process was repeated, reducing the mesh size of the filter with each centrifugation step.

Enzymatic lysis of the fractions

During the testing of this protocol, the cell lysis part during the colacosome isolation ended by adding 1 ml of TRIS buffer instead of 200 µl. Half of the volume of these samples was taken and spun down at 12000 G for 10 minutes. The TRIS buffer was replaced with 500 µl sodium acetate buffer (0,100 M, pH = 4). Endo-1,4 β-Mannanase (available from Megazyme with product code: E-BMABS) was added in a 1/30 and 1/120 enzyme/buffer ratio to the samples. These were incubated for 24 hours at 40 ˚C on a heat block and kept in motion at 250 rpm.

Bradford assay

To determine the amount of protein contents present within the enriched samples, a Bradford assay was utilized. For this, a series of dilutions of a stock of bovine serum albumin (2.0 mg/mL) was used to generate a standard protein concentration curve. The dilution series is shown in table 4. A 1/10 dilution was also made from the enriched samples. The bottle of Coomassie reagent was gently inverted and the required volume was taken out to adjust to room temperature. From the dilution series, as well as from the enriched samples, 20 µl was pipetted and mixed with 1 ml of Coomassie Reagent. These were left for 10 minutes and 250 µl was pipetted into a well of a 96 well plate. Bubbles were removed through usage of a pipet tip. The plate was put into a plate reader and the absorbance at 595 nm light was measured. The measurements of the dilution series formed the basis to generate a standard curve to compare the absorption of the enriched samples to.

SDS-PAGE protocol

For the SDS-PAGE, 4 µl of the enriched sample or enzymatically treated sample was taken and put into a new eppendorf. Next, 16 µl Bio-Rad 4x Laemmli Sample Buffer #1610747 was added to the samples. These were subsequently incubated for 1 hour at 40 ˚C on a heat block.

The 20 µl incubated samples were loaded up on SDS gel (Bio-Rad 12% Mini-PROTEAN TGX Stain-Free Protein Gels, 10 well, 30 µl #4568043) which was submerged in running buffer (Bio-Rad 10x Tris/Glycine/SDS #1610772). As a reference ladder, 10 µl of Precision Plus Protein Unstained Protein Standards #1610363 or 10 µl of Precision Plus Protein Dual Color Standards #1610374 was loaded

onto the gel. The SDS-PAGE was then run at 150 Volts for 1 hour.

After the electrophoresis, the gel was removed from the cast and washed 3 times with ddH_2O and subsequently stained with 20 ml of SimplyBlue SafeStain for 1 hour. During the staining procedure, the gel was kept in gentle movement on an orbital shaker. The destaining procedure is dependent on the intensity of the gel's colour and usually takes 1-3 hours. During this procedure the gel is submerged in ddH_2O and the water is replaced when appearing discoloured during the destaining procedure. Using a Bio-Rad GS-800 Calibrated Imaging Densitometer, the gel was captured digitally.

In gel digestion

First the gel is analyzed, and the bands of interest are excised. These gel bands are cut into smaller pieces and put into eppendorfs. Next, 200 µl of 200 mM ammonium bicarbonate solution is added after which the samples are vortexed for 20 minutes and the liquid is removed by using a pipette. This is repeated once more.

The next step in the procedure is the tryptic digestion process. For this, 100 µl of 0.002 µg/µl MS-Grade Trypsin/Lys-C Protease Mix is added to the cut up gel pieces. This was incubated overnight at 37 ˚C.

To extract the proteins from the gel, 100 µl of extraction buffer (80% acetonitrile and 0,3% Trifluoroacetic acid) was added and left for 5 minutes. Approximately 160 µl was extracted from the eppendorfs. The liquid was transferred to a new eppendorf and subsequently dried in a vacuum centrifuge.

MALDI preparation and MS/MS

The vacuum dried samples are redissolved in 12 µl of 0.1% Formic acid, 96,9% H_2O, 3% acetonitrile solution and pipetted up and down. Next, 1 µl of the sample was taken and put in a separate eppendorf. To each of these, 1 µl of 10 mg/ml α-cyano-4-hydroxycinnamic acid was added. By pipetting up and down, the matrix and the sample were mixed and the 2 µl mixture was subsequently spotted onto a MALDI-target plate. After this, MALDI-TOF combined with tandem mass spectrometry (MS/MS) was executed. The software MASCOT was used for the analysis.

Results

Cultivation and screening

As stated in the materials and methods, the initial screening process took place on agar plates. Out of the 32 available strains, only 6 strains proved to contain an abundance of colacosomes. However, this is not a unanimous finding for every type of medium. A summary can be seen in table 5. A complete table containing every strain for every medium type can be found in the annexes (table 6), as well as photographic results. All microscopy photographs were made at a 1000x magnification unless stated otherwise.

All strains were used to establish liquid cultures except for CBS 590.93. Since GYPA proved to be the best type of medium for colacosome formation, this was chosen to make small liquid cultures, as well as X-agar. The results can be seen in table 7. *Hyalopycnis blepharistoma* (CBS 591.93) and *Rhodosporidiobolus ruineniae* (CBS 5001) were the only successful strains to form colacosomes in liquid GYPA medium. These strains were used to further test the best lysis and enrichment protocol on. colacosomes seemed to be more visible and prominent in *Hyalopycnis blepharistoma* which is why these were preferred to experiment on.

Lysis and enrichment results

When comparing the centrifugation fractions of the different protocols, protocol 6 was the best when it came to cell lysis. As for purification and enrichment of the colacosome fraction, a new method was developed with a focus on separation through filtration instead of separation of organelles through ultracentrifugation. The *Sequential filter protocol* can be found in the annexes, but was also described in materials and methods above under the section 'Enrichment of the colacosome fraction'.

Species	Strain	GYPA	MEA	PDA	X-AGAR	N-DEP
Hyalopycnis blepharistoma/ Heterogastridium	CBS 149.68	YES	YES	NO	YES	NO
Hyalopycnis blepharistoma/ Heterogastridium	CBS 953.73	YES	NO	NO	NO	NO
Hyalopycnis blepharistoma/ Heterogastridium	CBS 582.80	YES	NO	YES	NO	YES
Hyalopycnis blepharistoma/ Heterogastridium	CBS 590.93	Not Ideal	NO	NO	NO	NO
Hyalopycnis blepharistoma/ Heterogastridium	CBS 591.93	YES	NO	YES	YES	YES
Rhodosporidiobolus ruineniae	CBS 5001	YES	NO	YES	NO	NO

Table 5: Summary of successful colacosome-forming strains on solid medium.

No = No colacosomes seen.
Yes = Colacosomes found in large amounts.
Not Ideal = Colacosomes found, but in insufficient amounts.

Species	Strain	GYPA	X-AGAR
Hyalopycnis blepharistoma/ Heterogastridium	CBS 149.68	Not Ideal	Not Ideal
Hyalopycnis blepharistoma/ Heterogastridium	CBS 953.73	NO	Not tested
Hyalopycnis blepharistoma/ Heterogastridium	CBS 582.80	Not Ideal	Not tested
Hyalopycnis blepharistoma/ Heterogastridium	CBS 591.93	YES	Not Ideal
Rhodosporidiobolus ruineniae	CBS 5001	YES	Not tested

Table 7: Tested strains on liquid medium.

No = No colacosomes seen.
Yes = Colacosomes found in large amounts.
Not Ideal = Colacosomes found, but in insufficient amounts.

Enzymatic lysis

Due to the aforementioned preference of mechanical lysis over enzymatic lysis, this alternative was tested on *Hyalopycnis blepharistoma* (CBS 591.93), but ultimately discarded due to time constraints for further testing and evaluation. During the testing of this protocol, samples were stained prior to the enzymatic treatment. Only the 1/30 enzyme/ sample ratio seemed to have an effect after approximately 21 hours of incubation on a heat block at 40 ˚C. This was mainly seen due to the cell wall becoming more faded when looking through the microscope.

Bradford assay

To ensure that there was not a loss of protein content during the sequential filter protocol, a Bradford assay was used. For this, 5 samples of *Hyalopycnis blepharistoma* (CBS 591.93) were used that each had a different final filter mesh size. These samples were: an unfiltered sample, a sample filtered to a 100µm mesh size, 40 µm, 20 µm and 10 µm mesh size. The mean concentration of these can be found in table 8. The full results of the Bradford assay can be found in the annexes in the tables section (Table 9 & 10), along with a graph of the standard curve and its equation.

Final filter mesh size	Undiluted measurement	1/10 dilution
Unfiltered	1352,6667 µg/ml	139,0 µg/ml
100 µm	NaN	195,0 µg/ml
40 µm	1258,3333 µg/ml	117,8 µg/ml
20 µm	1653,6667 µg/ml	176,9 µg/ml
10 µm	1408,6667 µg/ml	155,7 µg/ml

Table 7: Mean concentration acquired from the Bradford assay

SDS-PAGE

In total, 2 successful SDS-PAGEs were run. These can be seen in figure 4 and figure 5. The SDS-PAGE in figure 5 are the same samples used in the Bradford analysis.

Figure 4 contains samples that were treated with endo-1,4 β-Mannanase as after the filtration protocol. These were incubated for 24 hours prior to the gel electrophoresis. In contrast to the description in the materials and methods, these were not incubated in sodium acetate buffer, but instead on TRIS buffer (0,375 M, pH = 8,8). This will be discussed further on in the discussion. As we can see in figure x, there are clear bands seen in the fractions that were not enzymatically treated between 100 kD and 75 kD. There is also a band visible in between 37 kD and 25 kD and around 15 kD. Some of these bands are also visible in the enzymatically treated samples, such as the band in between 100 kD and 75 kD and the band around 15 kD. The band between 100 kD and 75 kD seems to be fading as the filtration mesh size decreases in the enzymatically treated fractions. In the enzymatically treated samples, there is a line visible around 37 kD, as well as in between 37 kD and 25 kD. These were excised according to figure 4 and used for mass spectrometry.

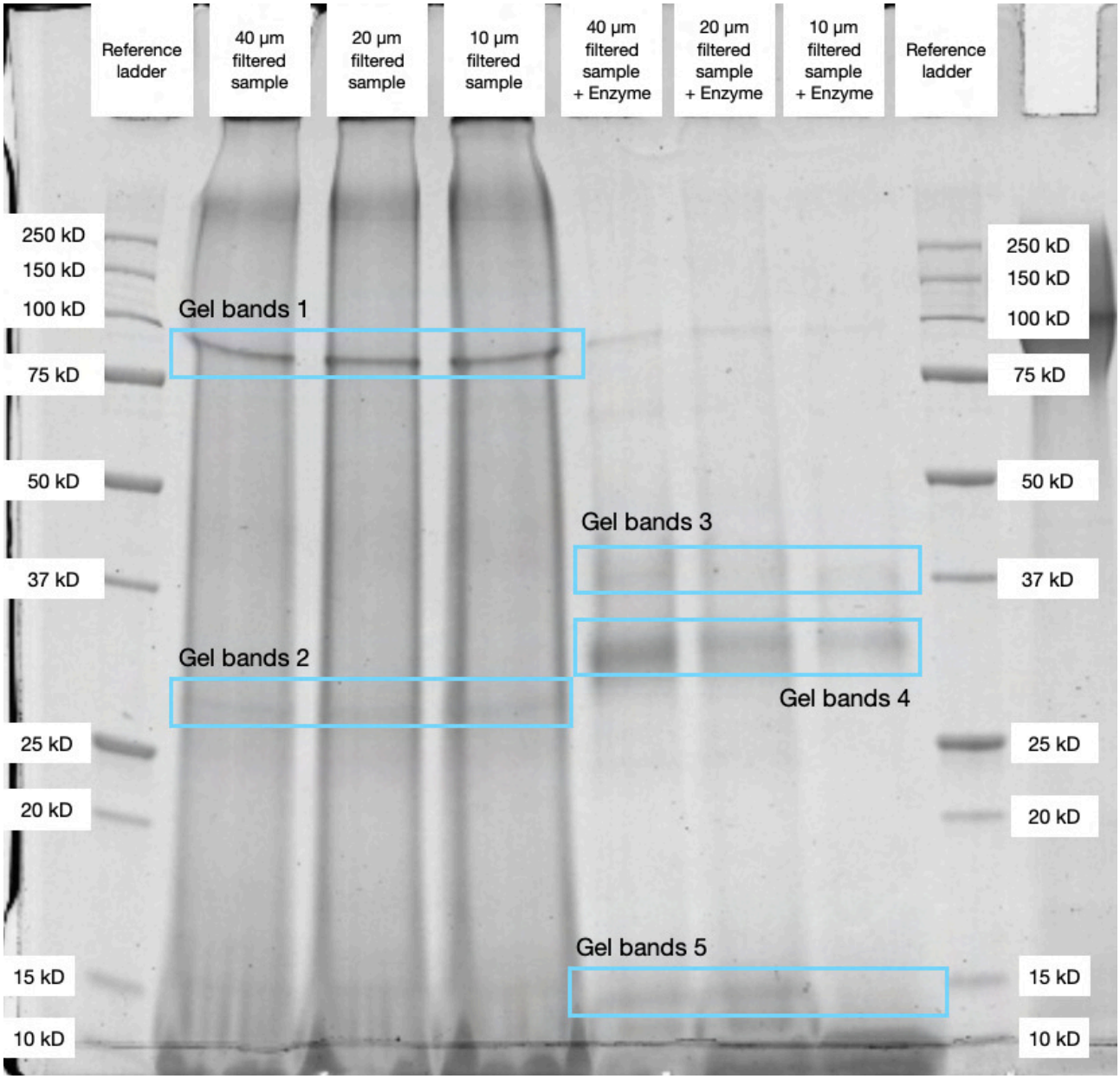

Figure 4: First successful SDS-PAGE with annotated excised bands.

Figure 5 contains the same samples as used in the Bradford analysis. As can be seen in the figure, for all the samples there is a clear band visible in between 150 kD and 100 kD. There might be a slight line visible between 37 kD and 25 kD for all the samples. The most prominent band is visible below 10 kD. This band was excised for each lane, and underwent sample preparation until the samples could be stored in the freezer for mass spectrometry on a later date.

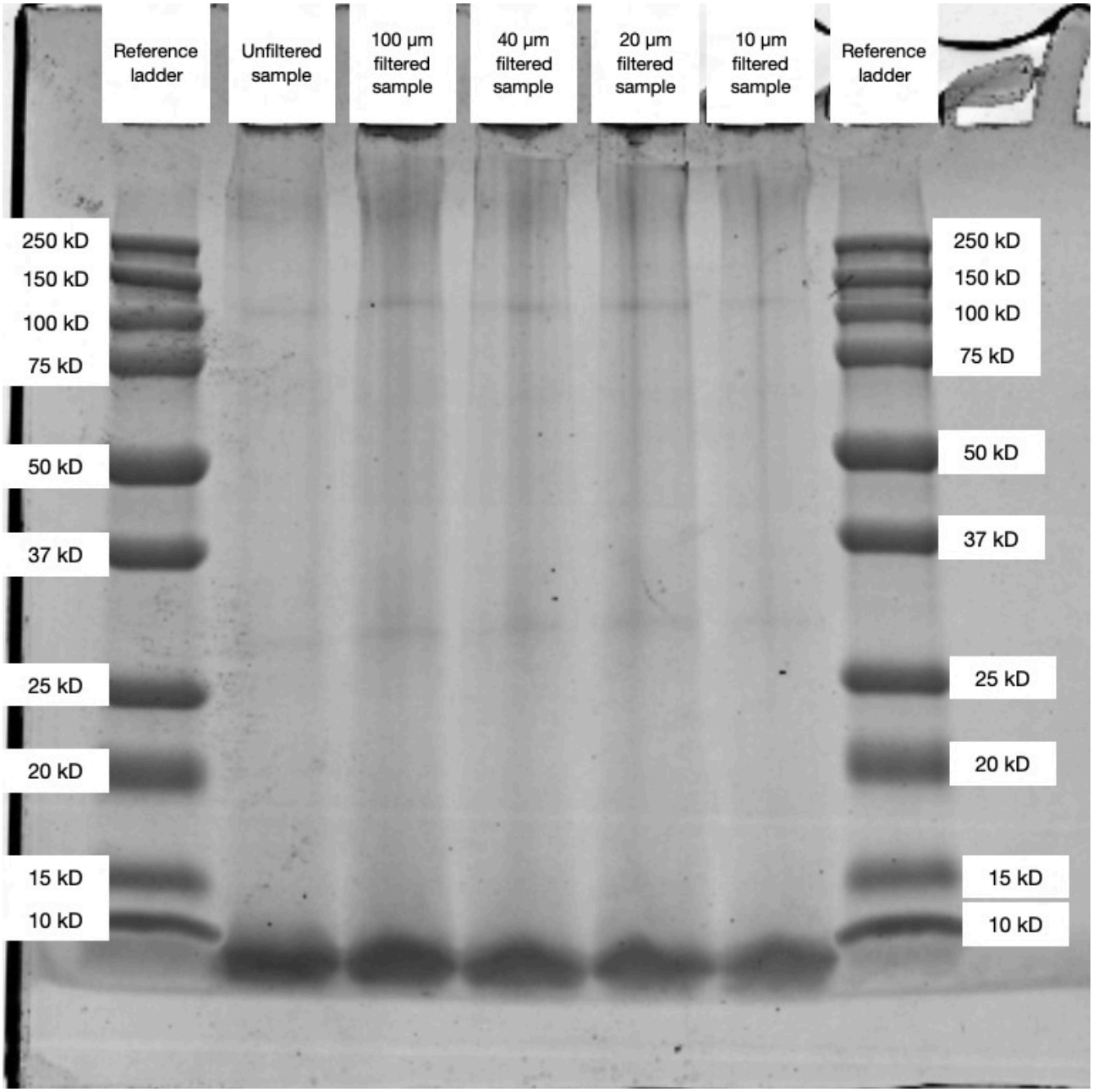

Figure 5: Second successful SDS-PAGE.

MALDI-TOF and MS/MS

In the spectrum visible in gel band 1, the 1884,9949 mass to charge ratio (m/z) pointed towards lysyl endopeptidase (figure 6). This same signal was also seen in gel band 2 (figure 7). The spikes visible at 1164,6288; 2324,3450 and 2865,6233 m/z are attributed to either lysyl endopeptidase or trypsin. In gel band 3, the signal of the spike at 1781,0592 was strong enough to analyze through tandem mass spectrometry (figure 8, 9 & 10). The amino acid sequence determined from this spectrum pointed towards this being mannanase, as can be seen in figure 9. These peaks occur in the gel bands 4 and 5 as well and have also been identified as mannanase (figure 11 & 12).

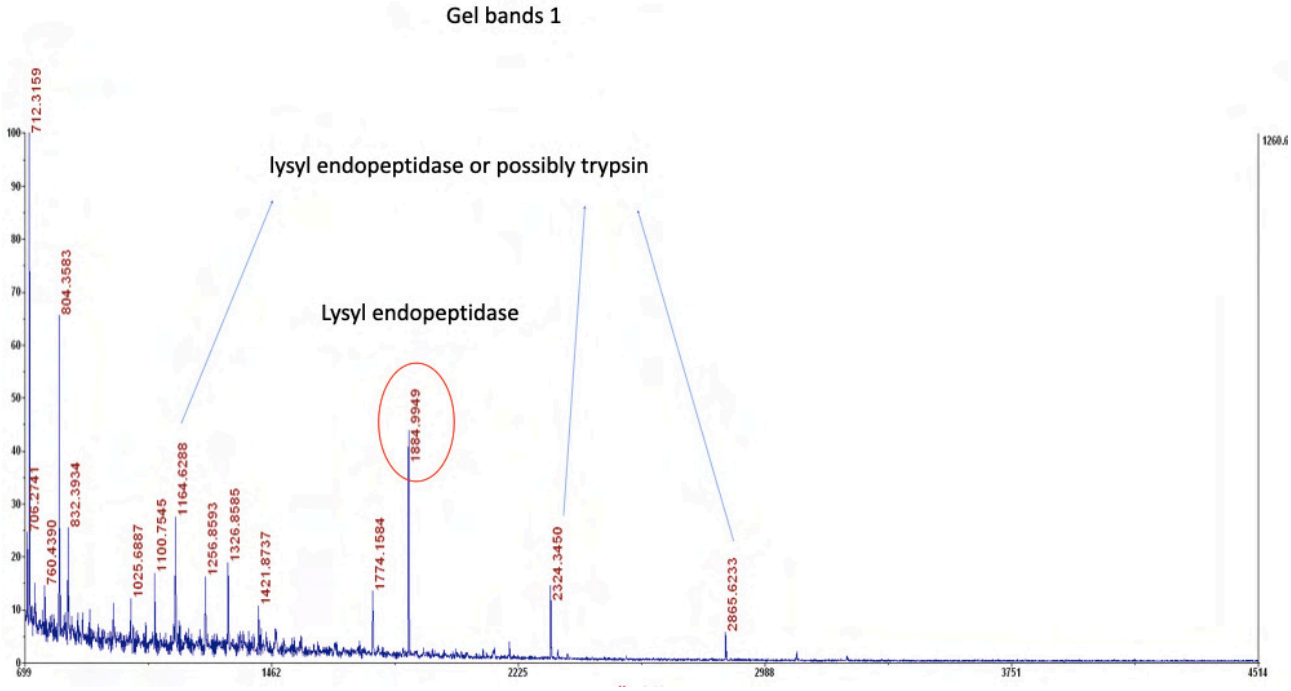

Figure 6: Mass spectrometry results from gel bands 1.

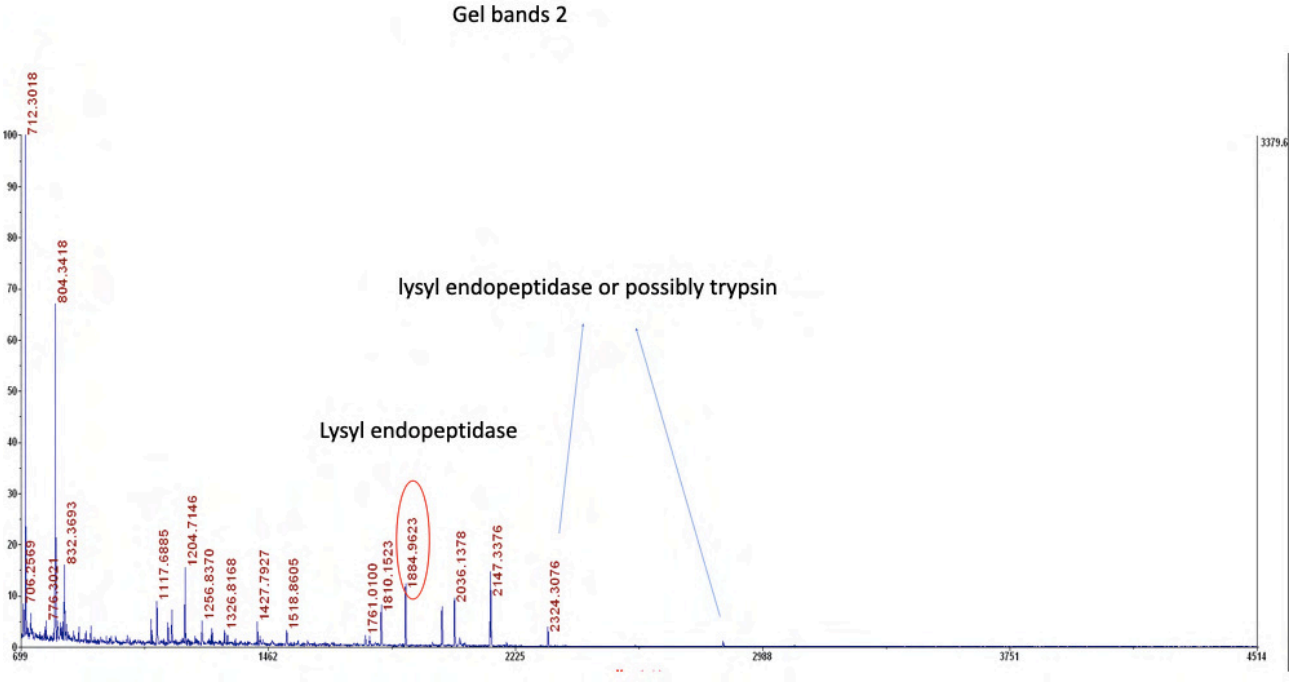

Figure 7: Mass spectrometry results from gel bands 2.

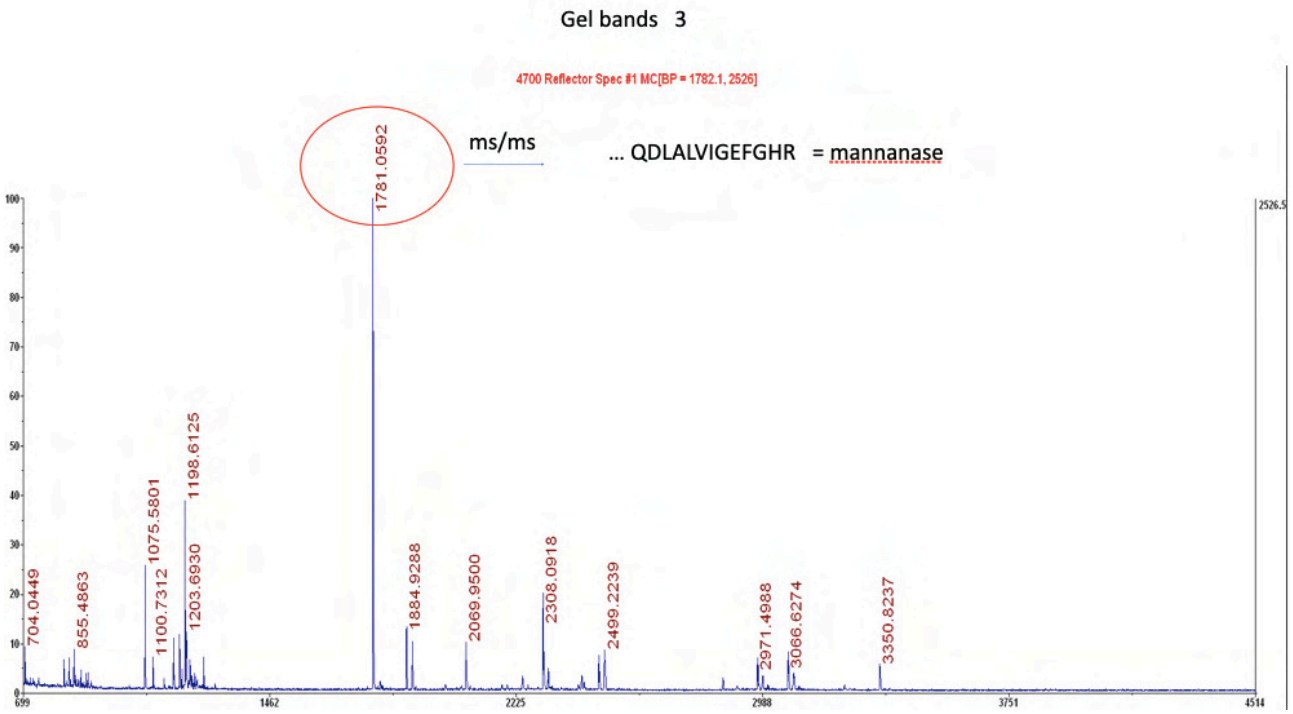

Figure 8: Mass spectrometry results from gel bands 3.

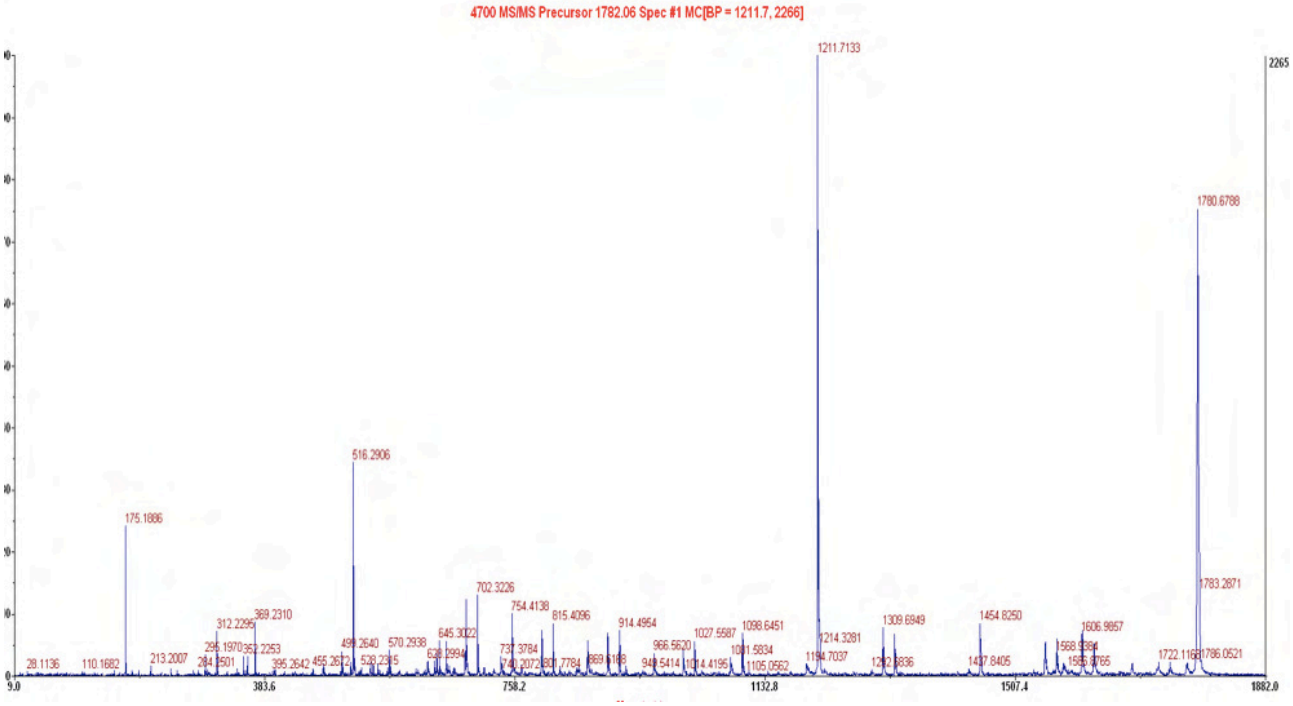

Figure 9: Tandem mass spectrometry results for the 1781,0592 m/z spike from gel bands 3.

Untitled
Average Mass = 1781.0455, Monoisotopic Mass = 1779.9632
Residues: 1-16, T1
N-Terminus = H, C-Terminus = OH
Fragment ions: Monoisotopic/Average (1750) m/z ratios with 1 positive charge(s).

b	100.1	213.2	327.2	455.3	570.3	683.4	754.4	867.5	966.6	1079.6	1136.7	1265.7	1412.8	1469.8	1606.9	-
i	72.1	86.1	87.1	101.1	88.0	86.1	44.1	86.1	72.1	86.1	30.0	102.1	120.1	30.0	110.1	129.1
	1	2	3	4	5	6	7	8	9	10	11	12	13	14	15	16
	Val	Leu	Asn	Gln	Asp	Leu	Ala	Leu	Val	Leu	Gly	Glu	Phe	Gly	His	Arg
	16	15	14	13	12	11	10	9	8	7	6	5	4	3	2	1
y"	-	1681.9	1568.8	1454.8	1326.7	1211.7	1098.6	1027.6	914.5	815.4	702.3	645.3	516.3	369.2	312.2	175.1

Figure 10: Animo acid sequence from the tandem mass spectrometry results for the 1781,0592 m/z spike from gel bands 3.

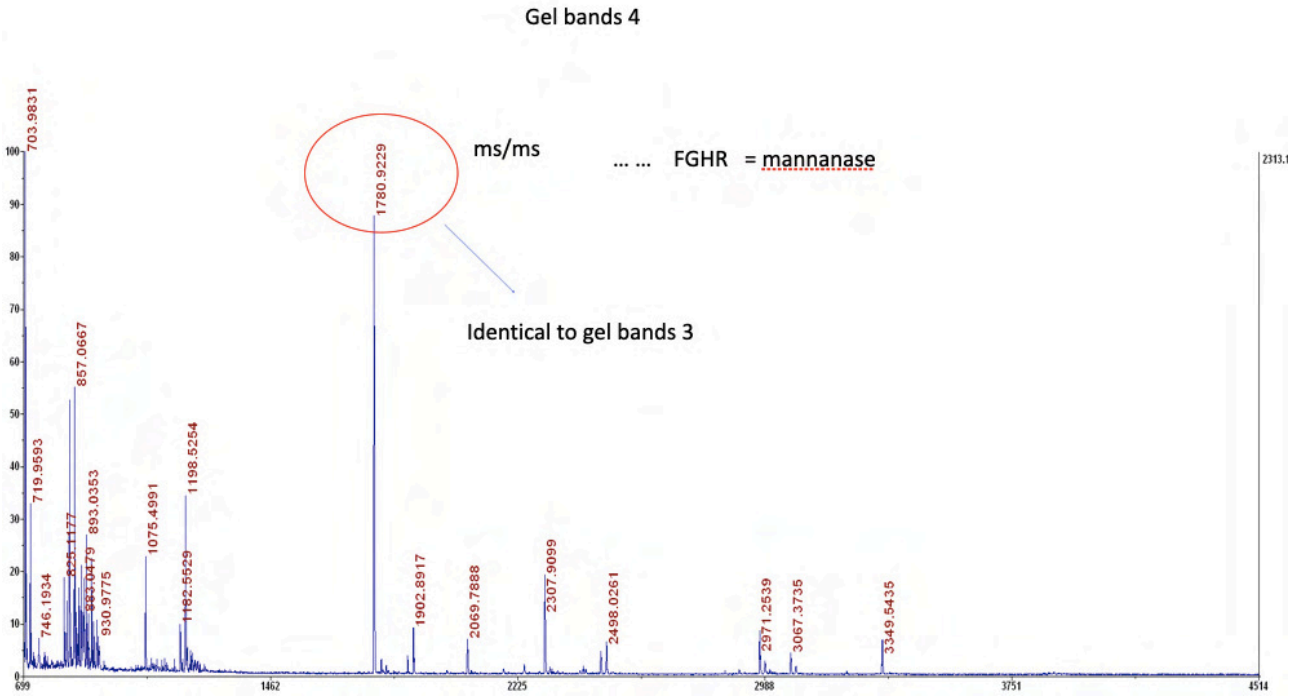

Figure 11: Mass spectrometry results from gel bands 4.

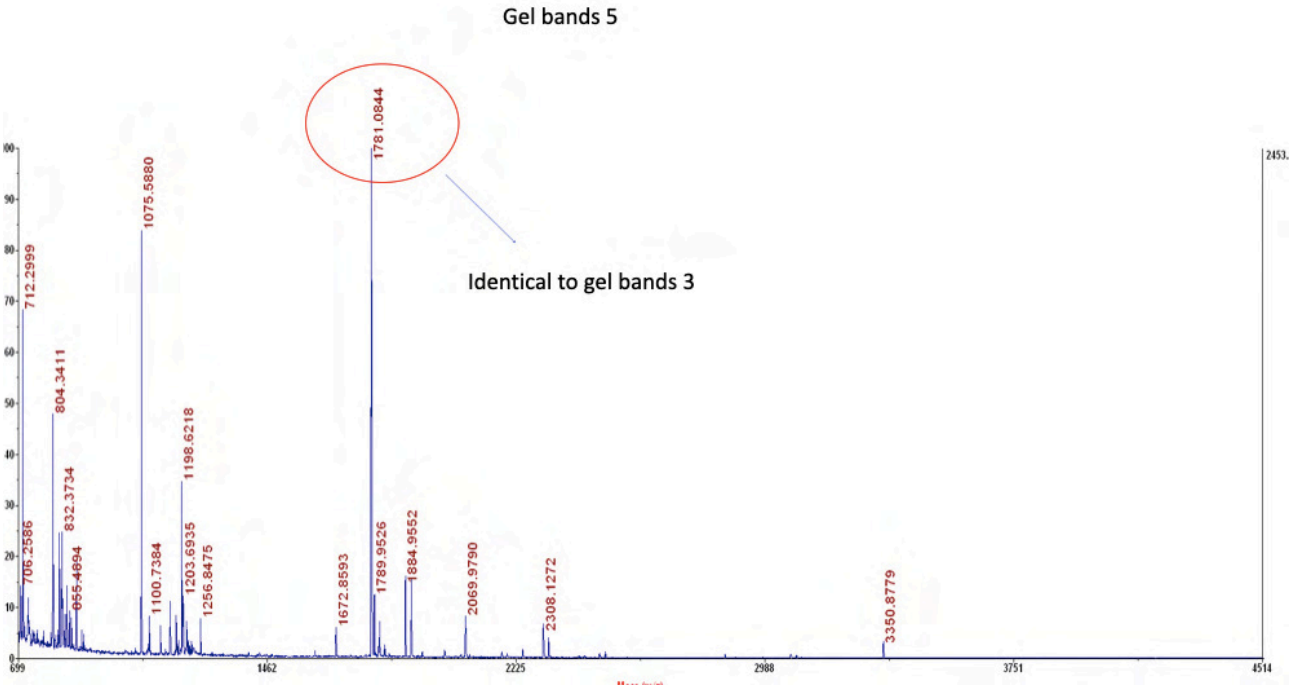

Figure 12: Mass spectrometry results from gel bands 5.

Discussion

As stated before, the main goal of this thesis is to characterize the contents of colacosomes, an objective that can be divided into multiple sub-objectives. These will be discussed here, one by one.

1. *Identification of strains that form an abundance of colacosomes on a specific medium.*

Out of the 19 species that have been known to form colacosomes (table 1), a select few species were available for the cultivation and screening process. Of these species, a collection of 32 strains was available. Curiously enough, only 2 species were capable of forming colacosomes in monocultures on a select amount of media. These were *Hyalopycnis blepharistoma* (Berk.) Seeler, Farlowia (CBS 149.68, CBS 953.73, CBS 582.80, CBS 590.93, CBS 591.93) and *Rhodosporidiobolus ruineniae* (Holzschu, Tredick & Phaff) Q.M. Wang, F.Y. Bai, M. Groenew. & Boekhout (CBS 5001).

The most successful species of these two, seems to be *Hyalopycnis blepharistoma*, as most strains successfully formed colacosomes on multiple media types. Not every strain formed colacosomes. In contrast to the other strains, strain CBS 587.93 doesn't form colacosomes on any type of the tested culture media. All the other strains of *Hyalopycnis blepharistoma* form colacosomes on at least one type of medium. Interestingly, the most successful medium turned out to be GYPA. This is in contrast to what was anticipated when taking into account the origins of the strains, as the best environment expected was more acidic. GYPA medium was the most alkalic medium in the set (pH = ±7).

Strain CBS 590.93 forms colacosomes as well, but not in the amount that was desired for the next step of the research. Ideally, the most suitable strains formed an abundance of colacosomes: this being an uncountably large amount of colacosomes which should appear prominently in nearly every hyphal cell. When it comes to *Rhodosporidiobolus ruineniae*, only one of the two strains seems to be successful in forming colacosomes.

Quite remarkably, none of the 32 strains formed colacosomes on MEA medium except for one strain of *Hyalopycnis blepharistoma* (CBS 149.68). This raises the question whether or not the MEA medium is suitable for colacosome formation. It has to be noted that MEA medium contains high concentrations of maltose, which have been proven to have an effect on gene transcription, specifically the MAL genes. MAL-gene clusters are activated by maltose and inhibited by glucose (Hasegawa et al. 2010; Hu et al. 2000). Since the formation process of colacosomes and its regulations are still unknown, maltose could potentially influence the capability of forming colacosomes. As of now, this is still pure speculation but its influence shouldn't be ruled out.

The most successful medium in general is GYPA. This medium is a nutrient rich medium which is preferred for a fast growth of fungi and contains high amounts of peptone and glucose. As such, this medium was used to start liquid cultures.

All the colacosome forming strains, except for CBS 590.93, were used to establish liquid GYPA cultures. CBS 590.93 was left out due to not forming enough colacosomes on solid medium. Since there still was some leftover liquid X-agar, CBS 149.68 and CBS 591.93 were also tested on this liquid medium. Interestingly, the same strains didn't all do equally well in liquid medium compared to their solid counterparts, only leaving *Hyalopycnis blepharistoma* (CBS 591.93) and *Rhodosporidiobolus ruineniae* (CBS 5001) as viable candidates to experiment further on to develop a lysis protocol. The most interesting strain is still that of *Hyalopycnis blepharistoma* (CBS 591.93) due to the species forming colacosomes in high amounts on multiple media. As such, the protocols were developed with CBS 591.93 as the experimental test subject.

2. *Development of an adequate lysis protocol and purification of colacosome fraction.*

During the development of the best lysis protocol, various options were considered and tested in pursuit of the best possible final result. Sometimes the differences between protocols were small, yet impacted the results clearly. The main changes made, were aimed at improving the lysis of the cells. The purification or enrichment method of the colacosome fraction was mainly focused on differential ultracentrifugation during the development of these lysis protocols. As such, the differences in these lysis protocols will first be described and discussed.

In the first protocol, the sample buffer utilized was CTAB. This would assist in the breaking down of cells, but would also come with some unexpected side effects: The tissue samples taken from the large liquid cultures were floating on top of the buffer. This wasn't the only side effect of CTAB, as it apparently reacts with Congo red dye under the epifluorescence microscope. This was seen during the screening of the first protocol, as all acquired fractions were screened using the same staining method as described in the screening section in materials and methods. The combination of Congo red together with CTAB results in the formation of thin, gel-like flakes which instantly contract upon exposure to fluorescent light (593/40 nm) during the epifluorescence microscopy. This can be seen in figure 13. To work around this problem, staining of the samples prior to the lysis treatment was proposed, tested and proven to be a viable alternative. This staining procedure has since become integrated into the lysis protocols as well, which can be found in the annexes.

The results of the first protocol proved to be not very stellar, as many of the cells were still intact and floating on top of the buffer as an unlysed mass of hyphae. The inefficiency of the lysis protocol can be mainly pointed towards the inability of the glass beads to reach the floating sample sufficiently to cause a complete lysis. Nevertheless, a minor amount of lysed cells were found in the long treatment samples.

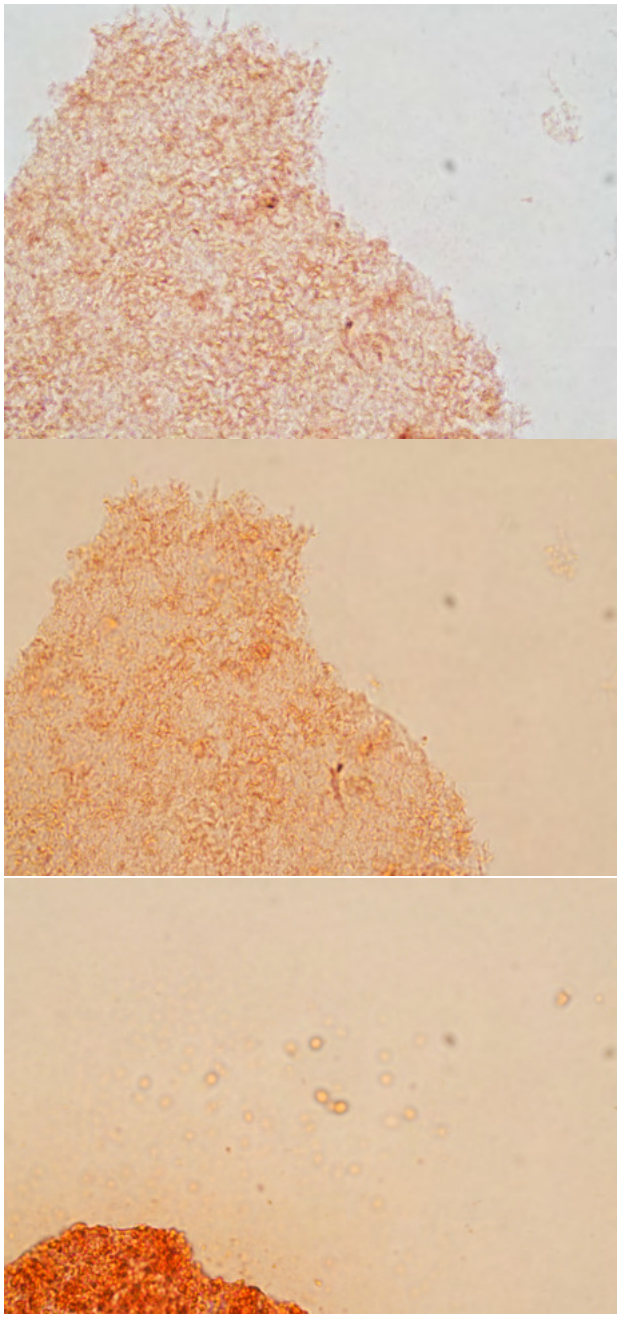

Figure 13: Gel-like flakes formed by the interaction of Congo red together and CTAB which instantly contract upon exposure to fluorescent light. This resulted in small round particles to appear as well. The first picture is before exposure to fluorescent light. After a brief exposure, the flake was quickly reacting until it reached the state in picture 3. This took place in less than 5 seconds.

The first protocol was reworked slightly and gave rise to protocol 2. From this protocol and onwards, the samples were stained prior to the lysis procedure. In this instance we tested two samples differing in lysis buffer: One sample used CTAB while the other sample used TRIS. There was an immediate visual difference after adding the buffer as the unlysed tissue sinks in the TRIS buffer, while the cells float in the CTAB buffer. This is beneficial for the lysis procedure, as the sinking tissue can be reached by the glass beads much more easily. Despite this, the amount of lysed cells was not satisfactory. Barely any cells broke open completely. It was clear that a stronger approach was required.

Utilizing a bead beater was the best option to tackle this problem. The samples used in this protocol were stained and incubated on CTAB for 48 hours at room temperature to assist in an even better lysis. One of these samples was bead beat with CTAB buffer while the other had its buffer removed. The difference in lysis was remarkable, not only in between the previous protocols, but also in between the samples. In the sample without buffer, there were much more lysed cells present in the 8000G pellet. Small round structures could also be observed in the 8000G pellet, but seemed to be rapidly breaking down during screening with epifluorescence microscopy. The sample that was bead beat with CTAB buffer showed clearly less lysed cells in all of the fractions. This is most likely due to the buffer slowing down the beads during the beating procedure and thus losing efficiency.

To ensure complete lysis, a treatment with liquid nitrogen was considered. As such, the first protocol using liquid nitrogen to completely freeze the samples and subsequently bead beat them was created (Protocol 4). In the first instance, positive results were noted: samples that were frozen in liquid nitrogen and bead beat without buffer proved to contain lysed cells within the 8000G pellet and 12000G pellet. However, a mistake was made during this protocol: The samples were frozen to the wall of the eppendorf. This led to a more inefficient lysis. Undoubtedly, using liquid nitrogen was a step in the right direction, but this protocol was not yet ideal. The round structures that were observed through epifluorescence microscopy seemed to be rather unstable and broke apart upon illumination with fluorescent light. This most likely was caused by the CTAB buffer. The buffer assists in cell lysis, but it does pose a hindrance when it disturbs the integrity of the secondary cell wall formed around the colacosomes, as this complicates the screening of the samples.

Due to this, only the TRIS buffer was used in further protocols. Not only is TRIS less invasive towards the proteins compared to the CTAB detergent, it is less dense than the samples, preventing the creation of a floating fraction of unlysed cells. Protocol 5 build further upon the previous findings, and showed one of the best lysis protocols. Most unlysed cells were found within the 4000G fraction, but also fragments and loose colacosomes could be viewed. Fragments and loose colacosomes were also found in the 8000G pellet but to a lesser extent in the 12000G pellet. In contrast to the CTAB samples, screening went more clearly and easily, as the colacosomes appeared more stable and didn't rupture under fluorescent light. The protocol was slightly altered afterwards in one specific point: the liquid nitrogen exposure.

In protocol 4 and 5, the complete eppendorfs were put into liquid nitrogen. Due to the brief exposure time, the sample itself might not have been completely frozen to the same degree as putting the sample directly into liquid nitrogen. Protocol 6 deviates from this: The sample is taken out of the eppendorf and put directly into liquid nitrogen. In this way, the sample becomes completely frozen solid, which is an advantage during the bead beating procedure. And indeed, this increased the efficiency of the lysis significantly. Just like in Protocol 5, the fractions with the most colacosomes and lysed cells were the pellets generated by spinning the samples down for 10 minutes at 4000G and 8000G. Unlysed cells were still present however. To enhance cell lysis even further, crushing the sample with a mortar and pestle was also tried in Protocol 7. However, the practicality of this step was rather low, as the

refined material is rather difficult to collect from the mortar without loss of the tissue due to the grinding.

All these protocols combined led to the final lysis protocol to be based off of Protocol 6. One problem that remained, was the purification of a colacosome fraction. Since the majority of the cell debris and colacosomes was found from 4000G to 8000G fractions, along with the majority of unlysed cells, ultracentrifugation might not be the ideal protocol. As such our views and approach shifted towards acquiring an enriched fraction i.e. a fraction that contains more colacosomes but does not exist out of purely colacosomes.

Since colacosomes are much smaller compared to unlysed cells, a filtration protocol was developed. As stated before, the diameter of colacosomes are estimated to be around 0,5-0,6µm. Ideally, fragments containing colacosomes and loose colacosomes would be isolated from the unlysed cells. This was achieved by testing filters of different mesh sizes, and proved to be the best when used in sequence.

As a potential other approach to mechanical lysis, enzymatic lysis was also considered. For this, an endo-1,4 β-Mannanase (available from Megazyme with Product code: E-BMABS) was chosen. This would affect the main sugar component in the cell wall of species belonging to the Microbotryomycetes. It was expected to make the cell wall more porous or at least more fragile. However, due to a mixup of data on the available enzymes, it was thought to be endo-1,4 β-Mannanase originating from *Aspergillus niger* to be available in the lab (enzyme available from Megazyme with product code: E-BMANN). This enzyme is active at a pH-level of 4 with optimum at pH-level of 3. Due to this mistake, the samples were prepared using a sodium acetate buffer of 100 mM with a pH of 4 while the actual enzyme used has an optimum around pH-level 8. This meant that the tests were run on a buffer that was 10^4 times more acidic than the enzyme's optimal active pH. As such, the results are most likely due to the exposure of the tissue to a high acidity buffer. This was perhaps one of the biggest flaws during the research. Due to time constraints, it was not possible to verify the effectiveness of the enzymatic treatment Using TRIS buffer.

3. Identification of the colacosome content.

One of the most notable things in the first gel electrophoresis is the reduction in intensity of staining of the proteins between 100 kD and 75 kD in the enzymatically treated fraction with decreasing filter mesh size. This can be explained however: Endo-1,4 β-Mannanase breaks down mannan chains into smaller mannose saccharides. Saccharides such as mannan influence the staining of peptides with Coomassie blue (Banik et al. 2009). This might explain why the staining of the proteins is less prominent in the enzymatically treated samples. Due to the fractions with smaller mesh size containing smaller cell wall fragments, it is likely that these were more accessible for the endo-1,4 β-Mannanase. This would facilitate the enzyme's reaction by liberating more mannose saccharides which will in turn sequester the Coomassie blue (Banik et al. 2009).

If this were true, it would make sense for the proteins visible in between 100 kD and 75 kD to be cell wall associated glycoproteins. From the mass spectrometry results, we can determine that in gel bands 3, 4 and 5, there have been found traces of mannanase, which is most likely the enzyme added from the enzymatic treatment.

This leaves the question: What is contained in the gel bands 1 and 2? Within the first gel, signs of lysyl endopeptidase were found, as well as possible signs of trypsin. Other signals weren't strong enough to perform tandem mass spectrometry on. These proteins are undoubtedly part of the protease mix that was added to digest the proteins during the in gel digestion protocol.

Gel bands 1 and 2 seem to appear in the second gel electrophoresis as well; however, due to time constraints and technical defects with the equipment, it was not possible to analyze these with mass spectrometry.

From the Bradford assay, we can deduce that there was not a loss of protein during the filtration procedure as the mean consentration stays about equal for all the samples with reducing mesh size. When looking at the accompanying electrophoresis we can see that the majority of the mass of

proteins is accounted for by small peptides that appear to be smaller than 10 kD. This could point towards a strong protease activity, leading to the destruction of proteins throughout the samples. As a suggestion for future research, a protease assay could be tested to verify whether or not there is protease activity within samples. If this is the case, protease inhibitors can be added to the samples. This could potentially clarify more about the exact contents of the colacosomes' content .

Conclusion

In conclusion, we have successfully determined that two species, specifically, *Hyalopycnis blepharistoma* and *Rhodosporidiobolus ruineniae* form colacosomes in monoculture on a few different types of medium. The strains that formed colacosomes were CBS 149.68, CBS 953.73, CBS 582.80, CBS 590.93 and CBS 591.93 for *Hyalopycnis blepharistoma* and CBS 5001 for *Rhodosporidiobolus ruineniae*.

Not every strain of these species gave the same results on the same types of media. GYPA, a nutrient rich medium, has proven to be the most successful medium on which all of the aforementioned strains form colacosomes in a monoculture on solid medium. MEA appears to be the least successful medium, raising the question if the maltose concentration acts as an environmental cue in the regulation of colacosome formation. Strain CBS 591.93 of *Hyalopycnis blepharistoma* and CBS 5001 of *Rhodosporidiobolus ruineniae* have shown to form colacosomes in high concentrations in liquid cultures, making them ideal candidates for further experimentation.

A lysis protocol has been successfully created together with a filtration procedure, resulting in an enriched fraction with high colacosome concentration. In the SDS-PAGE we have also seen something which could potentially point towards strong protease activity, something on which further research can be conducted upon.

With the discovery of colacosome forming strains in monocultures, as well as the media on which they grow and the created protocols, this thesis has laid a foundation for following research on a topic that has been dormant for decades.

Although the decisive answer as to what resides within colacosomes remains unanswered, the milestones reached during this thesis can act as a catalyst to spark future research regarding the creation, contents and subsequently, the function of colacosomes.

Summary - English

Mycoparasitic fungi can affect their hosts in a variety of ways through a variety of specific mechanisms. One example of such specialized cell structures are the colacosomes. Colacosomes are subcellular structures found in hyphae, that were first described as lenticular bodies by Kreger-van Rij & Veenhuis in 1971. Colacosome-forming fungi are only found within the Pucciniomycotina, more specifically, within the Cryptomycocolacomycetes and Microbotryomycetes. The latter will be the main focus point of this study. The Microbotryomycetes are known to contain Type 1-colacosomes, which are very electron-dense, and form a connection through the host and parasite cell wall but do not enter the plasmalemma of the host. The formation of colacosomes is thought to be very fast and occurs at contact points with a fungal host. However, colacosomes have been found in monocultures as well, which could be interpreted as a form of self-parasitism.

As of today, the exact function of colacosomes remains unclear as do their contents. Due to the change in electron density, a difference in contents between the colacosome and the cytosol is expected. Our main goal for this research is to characterize the contents of the colacosomes by finding colacosome-forming species, establishing cultures, lysing the cells and purifying the colacosome fractions to identify the proteins within through means of mass spectrometry.

The first step in this research was establishing monocultures of potential colacosome containing fungi on solid medium and evaluate the presence of colacosomes through Congo red staining combined with epifluorescence microscopy. This was tested on multiple media, as the environmental cues to activating colacosome formation are unknown. Out of the 32 available strains, only 6 strains proved to contain an abundance of colacosomes on solid medium.

When switching over to liquid medium, only two strains remained. These were *Hyalopycnis blepharistoma* (CBS 591.93) and *Rhodosporidiobolus ruineniae* (CBS 5001) with the medium being liquid GYPA. Out of these two, most experiments regarding lysis protocols and colacosome purification were developed using *Hyalopycnis blepharistoma* (CBS 591.93).

The most optimal lysis protocol freezes tissue samples using liquid nitrogen and bead beating using glass beads. When it came to purification of the colacosome fracion, the initial idea was to separate the colacosomes using ultracentrifugation, but this technique was not ideal as unlysed cells still were common in the colacosome rich pellets. This led to the creation of a sequential filtration protocol which proved to be effective at removing unlysed cells and larger fragments from the pellets.

Due to technical difficulties, the contents of the colacosomes couldn’t be determined, however, in the lysed fractions there appear to be many smaller peptides present, with might point towards strong protease activity. These findings function as a foundation for more in depth research regarding the contents of colacosomes.

Summary - Dutch

Mycoparasitaire schimmels kunnen hun gastheren op verschillende manieren beïnvloeden via een verschillende specifieke mechanismen. Een voorbeeld van dergelijke gespecialiseerde celstructuren zijn de colacosomen. Colacosomen zijn subcellulaire structuren die worden gevonden in hyfen, en werden voor het eerst beschreven door Kreger-van Rij & Veenhuis in 1971. Colacosoom-vormende schimmels worden alleen gevonden in de Pucciniomycotina, specifiek in de Cryptomycocolacomycetes en Microbotryomycetes. Deze laatste groep zal in dit onderzoek centraal staan. Van de Microbotryomycetes is bekend dat ze Type 1-colacosomen bevatten. Deze zijn zeer elektronendicht en maken een connectie doorheen zowel de celwand van de parasiet als die van de gastheer, maar dringt de plasmalemma van de gastheer niet binnen.De vorming van colacosomen wordt als een zeer snel process beschouwd en vindt plaats op contactpunten met hyfen van een gastheer. Er zijn echter ook colacosomen gevonden in monoculturen, wat kan worden geïnterpreteerd als een vorm van zelfparasitisme.

Tot op vandaag blijft de exacte functie van colacosomen onduidelijk, evenals hun inhoud. Door de verandering in elektronendichtheid wordt een verschil in inhoud tussen het colacosoom en het cytosol verwacht. Ons belangrijkste doel van dit onderzoek is om de inhoud van colacosomen te karakteriseren door colacosoomvormende soorten te vinden, culturen op te starten, de cellen te lyseren en de colacosoomfracties op te zuiveren om de eiwitten erin te identificeren door middel van massaspectrometrie.

De eerste stap in dit onderzoek was het opzetten van monoculturen van potentiële colacosoomvormende schimmels op vast medium en het controleren op de aanwezigheid van colacosomen door middel van Congoroodkleuring in combinatie met epifluorescentiemicroscopie. Dit werd getest op meerdere media, omdat de omgevingsfactoren die aanzetten tot colacosoomvorming nog onbekend zijn. Van de 32 beschikbare stammen bleken slechts 6 stammen een overvloed aan colacosomen op vast medium te bevatten.

Bij het overschakelen naar vloeibaar medium bleven er slechts twee stammen over. Dit waren *Hyalopycnis blepharistoma* (CBS 591.93) en *Rhodosporidiobolus ruineniae* (CBS 5001) met als medium vloeibaare GYPA. Van deze twee werden de meeste protocollen op vlak van cellysering en colacosoomopzuivering ontwikkeld met behulp van *Hyalopycnis blepharistoma* (CBS 591.93).

In het meest optimale lyseringsprotocol worden de stalen bevroren met behulp van vloeibare stikstof en met glasparels gebroken in een bead beater. Als het ging om de zuivering van de colacosome-fractie, was het oorspronkelijke idee om de colacosomen te scheiden met behulp van ultracentrifugatie, maar deze techniek was niet ideaal omdat niet-gelyseerde cellen nog steeds veel voorkomen in de colacosoomrijke pellets. Dit leidde tot de creatie van een sequentieel filtratieprotocol dat effectief bleek te zijn bij het verwijderen van niet-gelyseerde cellen en grotere fragmenten uit de pellets.

Door technische problemen kon de inhoud van de colacosomen niet worden bepaald, maar in de gelyseerde fracties lijken er veel kleinere peptiden aanwezig te zijn, wat zou kunnen wijzen op een sterke protease-activiteit. Deze bevindingen en ontwikkelde protocols kunnen fungeren als basis voor meer diepgaand onderzoek naar de inhoud van colacosomen.

Acknowledgments

First and foremost, I would like to thank my supervisors, prof. dr. Annemieke Verbeken and prof. dr. Bart Devreese for their time, guidance and advice during the making of this thesis.

I would like to express my gratitude to my advisor, Nathan Schoutteten, for all his support, insights and guidance during the experiments and creation of the protocols but also for keeping the morale high when progress seemed to go rather slow. I would also like to thank Olivier Leroux for his assistance with the fluorescence microscopy and insights to possible different approaches.

I would also like to thank the Research Group Mycology in the Department of Biology and the Laboratory of Microbiology in the Department of Biochemistry and Microbiology, specifically the Bart Devreese group. The positive work environment had a positive effect on my motivation throughout the year. I expected some minor difficulties in planning, as this subject is located in between the two departments, but communication and planning went very well in general.

During the practical work at the Department of Biochemistry and Microbiology, I was assisted by Isabel Vandenberghe, Gonzalez Van Driessche and Zhoujian Diao to whom I would also like to thank.

To all my friends and family, who supported me during the making of this thesis: Thank you!!!

Last but definitely not least, I would like fulfill a promise. A thank you to my grandfather, Etienne Leroy, who passed away during this research. He might not have understood anything in detail about my thesis, but supported me nevertheless.

References

Aime, M. C., Toome, M., & McLaughlin, D. J. (2014). 10 Pucciniomycotina. *In Systematics and Evolution* (pp. 271–294). Springer Berlin Heidelberg. https://doi.org/10.1007/978-3-642-55318-9_10

Banik, S. P., Pal, S., Ghorai, S., Chowdhury, S., & Khowala, S. (2009). Interference of sugars in the Coomassie Blue G dye binding assay of proteins. In *Analytical Biochemistry* (*Vol. 386, Issue 1*, pp. 113–115). Elsevier BV. https://doi.org/10.1016/j.ab.2008.12.006

Bauer R (2004) Basidiomycetous interfungal cellular interactions – a synopsis. In: *Agerer R, Piepenbring M, Blanz P (eds) Frontiers in Basidiomycote Mycology. IHW*, Eching, pp 325–337.

Bauer, R., & Oberwinkler, F. (1991). The Colacosomes: New Structures at the Host-parasite Interface of a Mycoparasitic Basidiomycete*. In: *Botanica Acta* (*Vol. 104, Issue 1*, pp. 53–57). Wiley. https://doi.org/10.1111/j.1438-8677.1991.tb00193.x

Bauer, R., & Oberwinkler, F. (2008). Cellular Basidiomycete–Fungus Interactions. In: *Plant Surface Microbiology* (pp. 267–279). Springer Berlin Heidelberg. https://doi.org/10.1007/978-3-540-74051-3_16

Bauer, R., Begerow, D., Sampaio, J. P., Weiβ, M., & Oberwinkler, F. (2006). The simple-septate basidiomycetes: a synopsis. In: *Mycological Progress* (*Vol. 5, Issue 1*, pp. 41–66). Springer Science and Business Media LLC. https://doi.org/10.1007/s11557-006-0502-0

Borner, G. H. H. (2020). Organellar Maps Through Proteomic Profiling – A Conceptual Guide. In *Molecular & Cellular Proteomics* (*Vol. 19, Issue 7*, pp. 1076–1087). Elsevier BV. https://doi.org/10.1074/mcp.r120.001971

Elshahawy, I. E., Saied, N. M., Abd-El-Kareem, F., & Morsy, A. A. (2017). FIELD APPLICATION OF SCLEROTIAL MYCOPARASITES AS BIOCONTROL AGENTS TO STROMATINIA CEPIVORA, THE CAUSE OF ONION WHITE ROT. *Journal of Plant Pathology, 99*(2), 391–401. http://www.jstor.org/stable/44686784

Eriksson, J., & Ryvarden, L. (1975). The Corticiaceae of North Europe Volume 3, Coronicium - Hyphoderma.

Geladaki, A., Kočevar Britovšek, N., Breckels, L. M., Smith, T. S., Vennard, O. L., Mulvey, C. M., Crook, O. M., Gatto, L., & Lilley, K. S. (2019). Combining LOPIT with differential ultracentrifugation for high-resolution spatial proteomics. In *Nature Communications* (*Vol. 10*, Issue 1). Springer Science and Business Media LLC. https://doi.org/10.1038/s41467-018-08191-w

Gryta, H., Carriconde, F., Charcosset, J.-Y., Jargeat, P., & Gardes, M. (2006). Population dynamics of the ectomycorrhizal fungal species Tricholoma populinum and Tricholoma scalpturatum associated with black poplar under differing environmental conditions. In *Environmental Microbiology* (*Vol. 8*, Issue 5, pp. 773–786). Wiley. https://doi.org/10.1111/j.1462-2920.2005.00957.x

He, MQ., Zhao, RL., Hyde, K.D. et al. (2019). Notes, outline and divergence times of Basidiomycota. In *Fungal Diversity* (*Vol. 99*, Issue 1, pp. 105–367). Springer Science and Business Media LLC. https://doi.org/10.1007/s13225-019-00435-4

Highley, T. L. (1979). Mechanisms of Wood Decay and the Unique Features of Heartrots. In *Phytopathology* (*Vol. 69*, Issue 10, p. 1151). Scientific Societies. https://doi.org/10.1094/phyto-69-1151

Korhonen, A., Miettinen, O., Kotze, J. D., & Hamberg, L. (2022). Landscape context and substrate characteristics shape fungal communities of dead spruce in urban and semi-natural forests. In *Environmental Microbiology*. Wiley. https://doi.org/10.1111/1462-2920.15903

Kottke, I., Suárez, J. P., Herrera, P., Cruz, D., Bauer, R., Haug, I., & Garnica, S. (2010). Atractiellomycetes belonging to the 'rust' lineage (Pucciniomycotina) form mycorrhizae with terrestrial and epiphytic neotropical orchids. In *Proceedings of the Royal Society B: Biological Sciences* (*Vol. 277*, Issue 1685, pp. 1289–1298). The Royal Society. https://doi.org/10.1098/rspb.2009.1884

Kreger-van Rij, N. J. W., & Veenhuis, M. (1971a). A Comparative Study of the Cell Wall Structure of Basidiomycetous and Related Yeasts. In *Journal of General Microbiology* (*Vol. 68*, Issue 1, pp. 87–95). Microbiology Society. https://doi.org/10.1099/00221287-68-1-87

Kreger-van Rij, N. J. W., & Veenhuis, M. (1971b). Some features of yeasts of the genusSporidiobolus observed by electron microscopy. In *Antonie van Leeuwenhoek* (*Vol. 37*, Issue 1, pp. 253–255). Springer Science and Business Media LLC. https://doi.org/10.1007/bf02218489

Kumar, J., & Atri, N. (2019). CHARACTERISATION AND IDENTIFICATION OF ECTOMYCORRHIZAE OF RUSSULA (RUSSULACEAE: BASIDIOMYCOTA) ASSOCIATED WITH SHOREA ROBUSTA. *Journal of Tropical Forest Science, 31*(1), 114–124. https://www.jstor.org/stable/26565766

Laperriere, G., Desgagné-Penix, I., & Germain, H. (2018). DNA distribution pattern and metabolite profile of wild edible lobster mushroom (Hypomyces lactifluorum/Russula brevipes). In *Genome* (*Vol. 61*, Issue 5, pp. 329–336). Canadian Science Publishing. https://doi.org/10.1139/gen-2017-0168

Naranjo-Ortiz, M. A., & Gabaldón, T. (2019). Fungal evolution: major ecological adaptations and evolutionary transitions. In *Biological Reviews* (*Vol. 94*, Issue 4, pp. 1443–1476). Wiley. https://doi.org/10.1111/brv.12510

Oberwinkler, F. (2017). Yeasts in Pucciniomycotina. In *Mycological Progress* (*Vol. 16*, Issue 9, pp. 831–856). Springer Science and Business Media LLC. https://doi.org/10.1007/s11557-017-1327-8

Oberwinkler, F., & Bauer, R. (1990). Cryptomycocolax:A New Mycoparasitic Heterobasidiomycete. In *Mycologia* (*Vol. 82*, Issue 6, pp. 671–692). Informa UK Limited. https://doi.org/10.1080/00275514.1990.12025948

Oberwinkler, F., Bauer, R., & Tschen, J. (1999). The Mycoparasitism of Platygloea bispora. In *Kew Bulletin* (*Vol. 54*, Issue 3, p. 763). JSTOR. https://doi.org/10.2307/4110873

Pitt, J. I., & Hocking, A. D. (2009). Methods for Isolation, Enumeration and Identification. In *Fungi and Food Spoilage* (pp. 19–52). Springer US. https://doi.org/10.1007/978-0-387-92207-2_4

Prasanna, A. N., Gerber, D., Kijpornyongpan, T., Aime, M. C., Doyle, V. P., & Nagy, L. G. (2019). Model Choice, Missing Data, and Taxon Sampling Impact Phylogenomic Inference of Deep Basidiomycota Relationships. In *Systematic Biology* (*Vol. 69*, Issue 1, pp. 17–37). Oxford University Press (OUP). https://doi.org/10.1093/sysbio/syz029

Prillinger, H., Oberwinkler, F., Umile, C., Tlachac, K., Bauer, R., Dörfler, C., and Taufratzhofer, E. (1993). Analysis of cell wall carbohydrates (neutral sugars) from ascomycetous and basidiomycetous yeasts with and without derivatization. In *The Journal of General and Applied Microbiology* (*Vol. 39*, Issue 1, pp. 1–34). Microbiology Research Foundation. https://doi.org/10.2323/jgam.39.1

Hasegawa, S., Takizawa, M., Suyama, H., Shintani, T., & Gomi, K. (2010). Characterization and expression analysis of a maltose-utilizing (MAL) cluster in Aspergillus oryzae. In *Fungal Genetics and Biology* (*Vol. 47*, Issue 1, pp. 1–9). Elsevier BV. https://doi.org/10.1016/j.fgb.2009.10.005

Skrzypczak, C. (1988). Diseases of Dutch irises (Iris x hollandica), in particular of basal rot and blue mold, and their chemical control. Pt. 3. Identification, pathogenicity and biology of Penicillium corymbiferum casual agent of blue mold of Dutch iris. Experimental Work of the Institute of Pomology and Floriculture. Series B-Ornamental Plants.

Sun, J.-Z., Liu, X.-Z., McKenzie, E. H. C., Jeewon, R., Liu, J.-K. (Jack), Zhang, X.-L., Zhao, Q., & Hyde, K. D. (2019). Fungicolous fungi: terminology, diversity, distribution, evolution, and species checklist. In *Fungal Diversity* (*Vol. 95*, Issue 1, pp. 337–430). Springer Science and Business Media LLC. https://doi.org/10.1007/s13225-019-00422-9

Yang, S., Wang, W., Wei, H., Van Wychen, S., Pienkos, P., Zhang, M., & Himmel, M. (2016). Comparison of Nitrogen Depletion and Repletion on Lipid Production in Yeast and Fungal Species. In *Energies* (*Vol. 9*, Issue 9, p. 685). MDPI AG. https://doi.org/10.3390/en9090685

Hu, Z., Yue, Y., Jiang, H., Zhang, B., Sherwood, P. W., & Michels, C. A. (2000). Analysis of the Mechanism by Which Glucose Inhibits Maltose Induction of MAL Gene Expression in Saccharomyces. In *Genetics* (*Vol. 154*, Issue 1, pp. 121–132). Oxford University Press (OUP). https://doi.org/10.1093/genetics/154.1.121

Annexes

Annexes - Photographs

NS 20-141-C2 - Culture Plates	
GYPA	**MEA**
	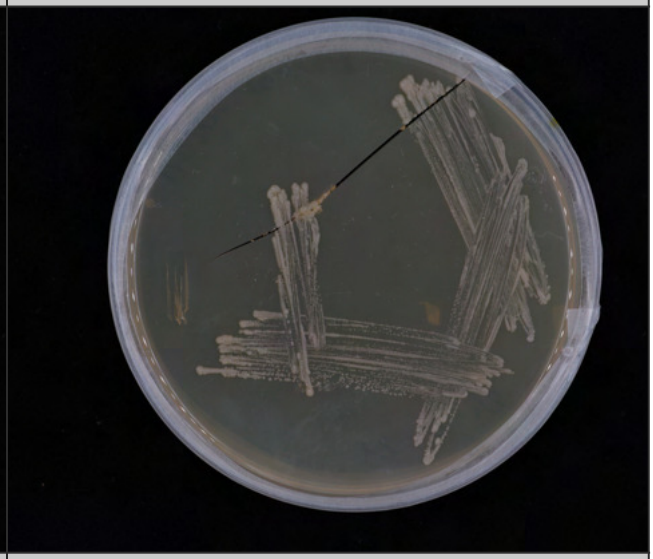
PDA	**X-AGAR**
	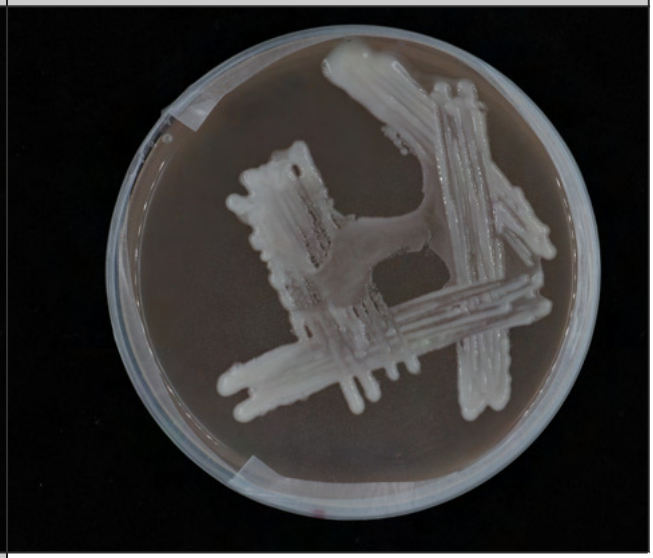
NITROGEN DEPLETED	
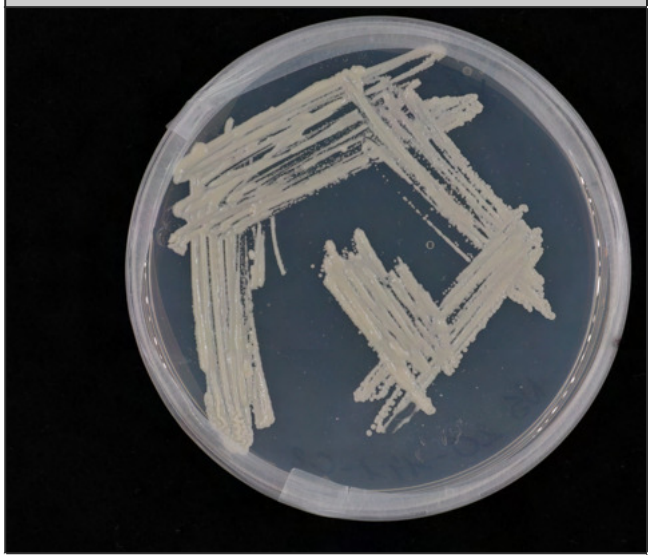	

NS 20-141-C2 - Culture Plates

NS 20-141-C2 - Microscopy Photographs	
GYPA	**MEA**
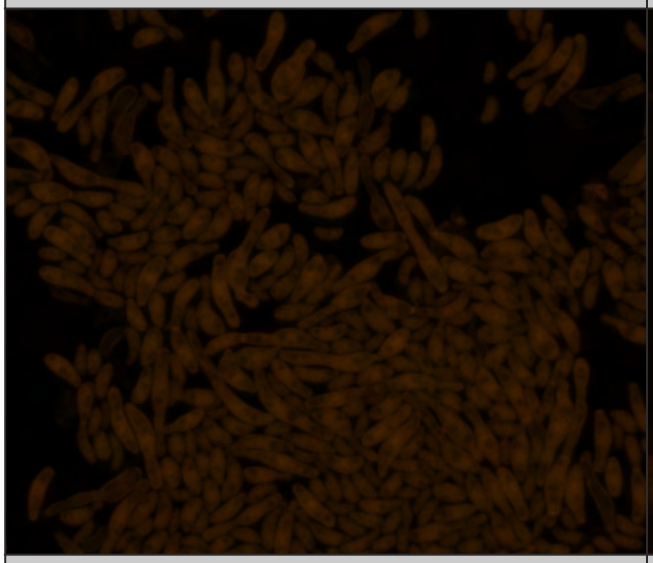	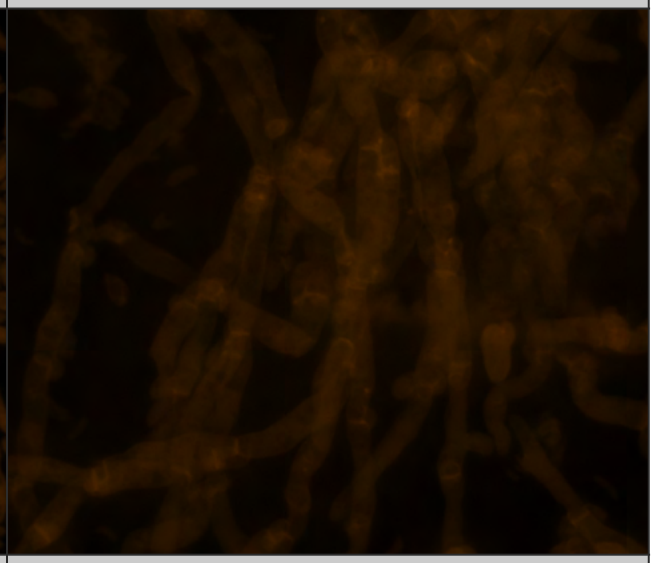
PDA	**X-AGAR**
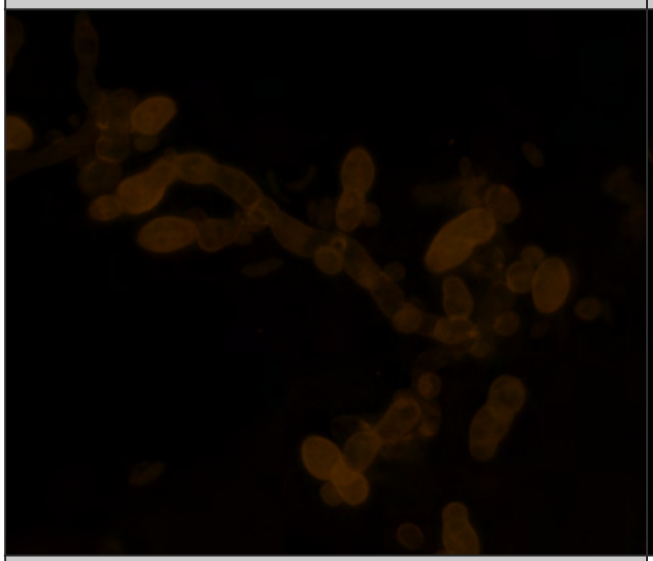	
NITROGEN DEPLETED	
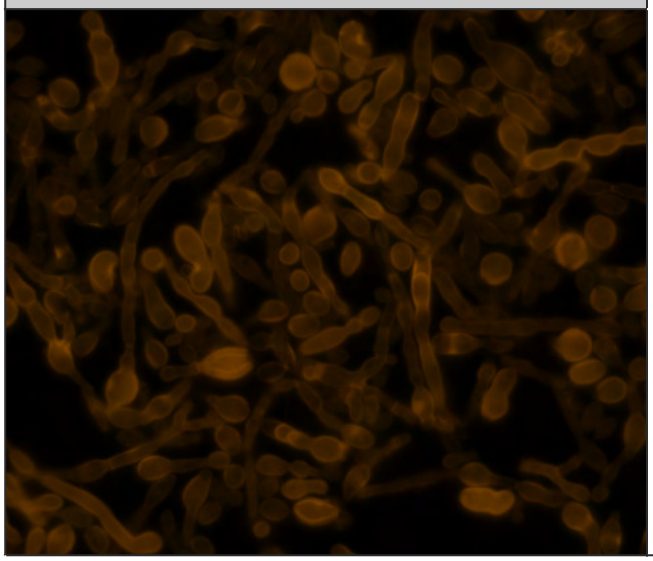	

NS 20-141-C2 - Microscopy Photographs

ENZ 20-052-C1 - Culture Plates	
GYPA	**MEA**
	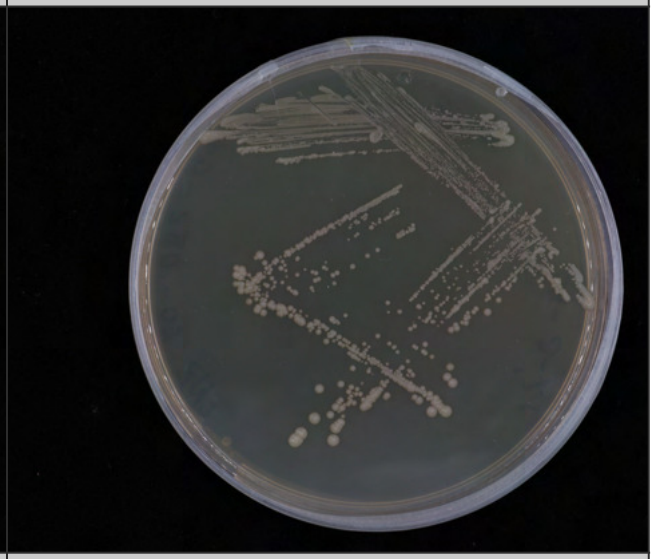
PDA	**X-AGAR**
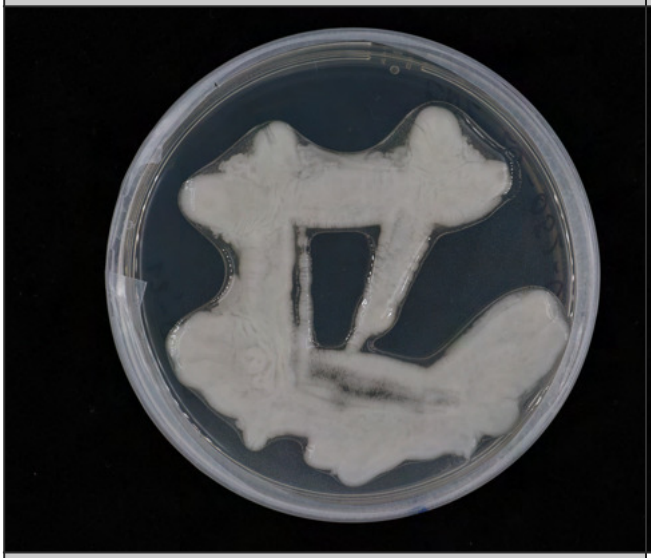	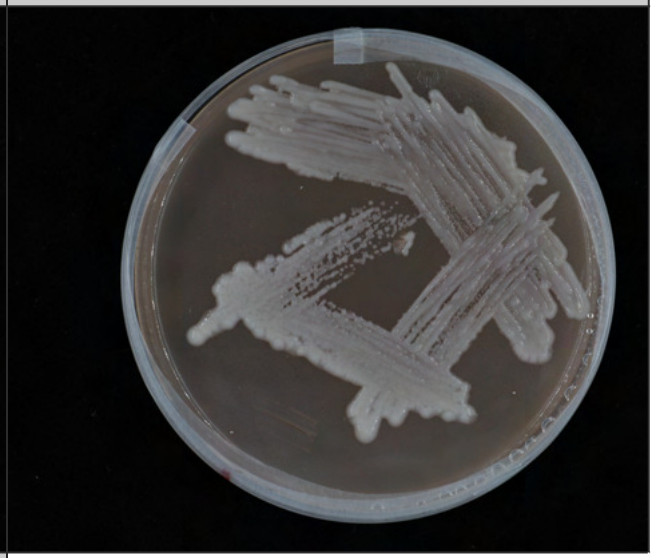
NITROGEN DEPLETED	
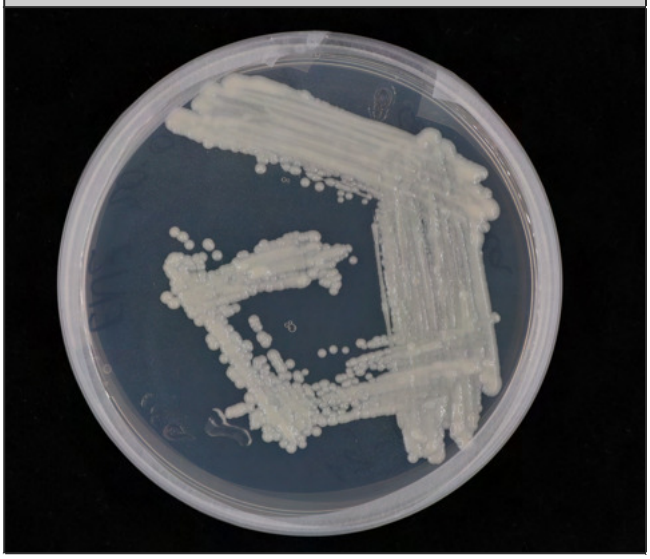	

ENZ 20-052-C1 - Culture Plates

ENZ 20-052-C1 - Microscopy Photographs	
GYPA	**MEA**
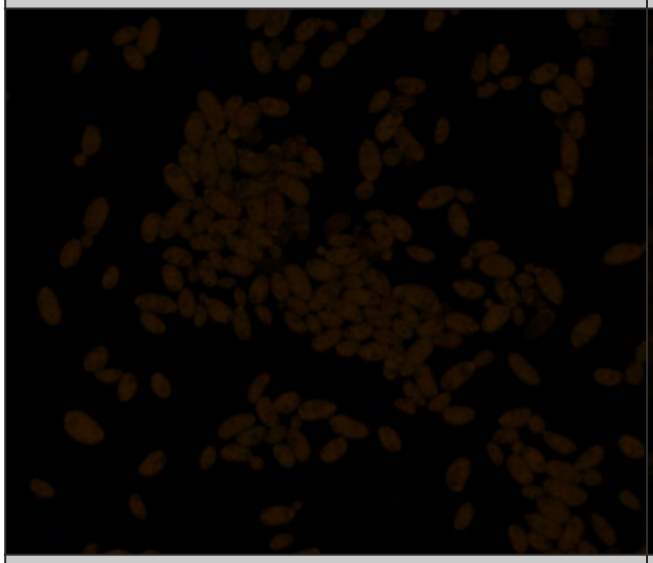	
PDA	**X-AGAR**
	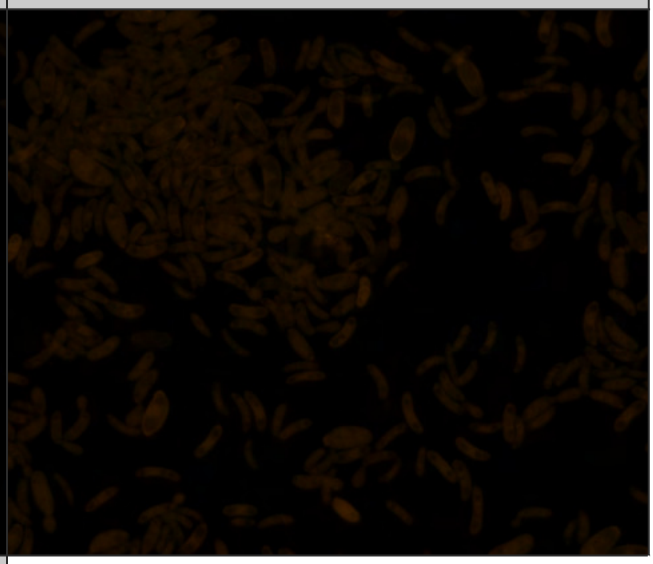
NITROGEN DEPLETED	
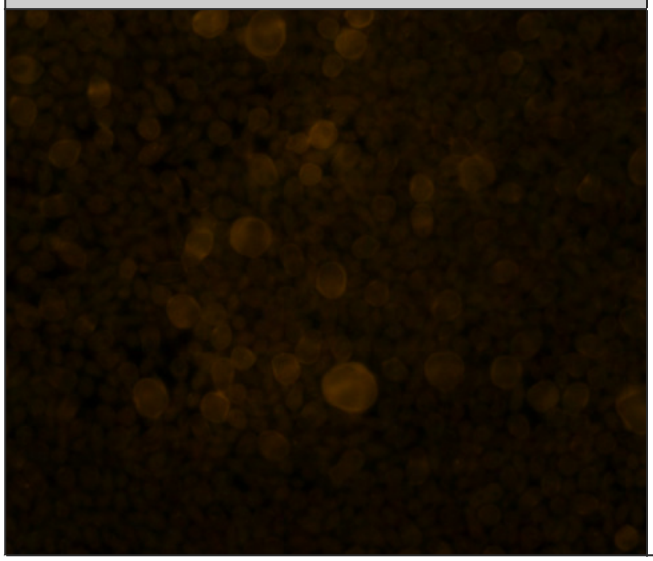	

ID 7149-C1 - Culture Plates	
GYPA	**MEA**
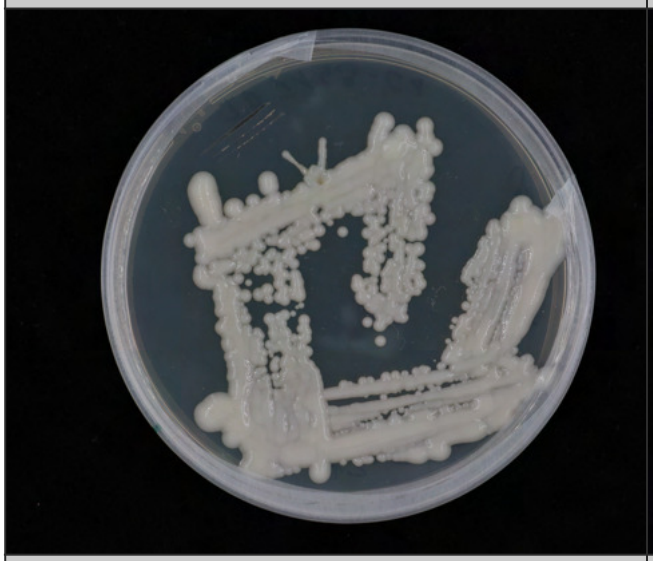	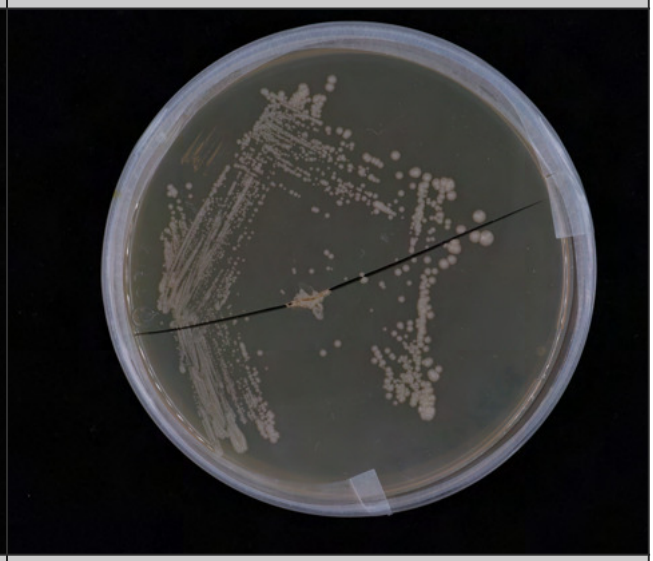
PDA	**X-AGAR**
	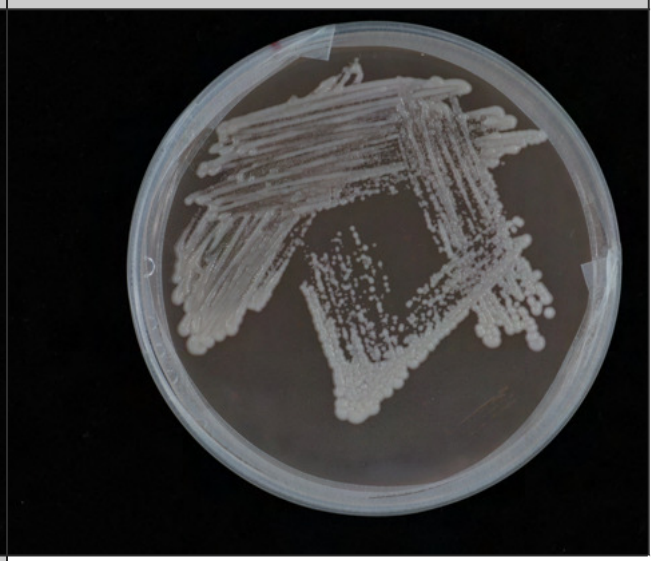
NITROGEN DEPLETED	
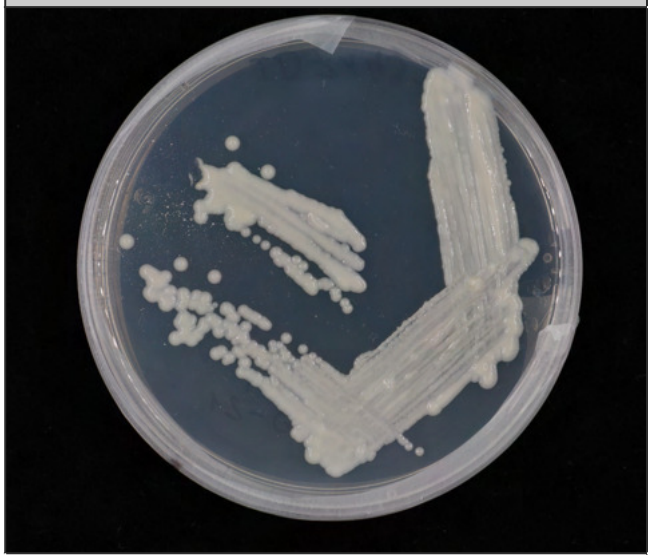	

ID 7149-C1 - Culture Plates

ID 7149-C1 - Microscopy Photographs	
GYPA	**MEA**
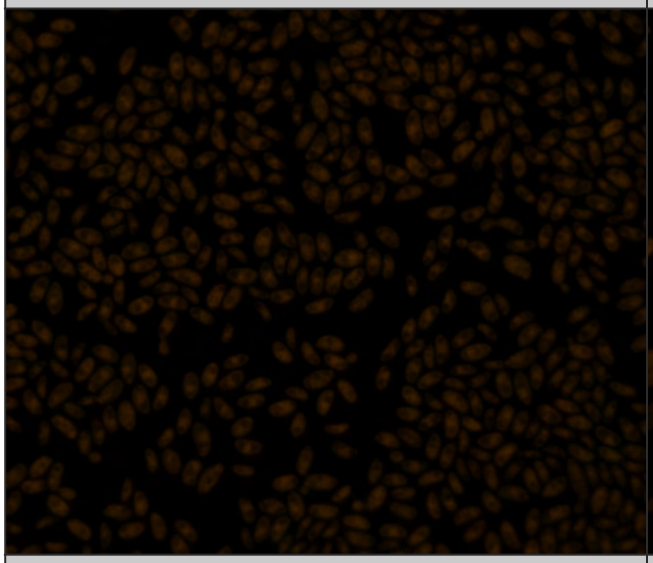	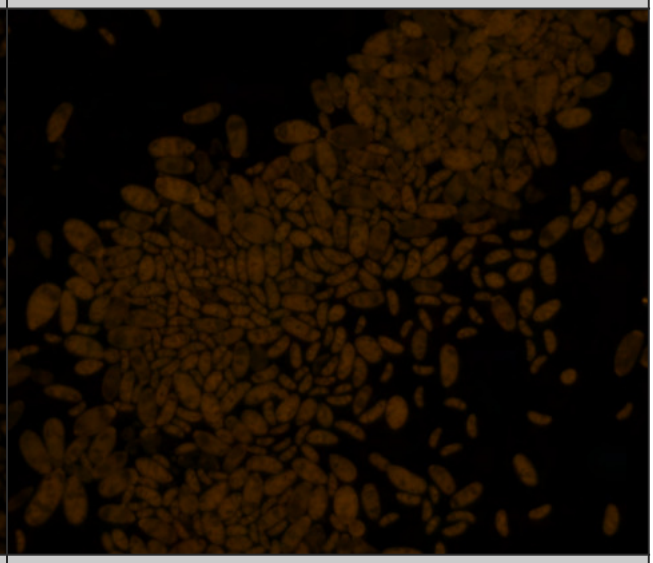
PDA	**X-AGAR**
	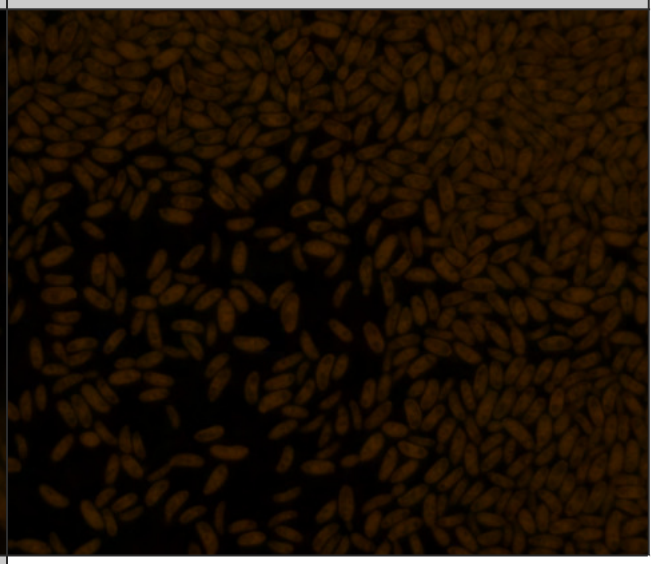
NITROGEN DEPLETED	
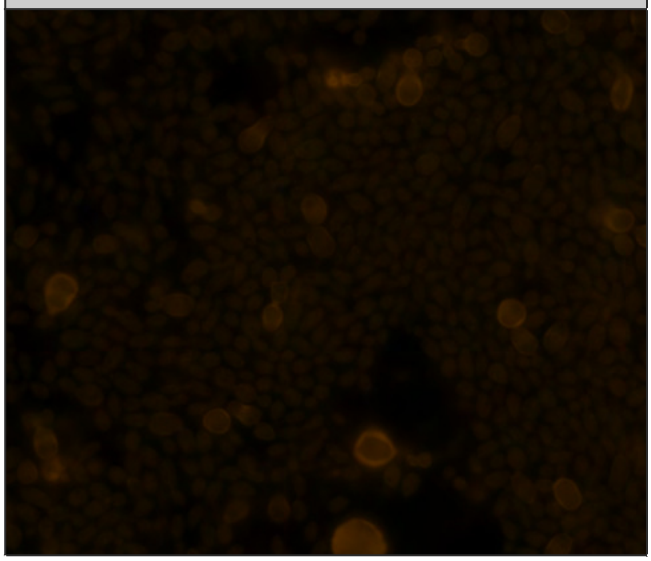	

ID 7149-C1 - Microscopy Photographs

OMC 2212-C2 - Culture Plates	
GYPA	**MEA**
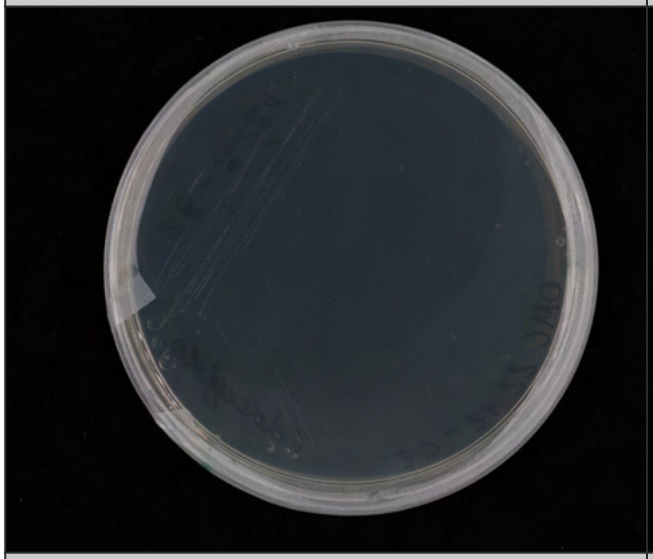	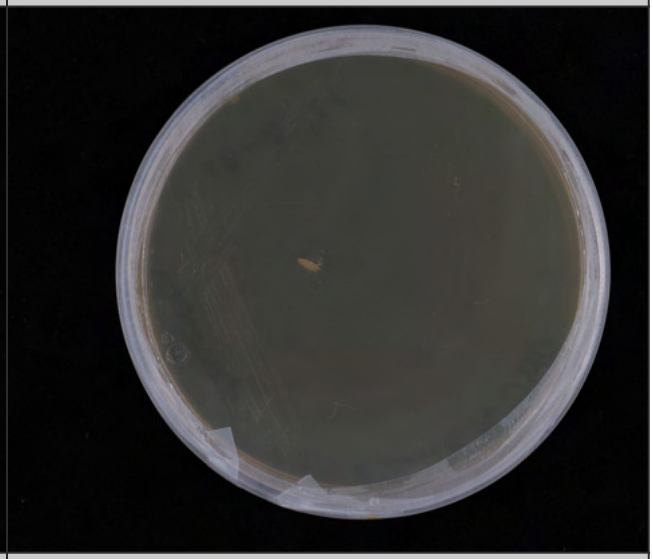
PDA	**X-AGAR**
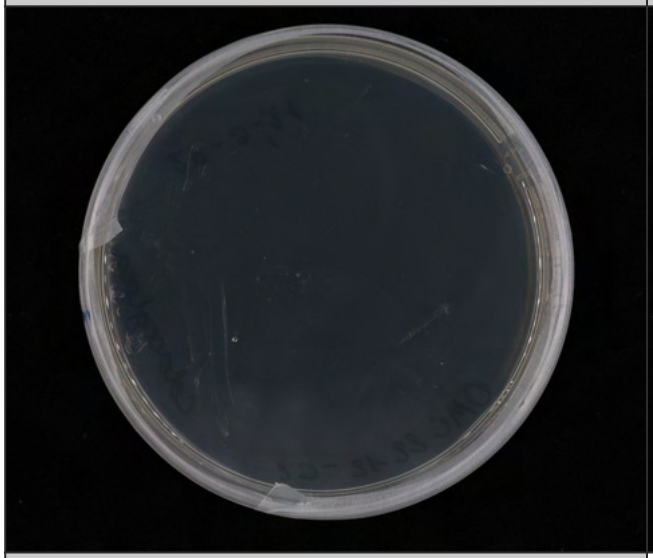	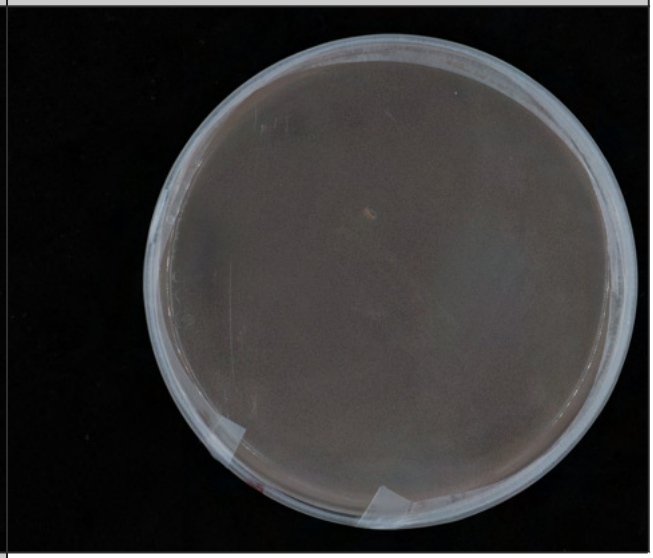
NITROGEN DEPLETED	
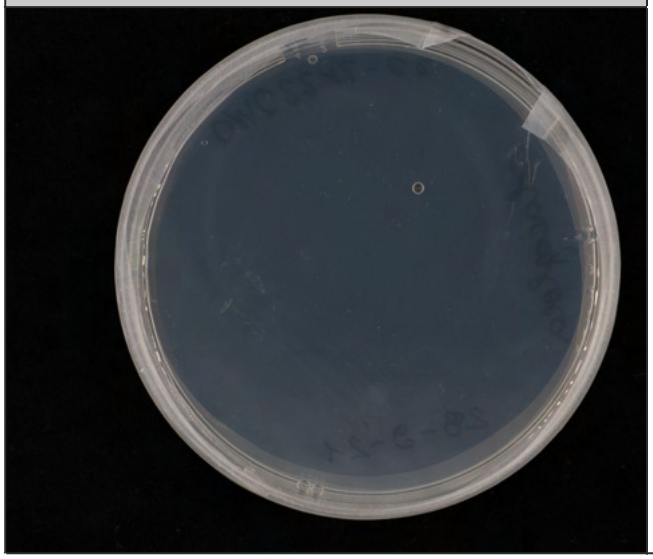	

OMC 2212-C2 - Culture Plates

OMC 2212-C2 - Microscopy Photographs	
GYPA	**MEA**
No growth detected.	No growth detected.
PDA	**X-AGAR**
No growth detected.	No growth detected.
NITROGEN DEPLETED	
No growth detected.	

VS 12415-C1 - Culture Plates	
GYPA	**MEA**
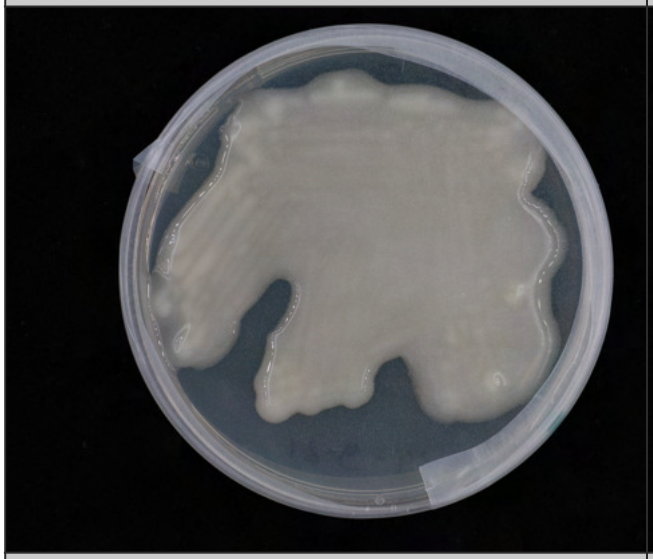	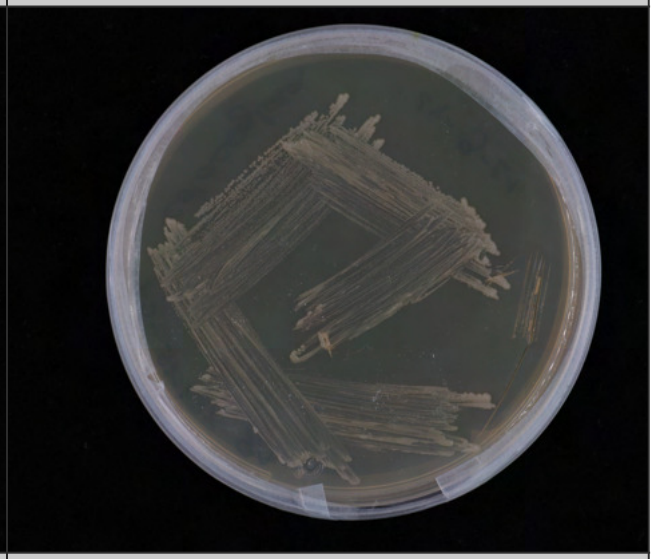
PDA	**X-AGAR**
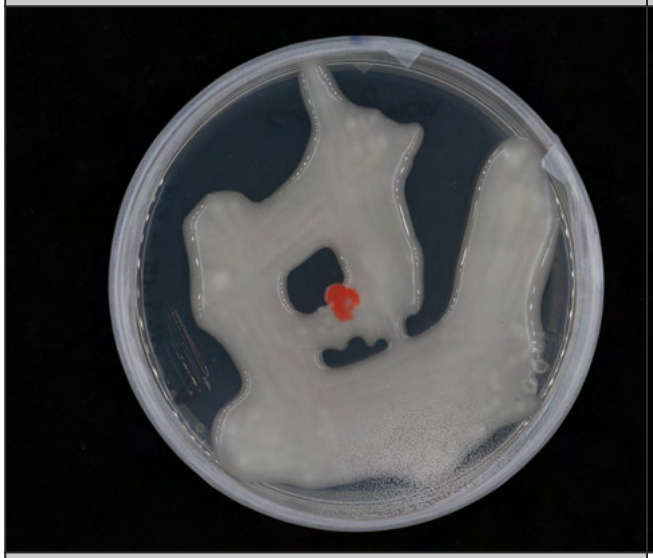	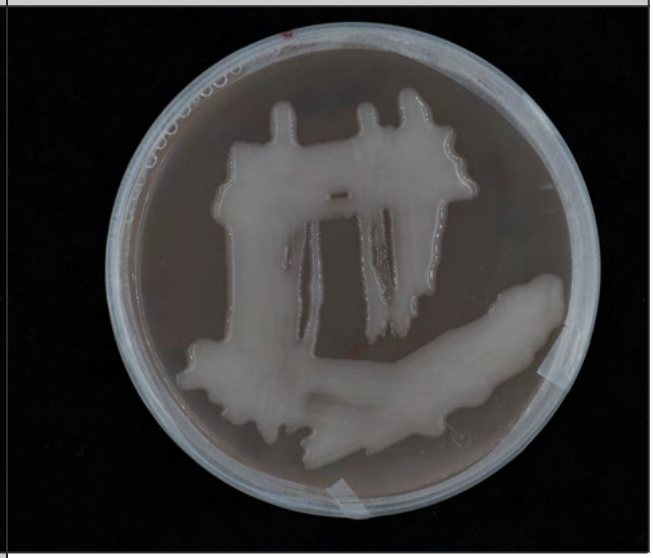
NITROGEN DEPLETED	
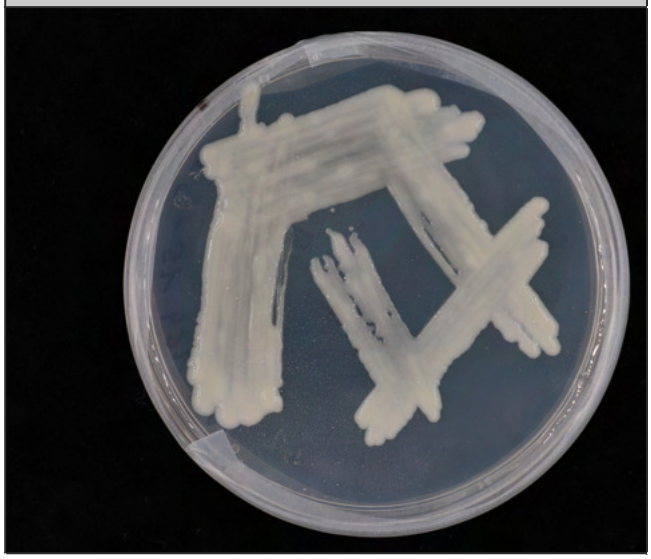	

VS 12415-C1 - Culture Plates

VS 12415-C1 - Microscopy Photographs	
GYPA	**MEA**
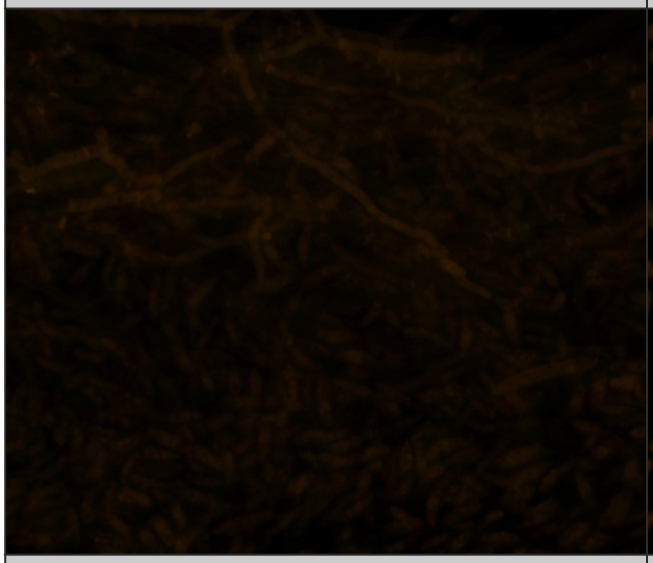	
PDA	**X-AGAR**
	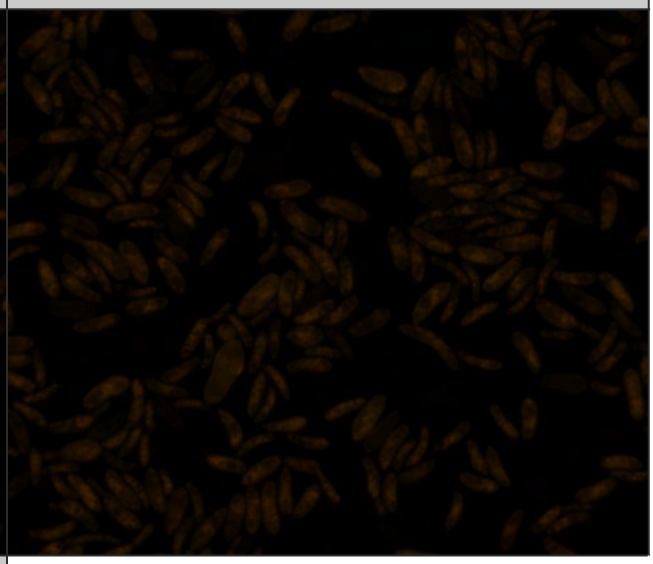
NITROGEN DEPLETED	
	

VS 12415-C1 - Microscopy Photographs

MG 407-C1 - Culture Plates	
GYPA	**MEA**
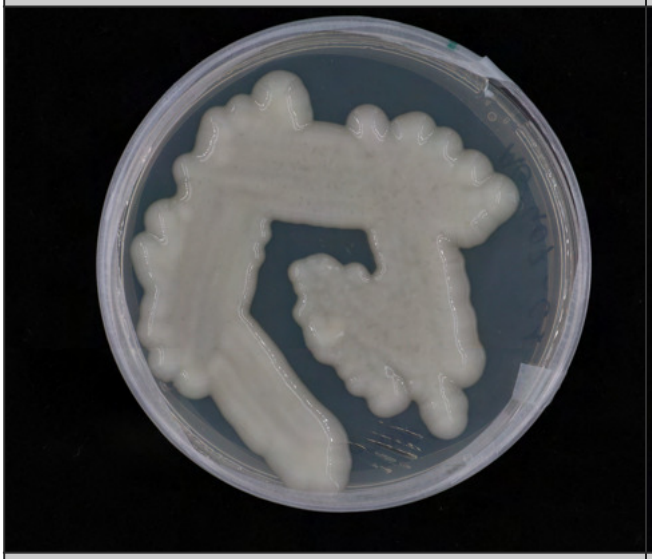	
PDA	**X-AGAR**
	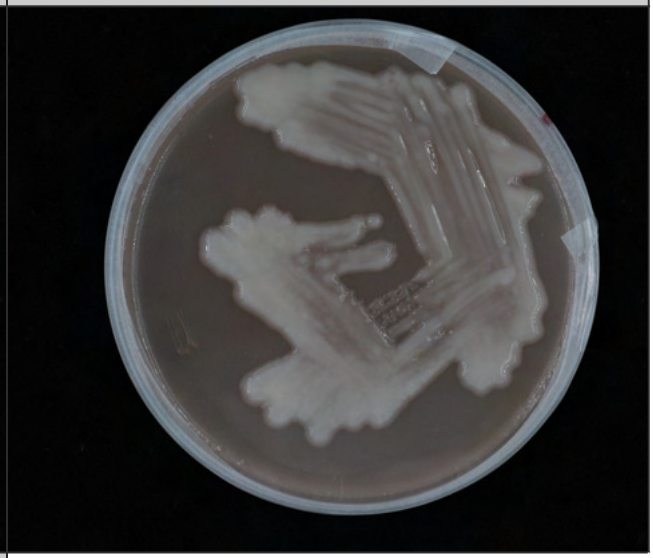
NITROGEN DEPLETED	
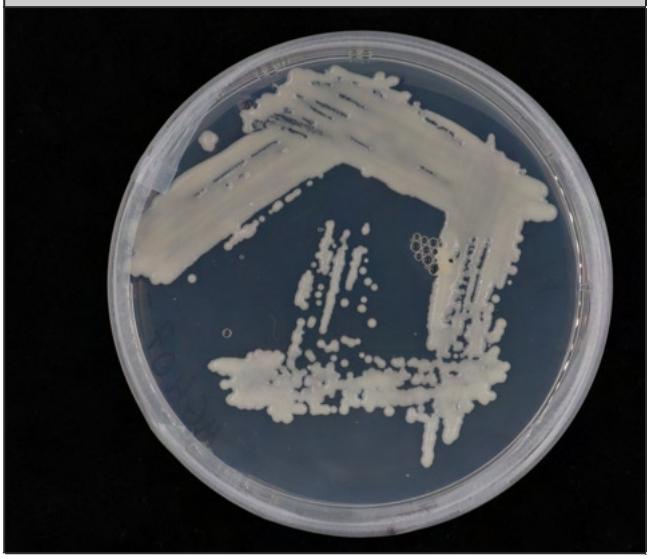	

MG 407-C1 - Culture Plates

MG 407-C1 - Microscopy Photographs	
GYPA	**MEA**
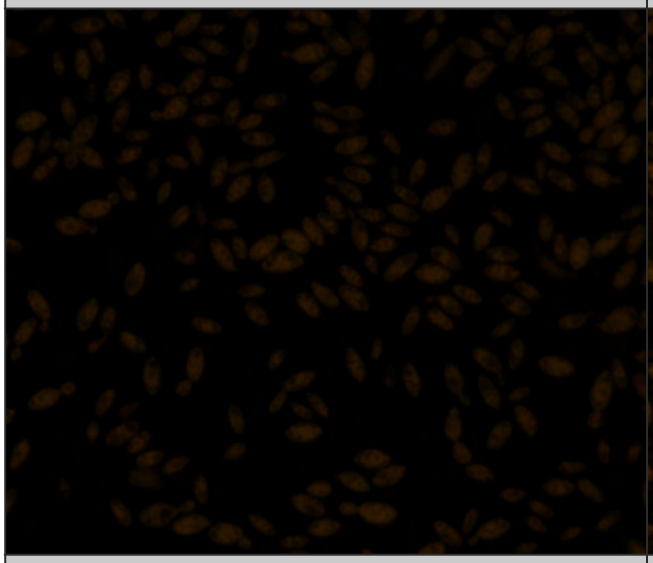	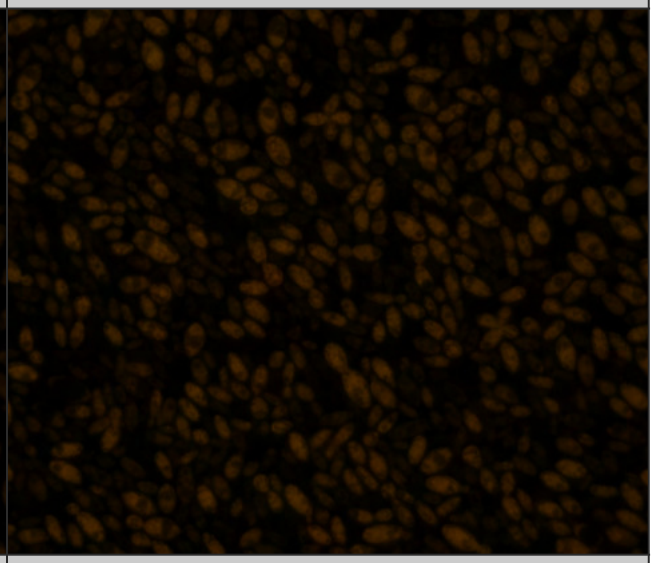
PDA	**X-AGAR**
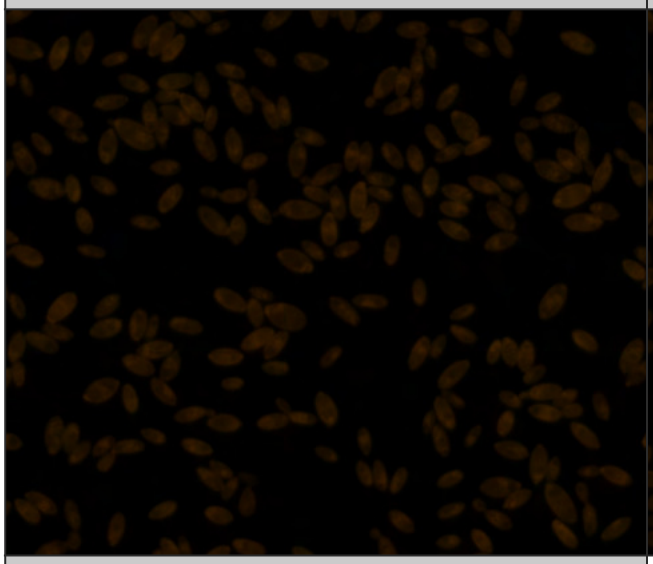	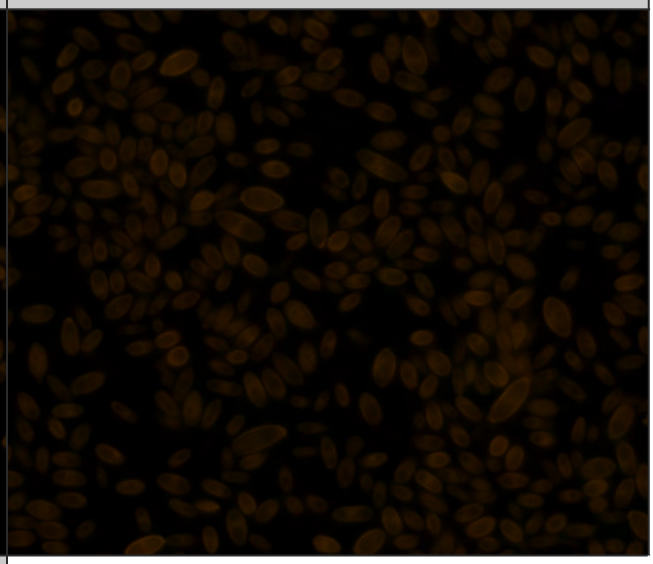
NITROGEN DEPLETED	
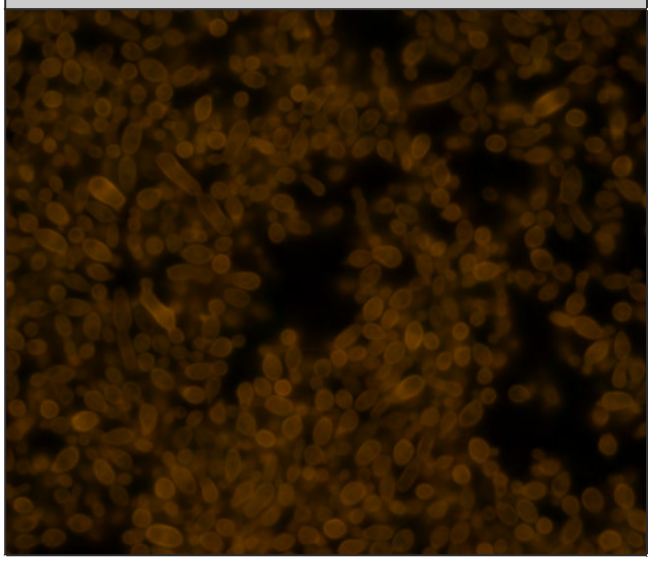	

MG 407-C1 - Microscopy Photographs

MG 438-C2 - Culture Plates	
GYPA	**MEA**
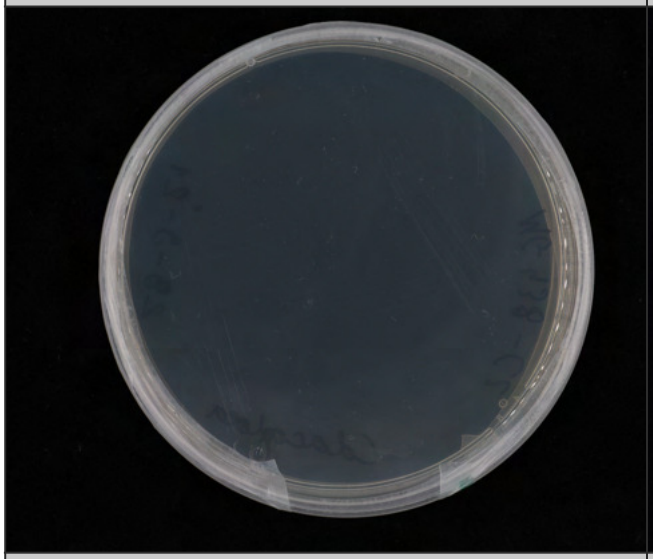	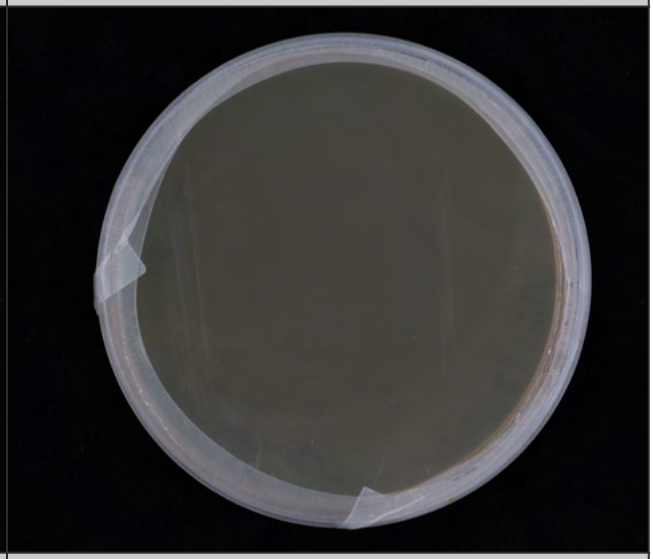
PDA	**X-AGAR**
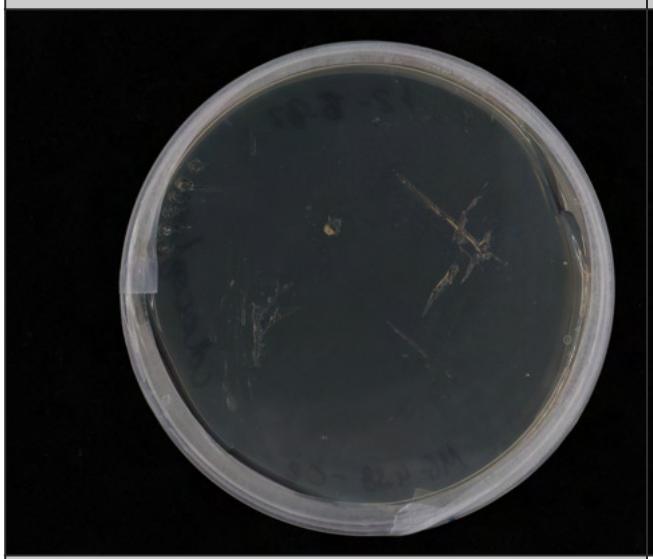	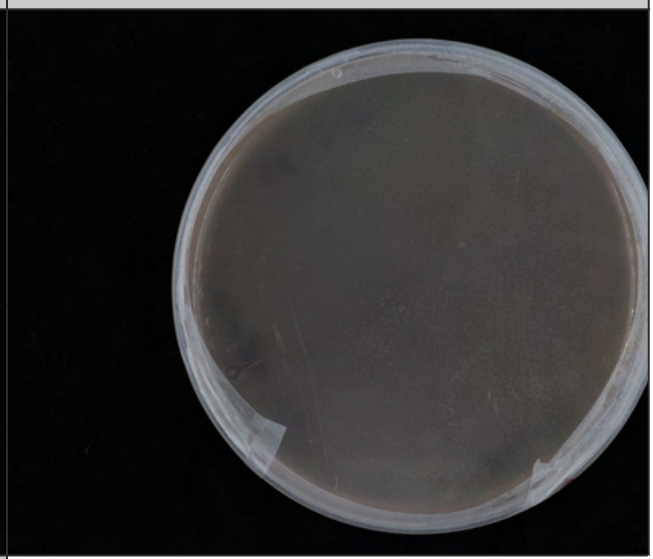
NITROGEN DEPLETED	
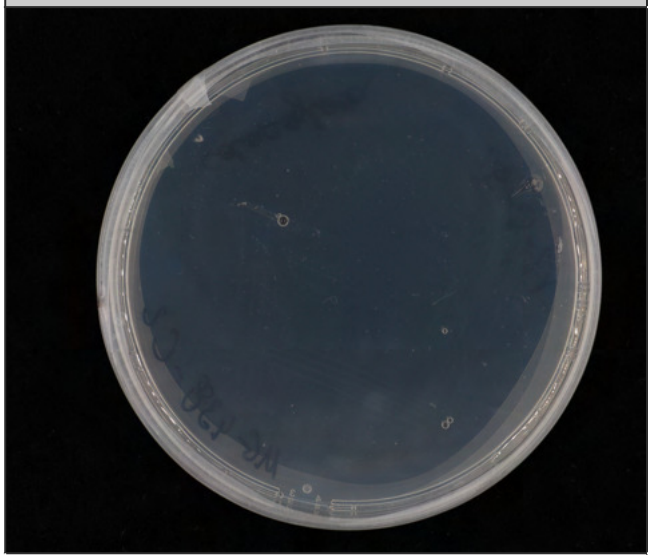	

MG 438-C2 - Culture Plates

MG 438-C2 - Microscopy Photographs	
GYPA	**MEA**
No growth detected.	No growth detected.
PDA	**X-AGAR**
No growth detected.	No growth detected.
NITROGEN DEPLETED	
No growth detected.	

MG 438-C2 - Microscopy Photographs

IS 20-006-C1 - Culture Plates	
GYPA	**MEA**
	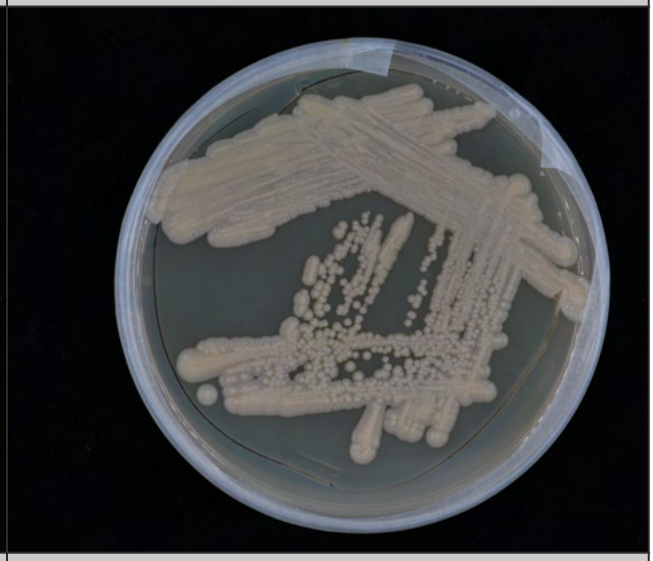
PDA	**X-AGAR**
	
NITROGEN DEPLETED	
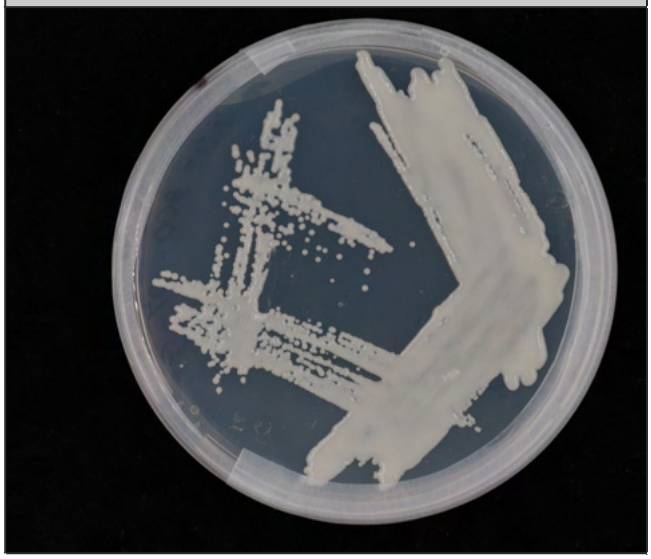	

IS 20-006-C1 - Culture Plates

IS 20-006-C1 - Microscopy Photographs	
GYPA	**MEA**
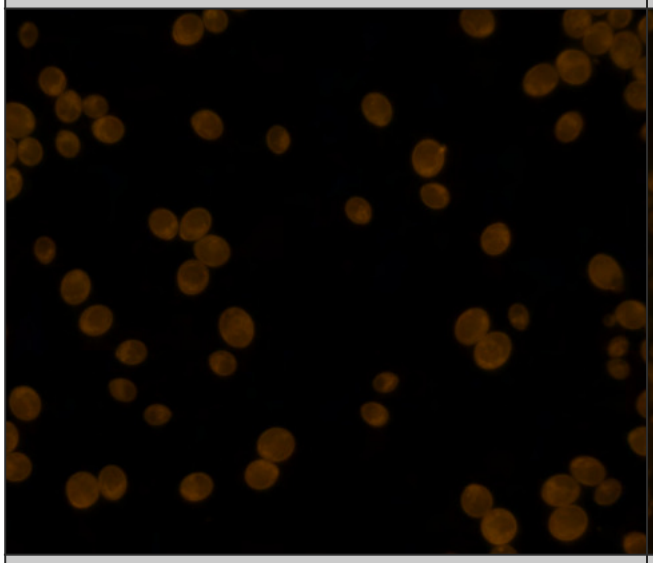	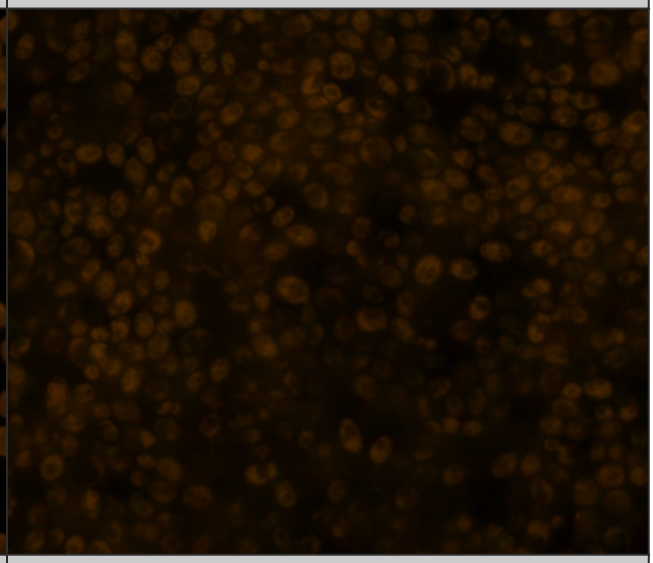
PDA	**X-AGAR**
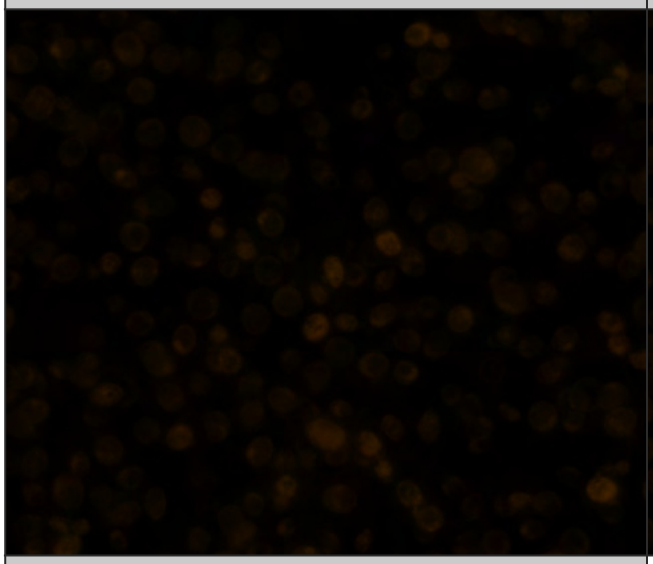	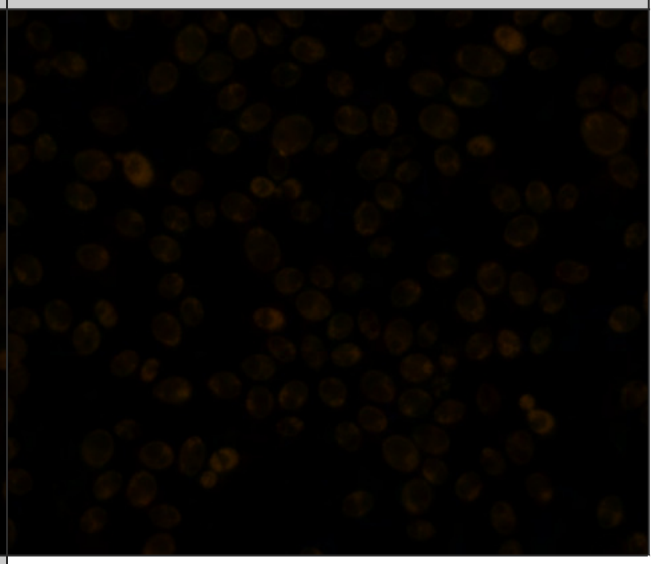
NITROGEN DEPLETED	
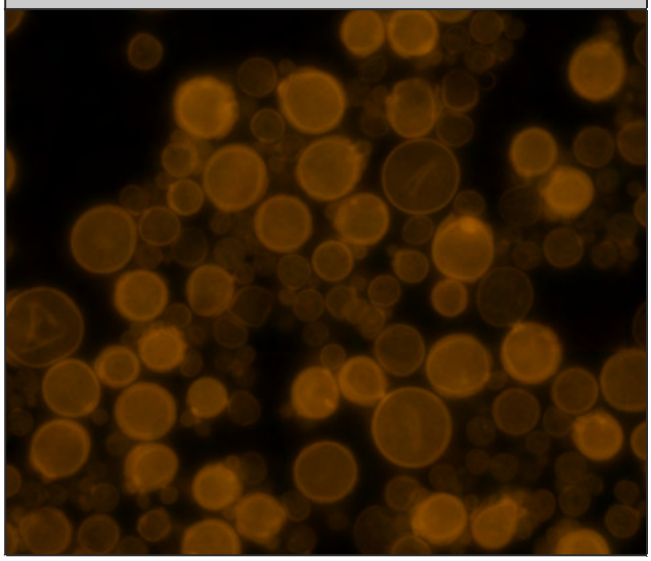	

IS 20-006-C1 - Microscopy Photographs

HW 347-C1 - Culture Plates	
GYPA	**MEA**
	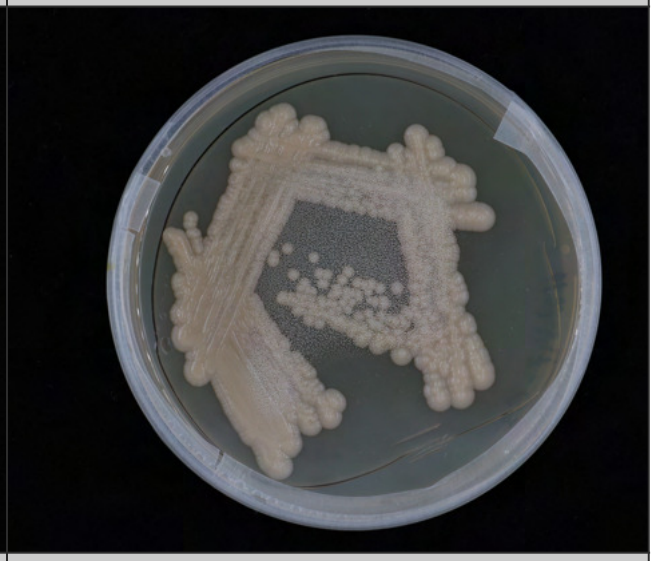
PDA	**X-AGAR**
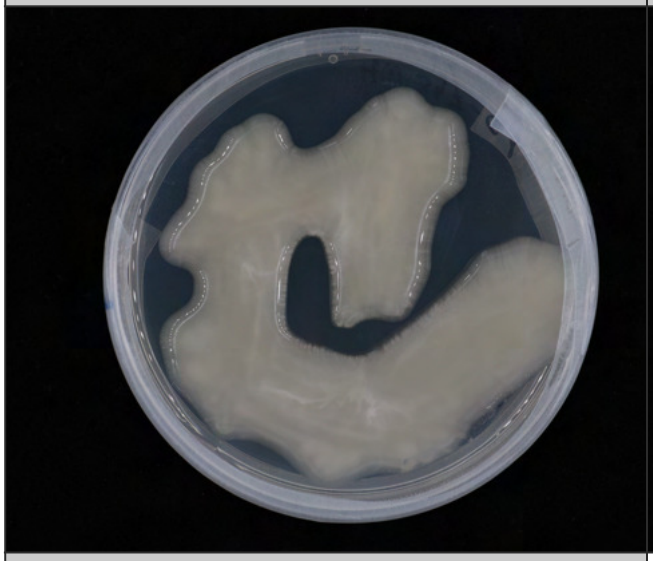	
NITROGEN DEPLETED	
	

HW 347-C1 - Culture Plates

HW 347-C1 - Microscopy Photographs	
GYPA	**MEA**
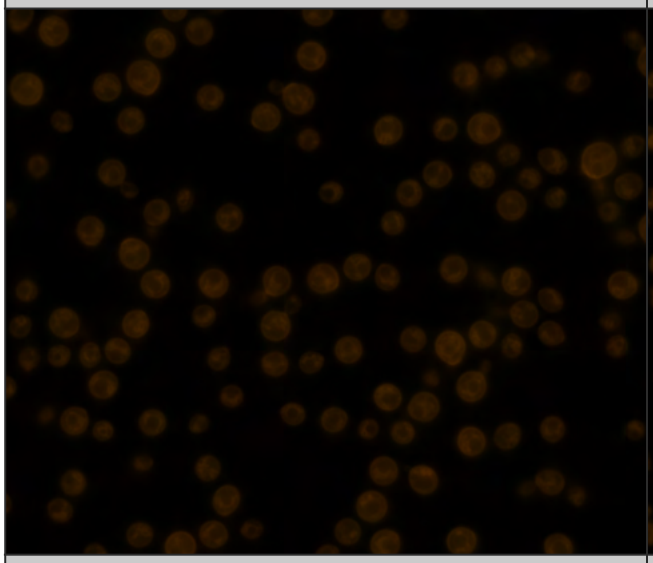	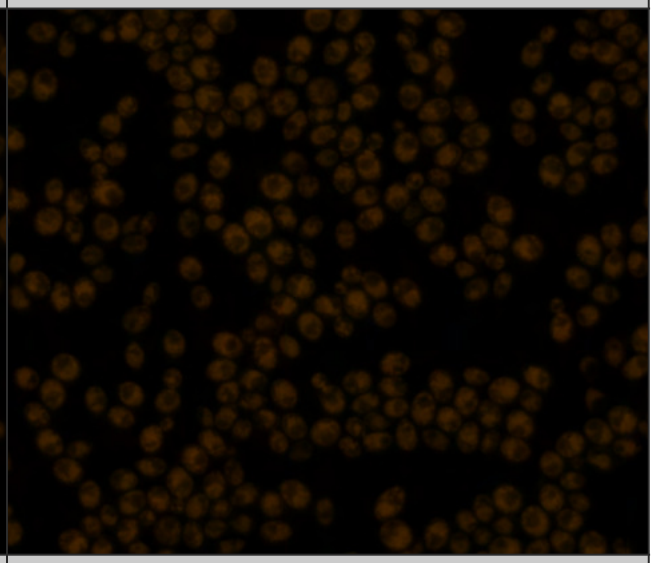
PDA	**X-AGAR**
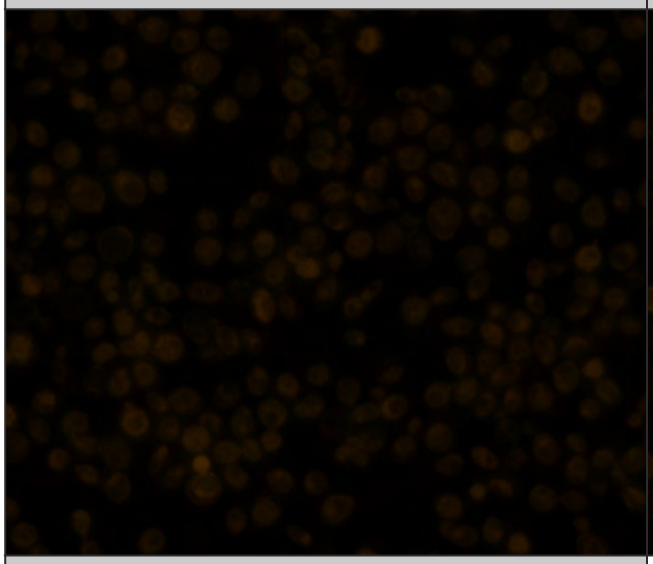	
NITROGEN DEPLETED	
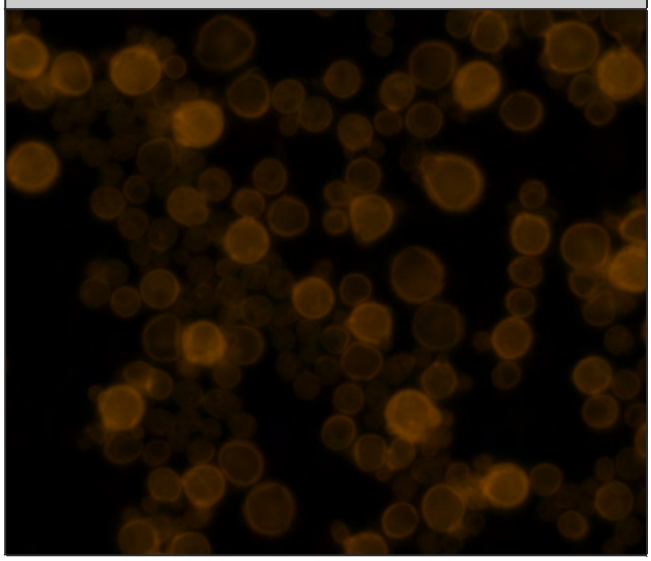	

HW 347-C1 - Microscopy Photographs

TR 04096-C1 - Culture Plates	
GYPA	**MEA**
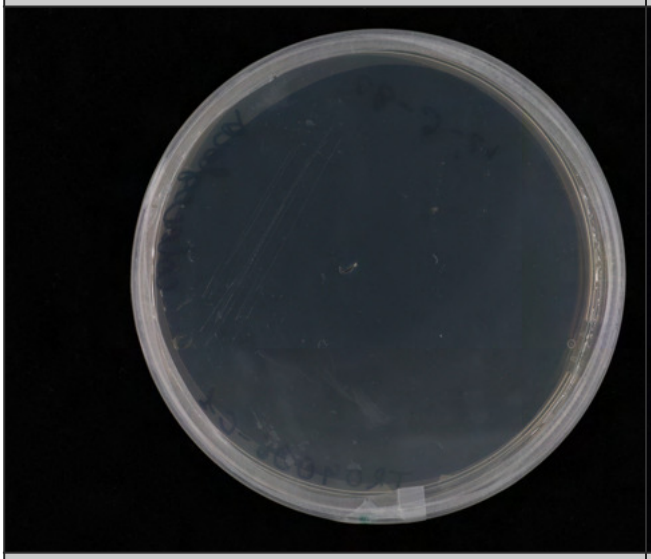	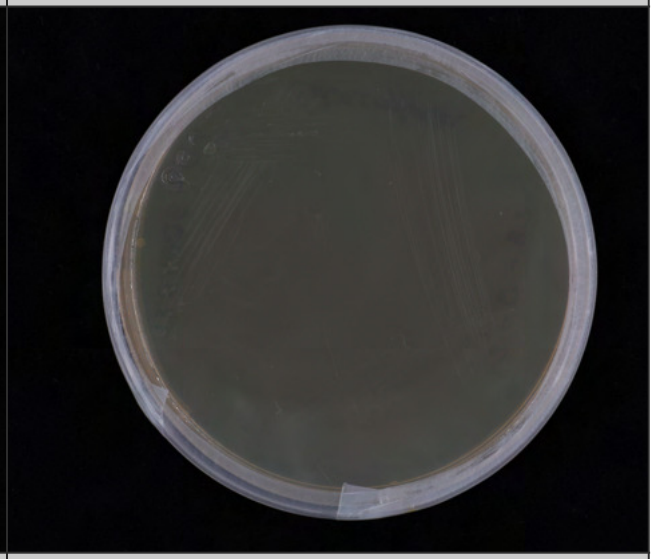
PDA	**X-AGAR**
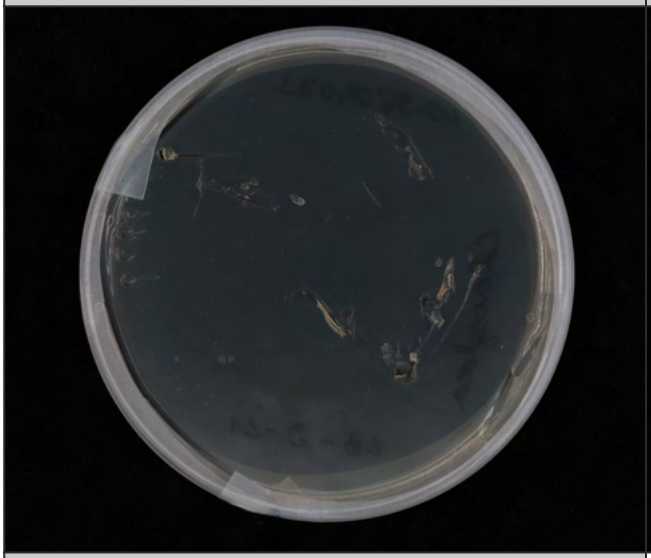	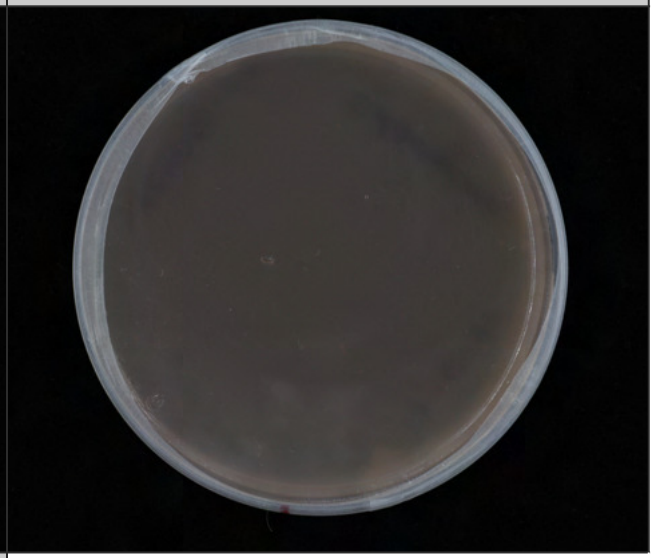
NITROGEN DEPLETED	
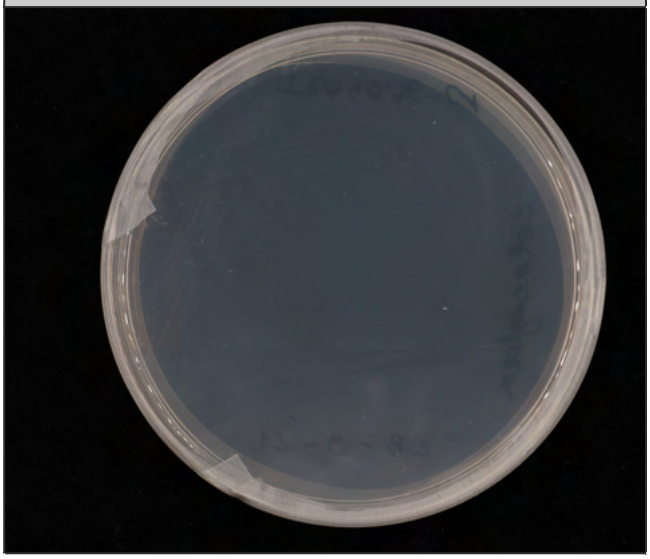	

TR 04096-C1 - Culture Plates

TR 04096-C1 - Microscopy Photographs	
GYPA	**MEA**
No growth detected.	No growth detected.
PDA	**X-AGAR**
No growth detected.	No growth detected.
NITROGEN DEPLETED	
No growth detected.	

CBS 149.68 - Culture Plates	
GYPA	**MEA**
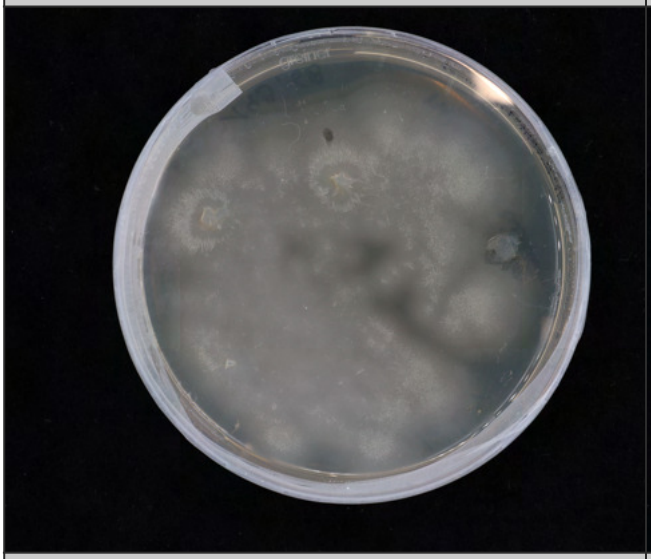	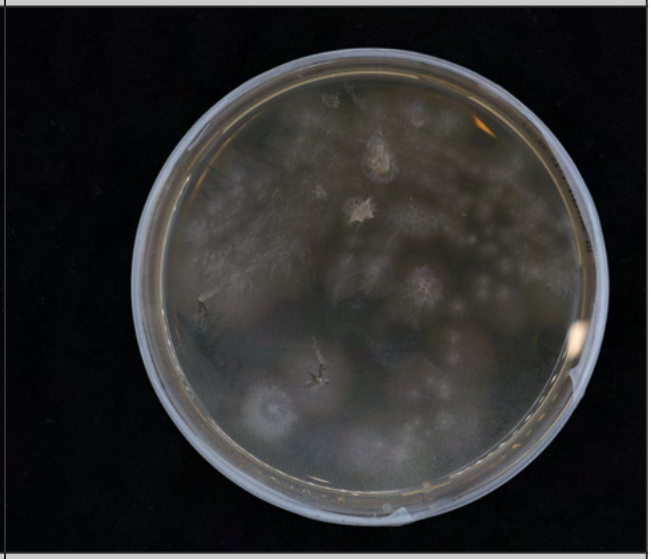
PDA	**X-AGAR**
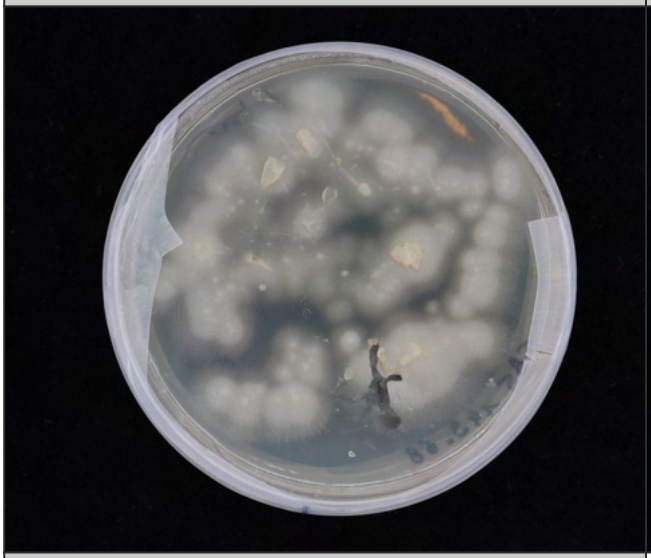	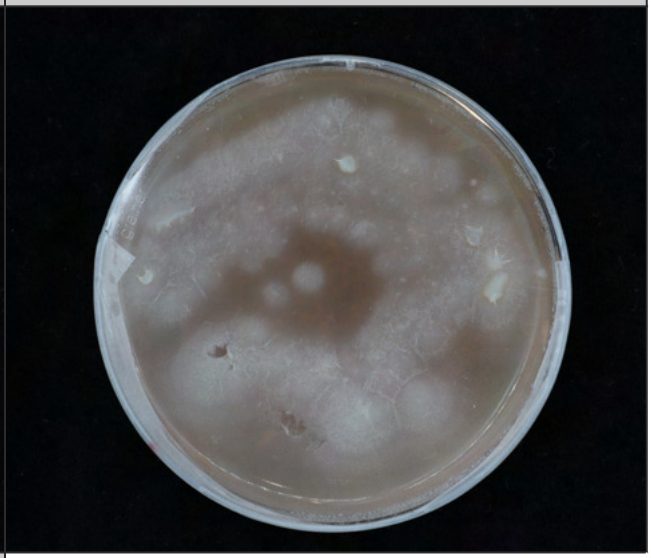
NITROGEN DEPLETED	
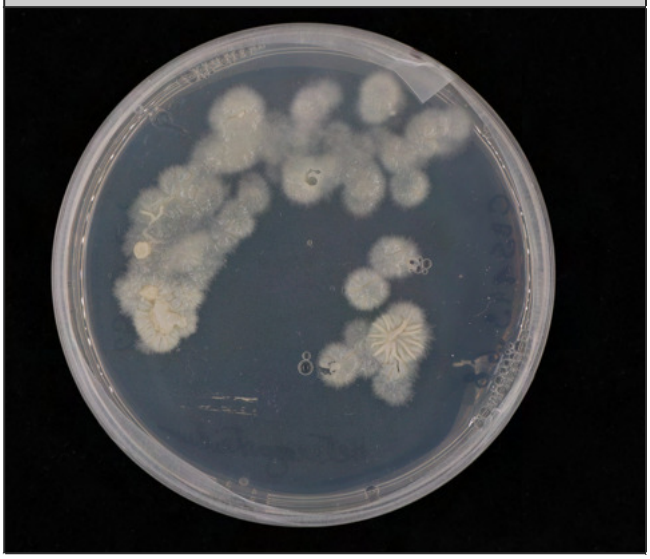	

CBS 149.68 - Culture Plates

CBS 149.68 - Microscopy Photographs	
GYPA	**MEA**
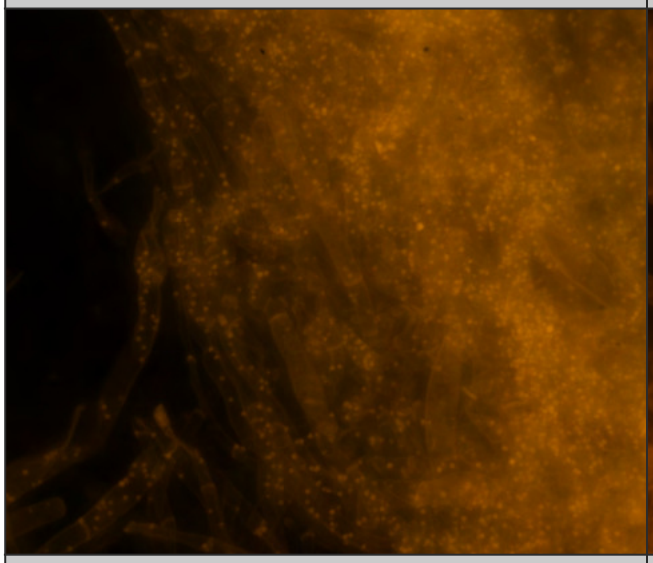	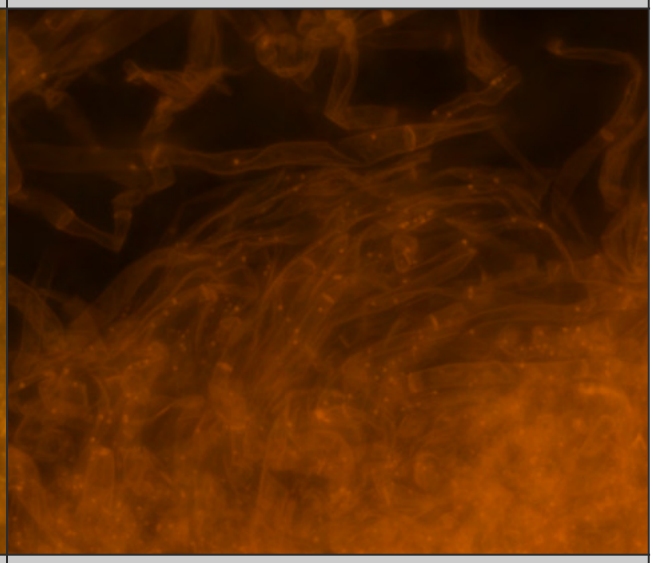
PDA	**X-AGAR**
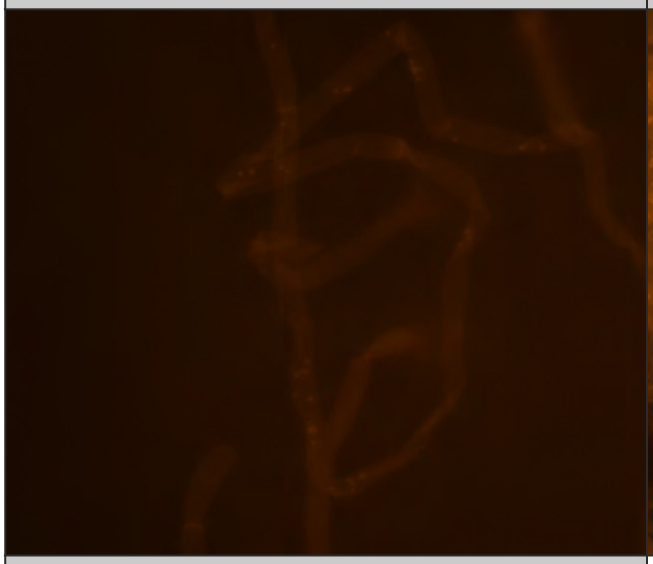	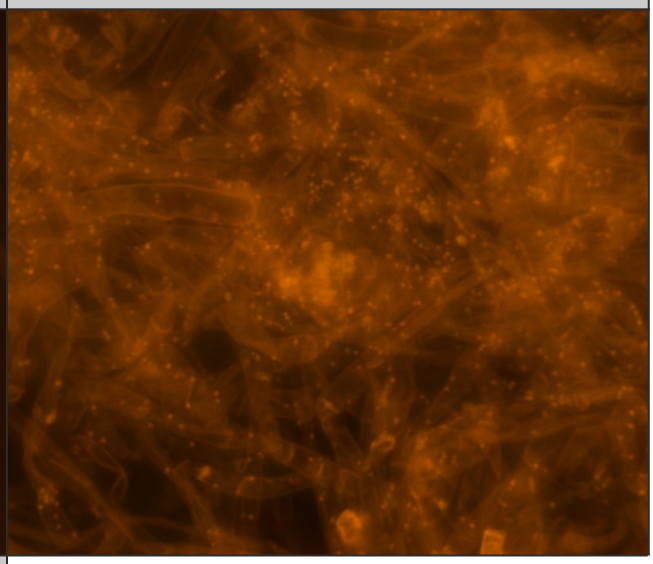
NITROGEN DEPLETED	
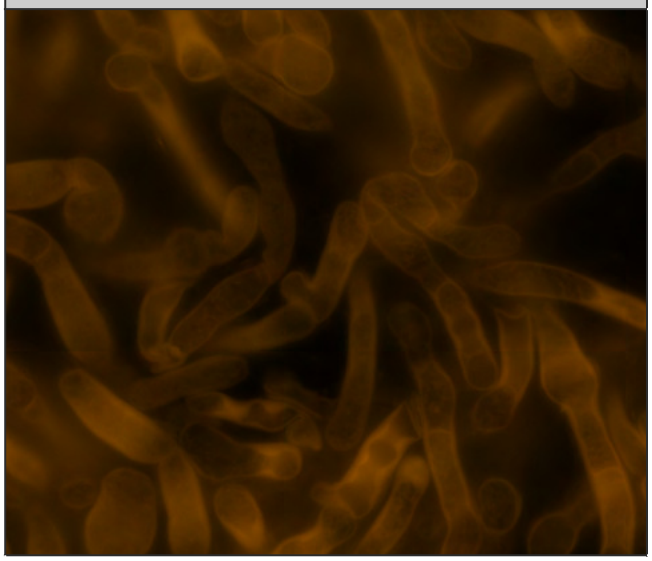	

CBS 149.68 - Microscopy Photographs

CBS 953.73 - Culture Plates	
GYPA	**MEA**
	
PDA	**X-AGAR**
	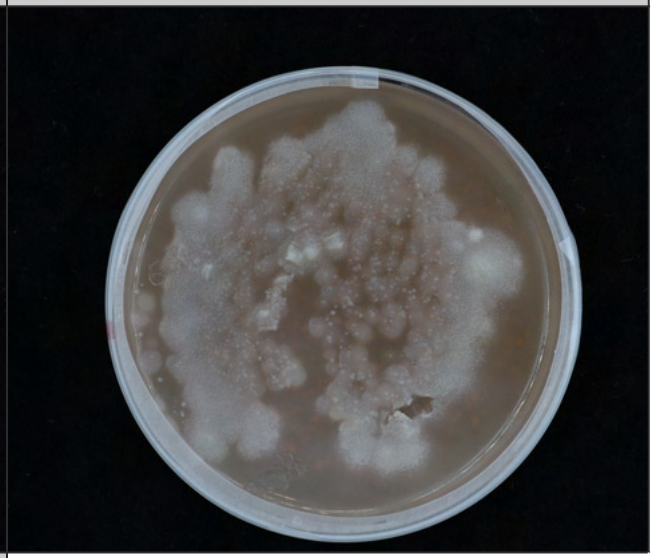
NITROGEN DEPLETED	
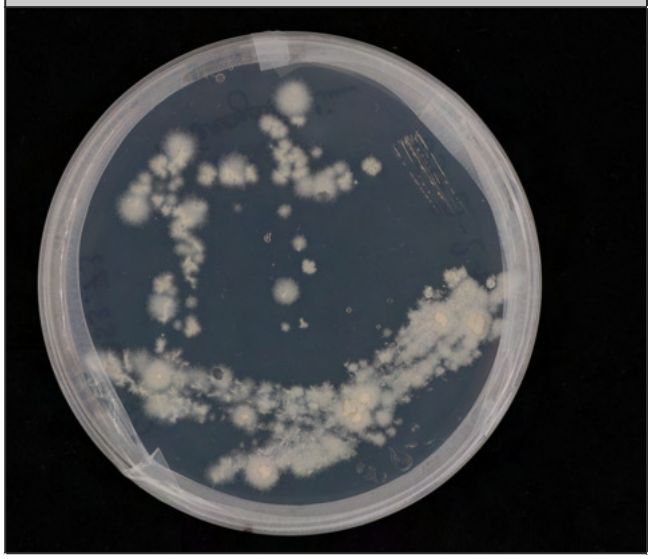	

CBS 953.73 - Culture Plates

CBS 953.73 - Microscopy Photographs	
GYPA	**MEA**
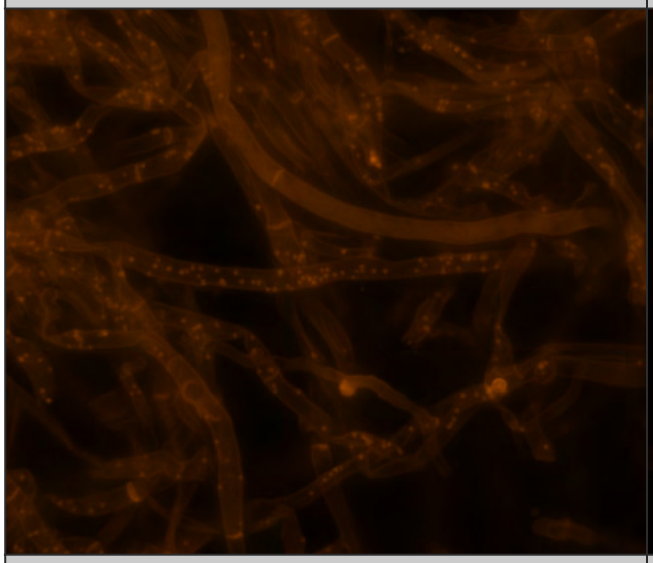	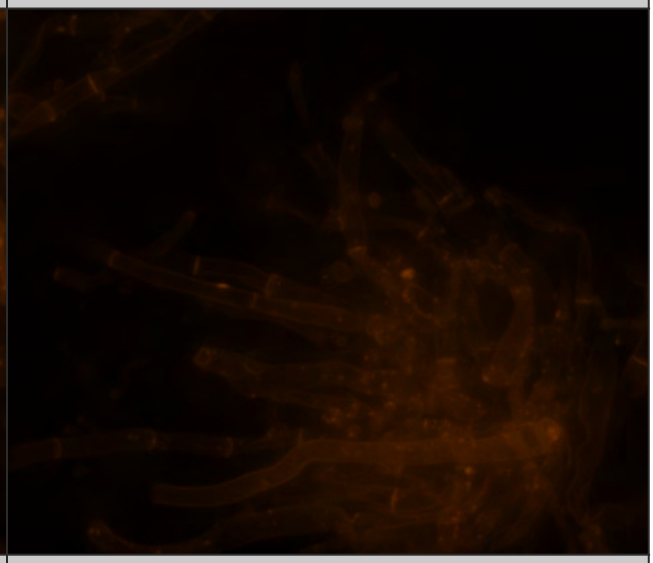
PDA	**X-AGAR**
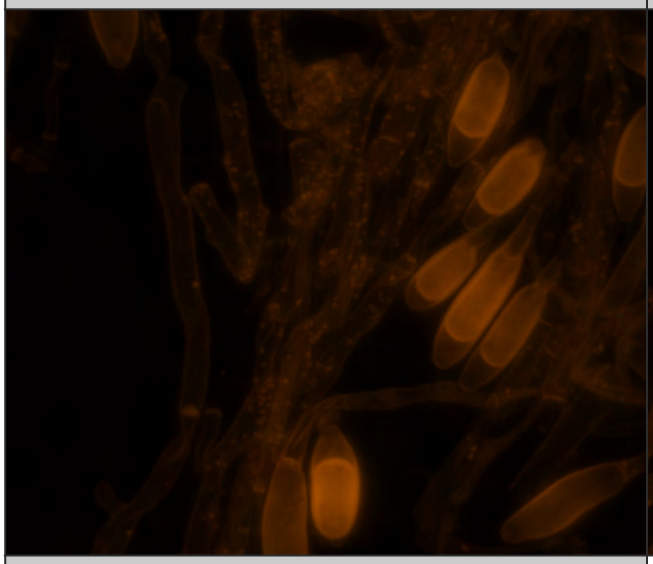	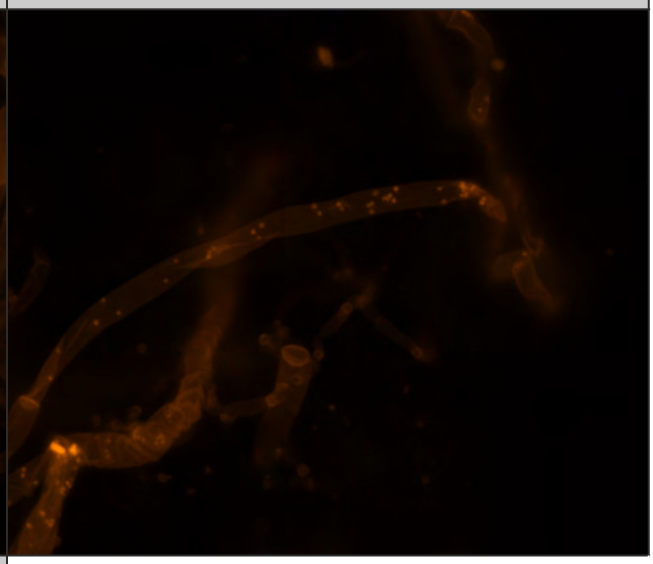
NITROGEN DEPLETED	
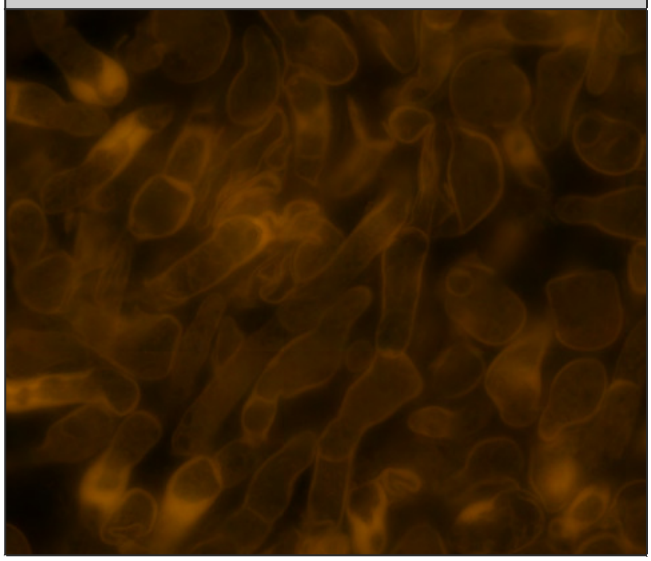	

CBS 953.73 - Microscopy Photographs

CBS 582.80 - Culture Plates	
GYPA	**MEA**
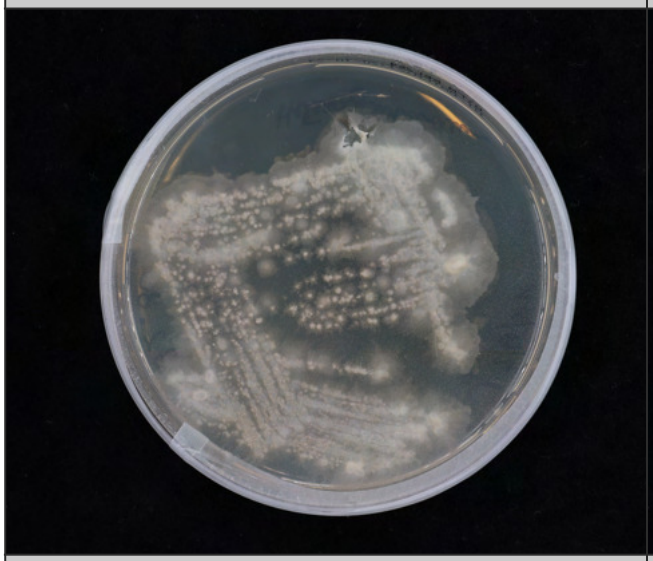	
PDA	**X-AGAR**
	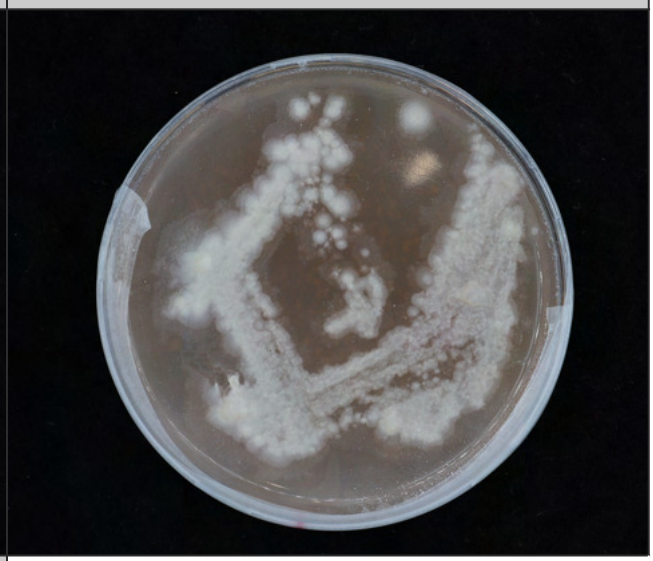
NITROGEN DEPLETED	
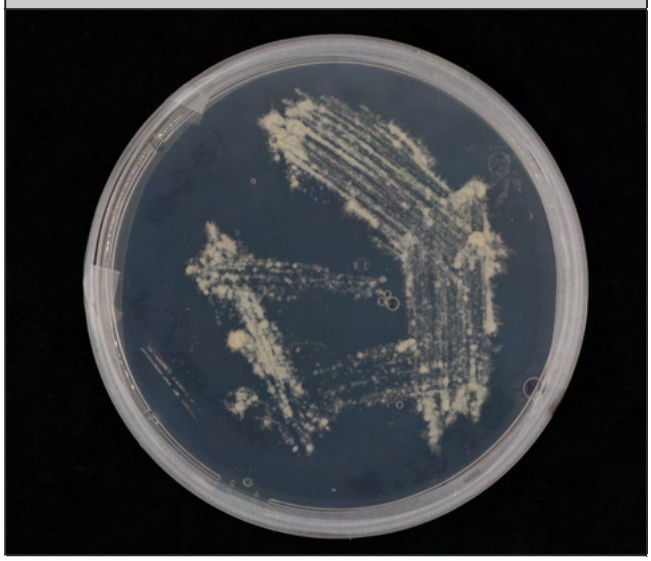	

CBS 582.80 - Culture Plates

CBS 582.80 - Microscopy Photographs	
GYPA	**MEA**
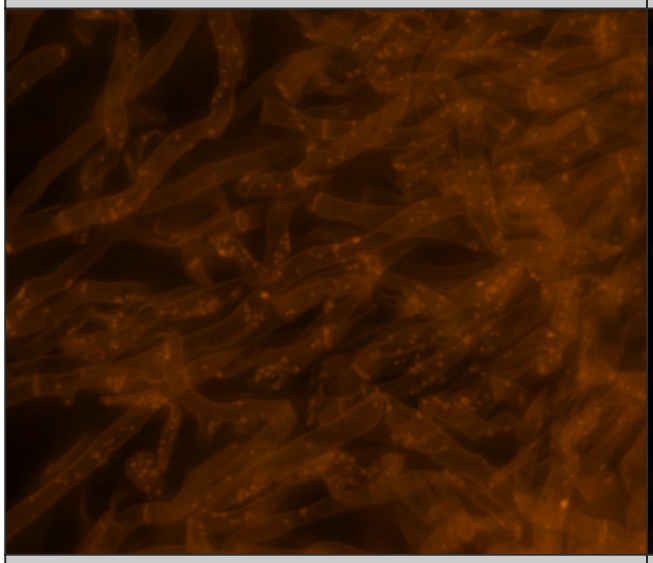	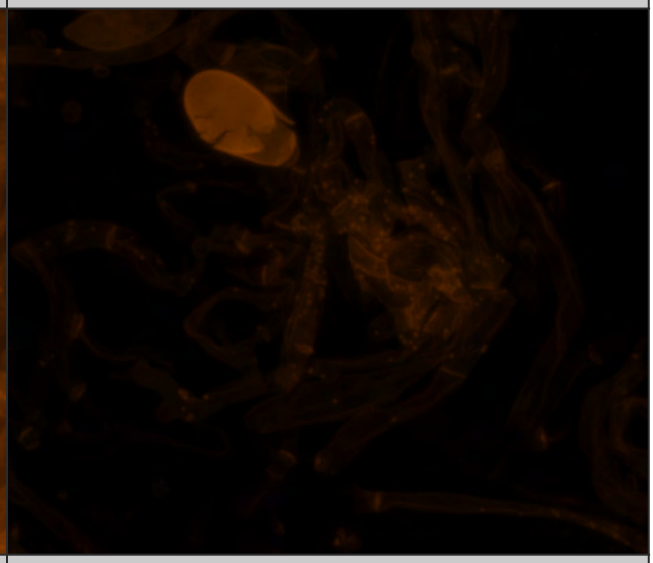
PDA	**X-AGAR**
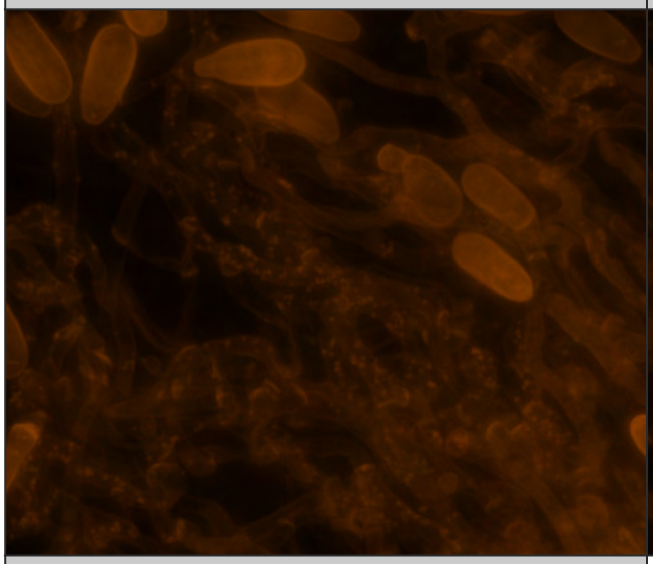	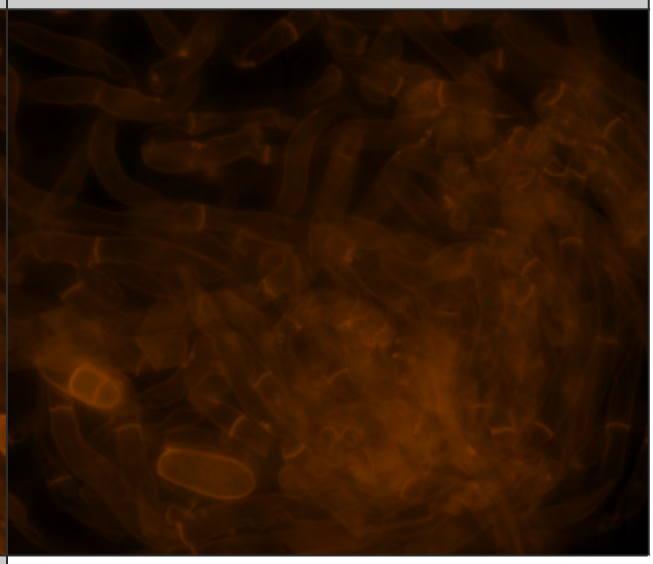
NITROGEN DEPLETED	
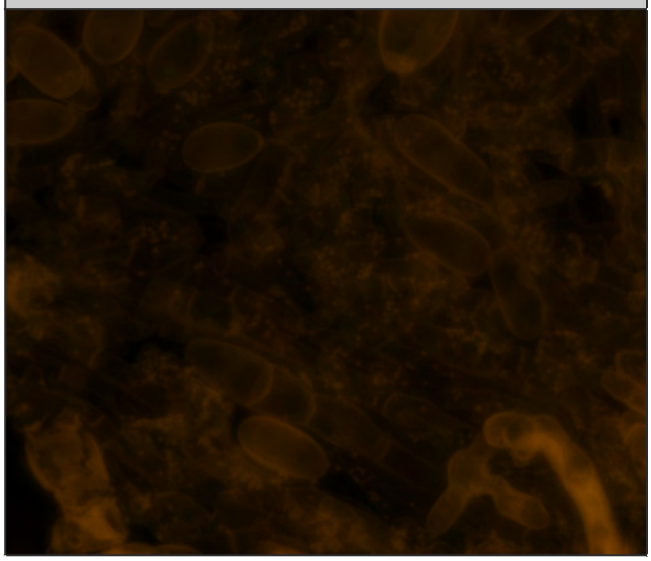	

CBS 582.80 - Microscopy Photographs

CBS 587.93 - Culture Plates	
GYPA	**MEA**
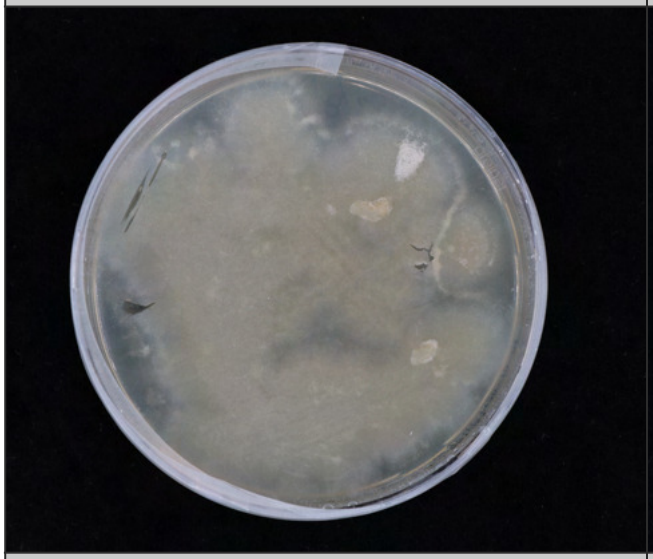	
PDA	**X-AGAR**
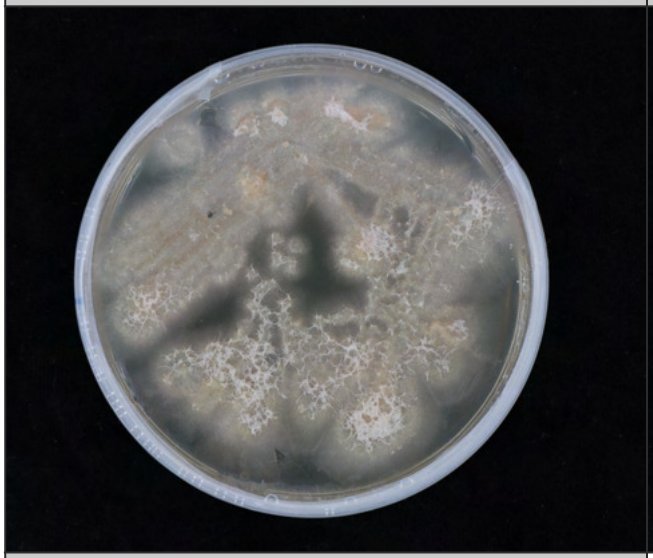	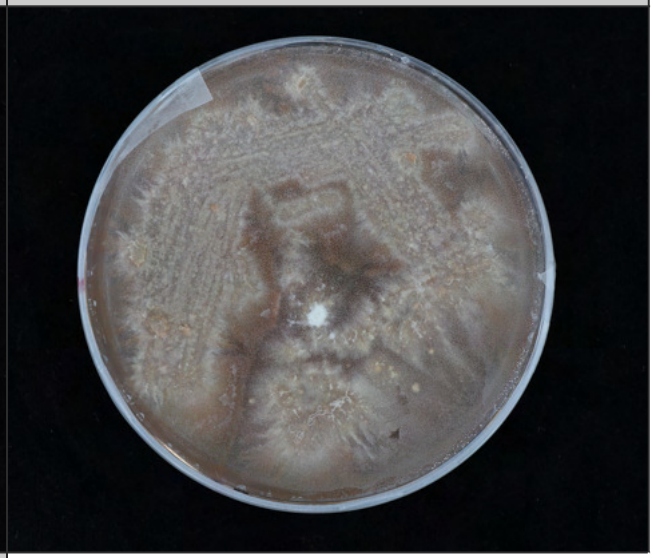
NITROGEN DEPLETED	
	

CBS 587.93 - Culture Plates

CBS 587.93 - Microscopy Photographs	
GYPA	**MEA**
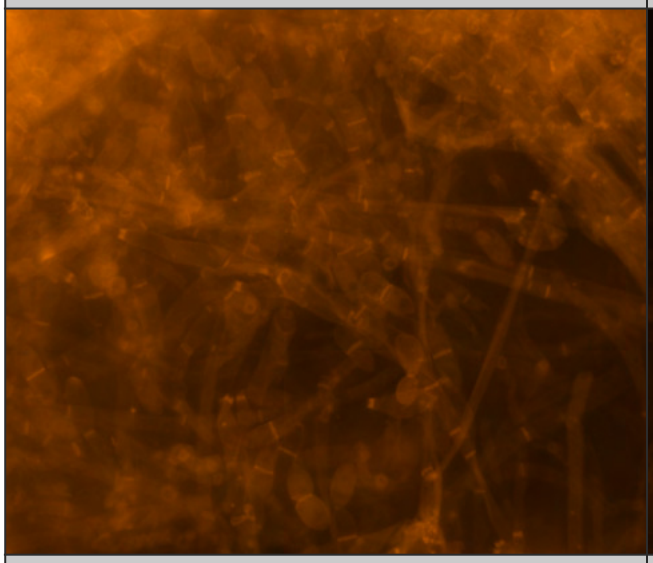	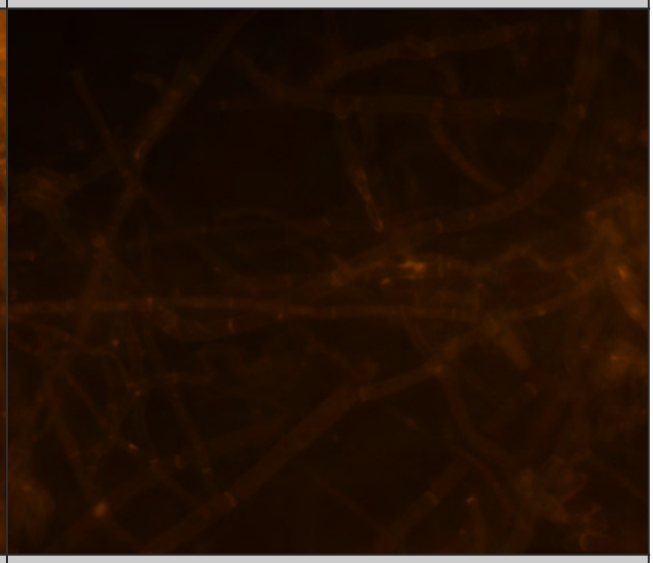
PDA	**X-AGAR**
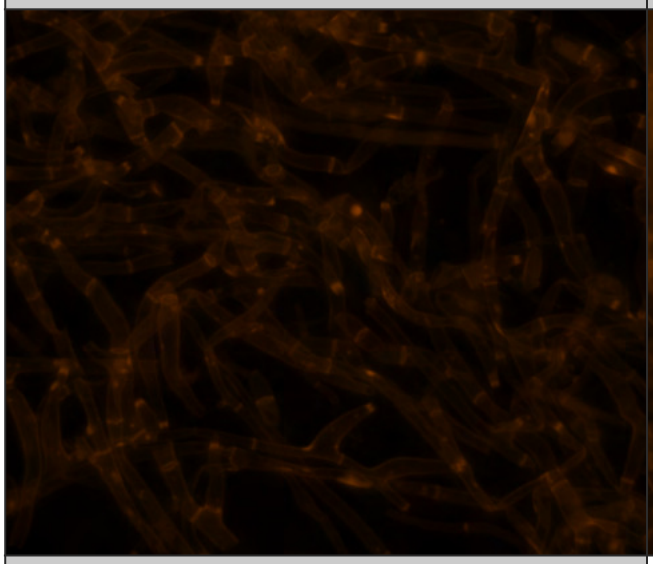	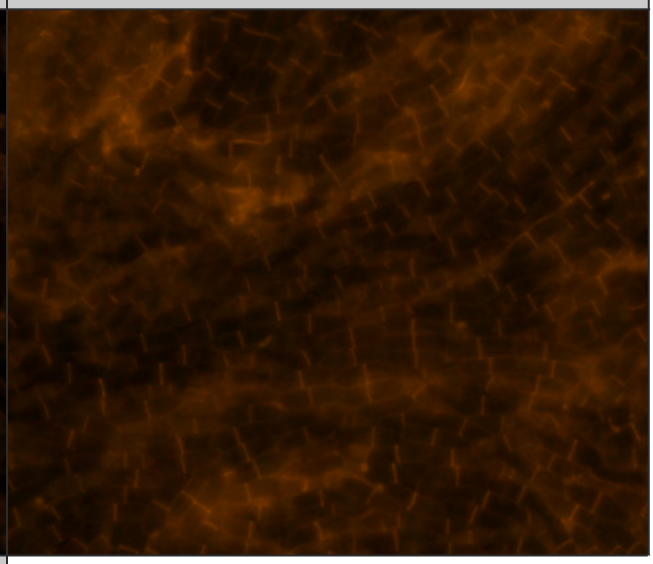
NITROGEN DEPLETED	
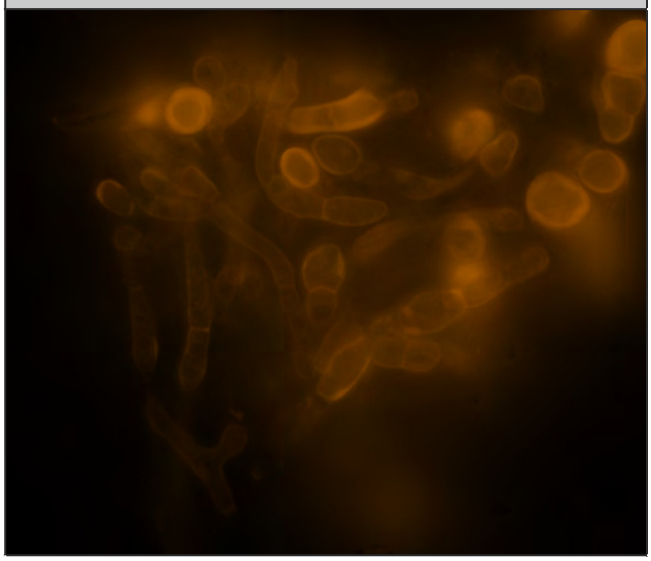	

CBS 587.93 - Microscopy Photographs

CBS 590.93 - Culture Plates	
GYPA	**MEA**
	
PDA	**X-AGAR**
	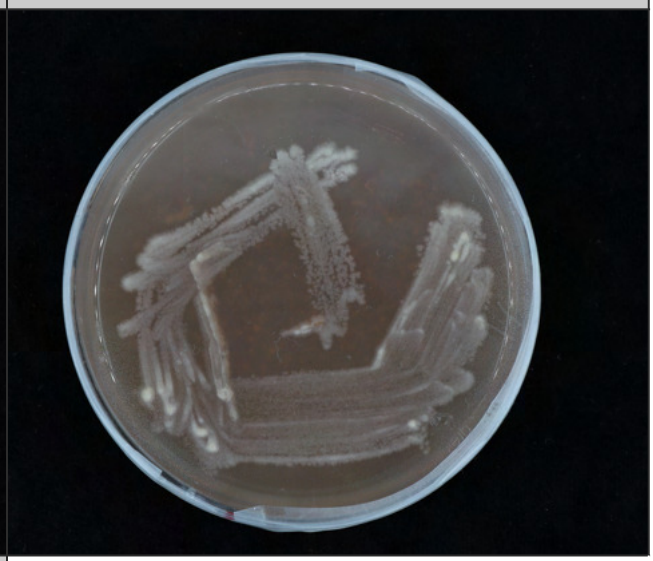
NITROGEN DEPLETED	
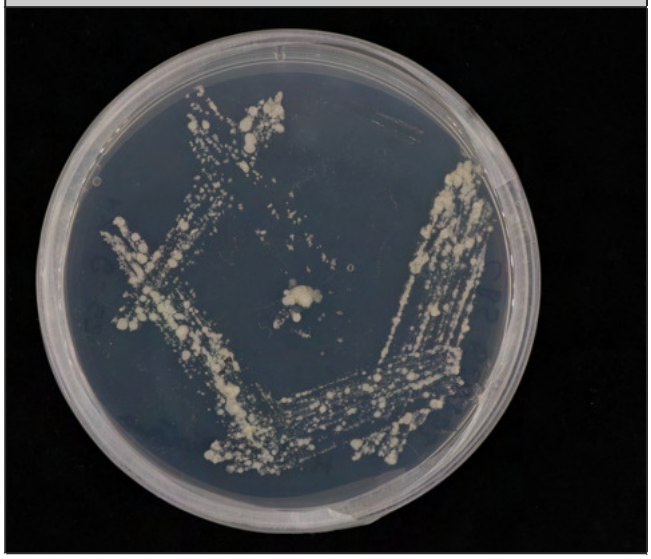	

CBS 590.93 - Culture Plates

CBS 590.93 - Microscopy Photographs	
GYPA	**MEA**
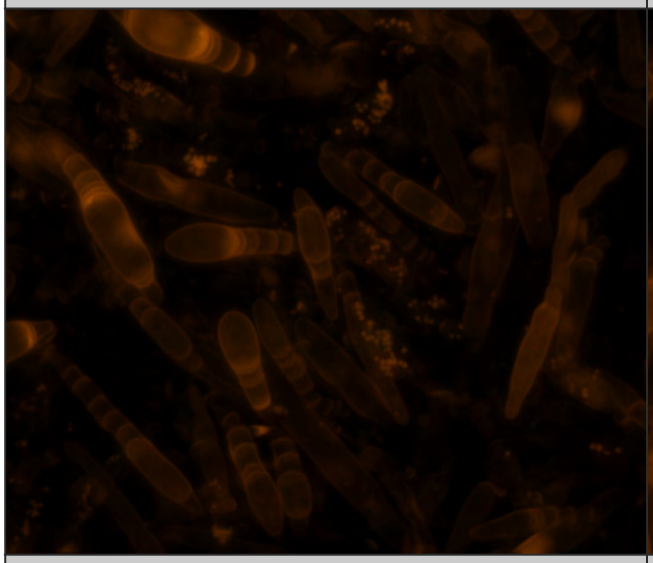	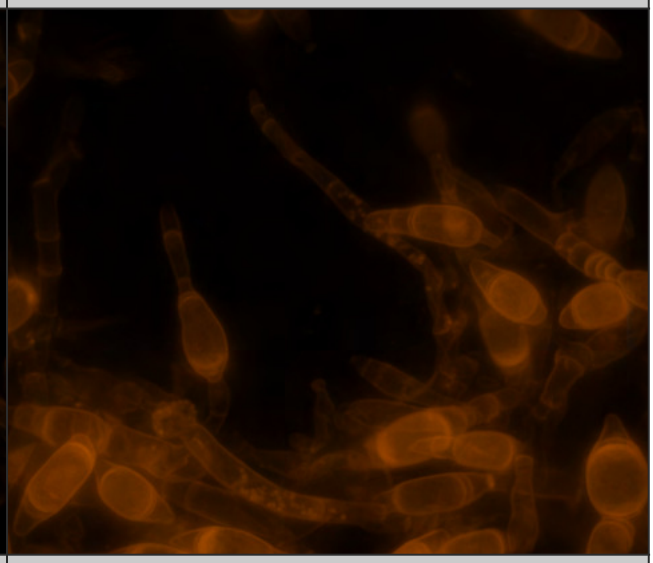
PDA	**X-AGAR**
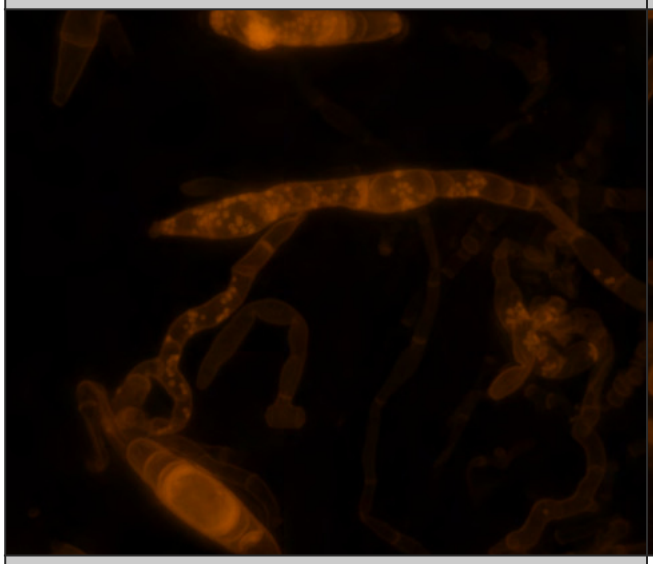	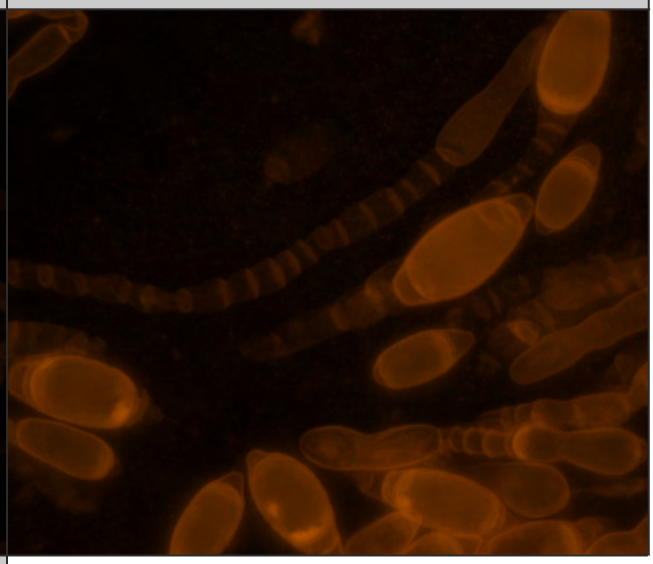
NITROGEN DEPLETED	
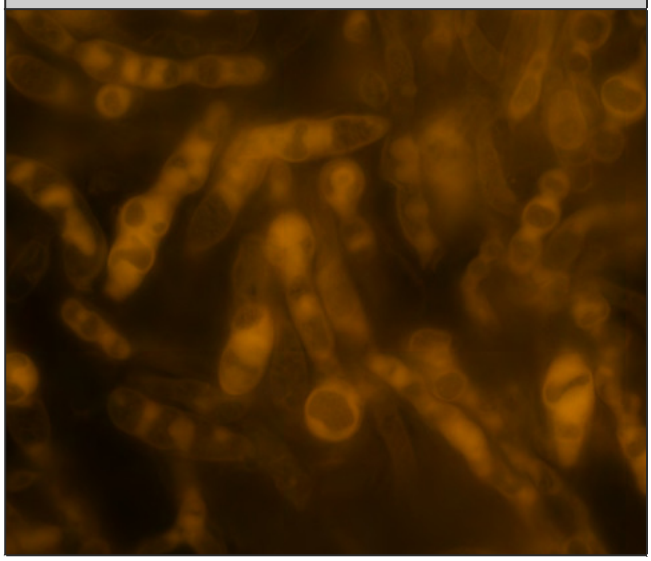	

CBS 590.93 - Microscopy Photographs

CBS 591.93 - Culture Plates	
GYPA	**MEA**
	
PDA	**X-AGAR**
	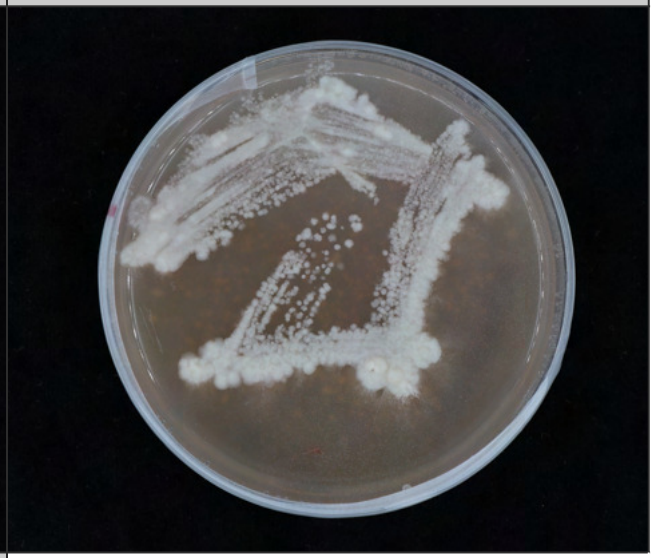
NITROGEN DEPLETED	
	

CBS 591.93 - Culture Plates

CBS 591.93 - Microscopy Photographs	
GYPA	**MEA**
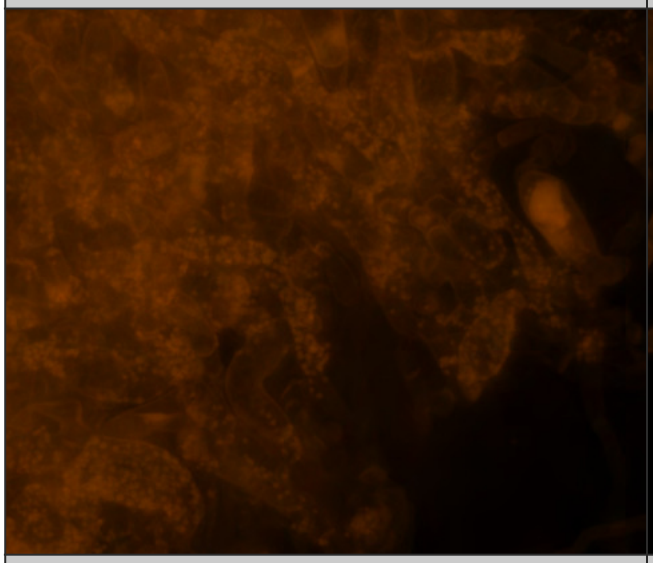	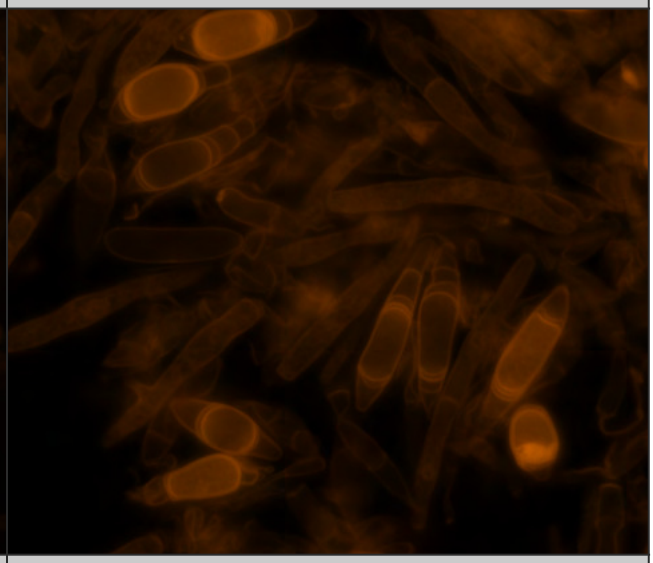
PDA	**X-AGAR**
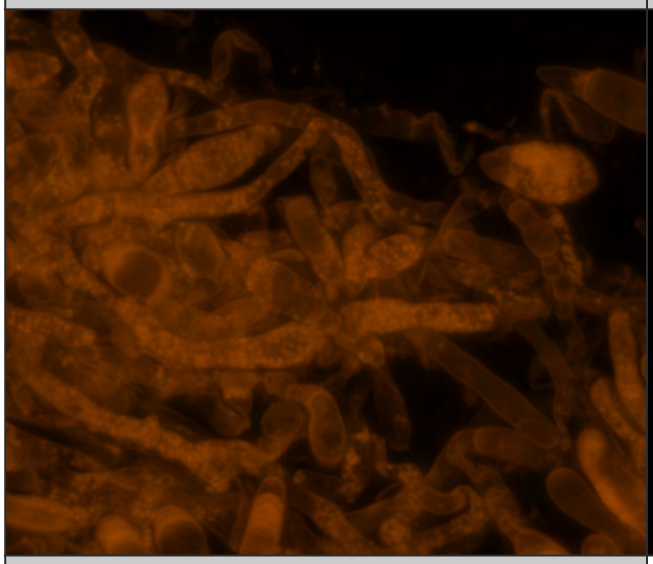	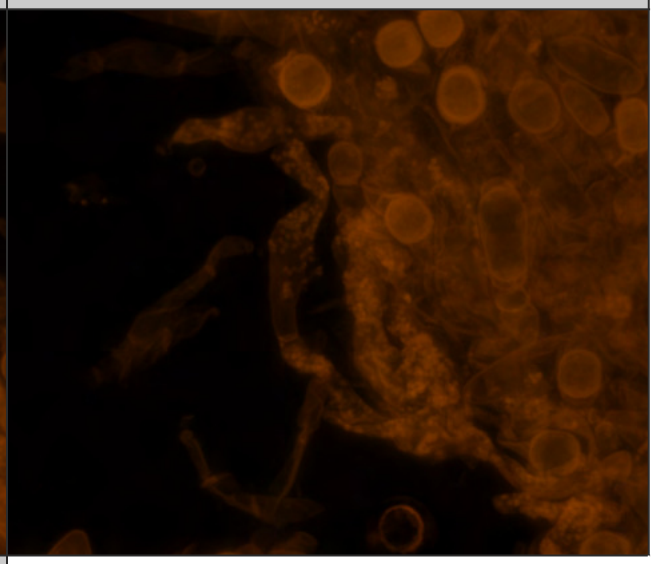
NITROGEN DEPLETED	
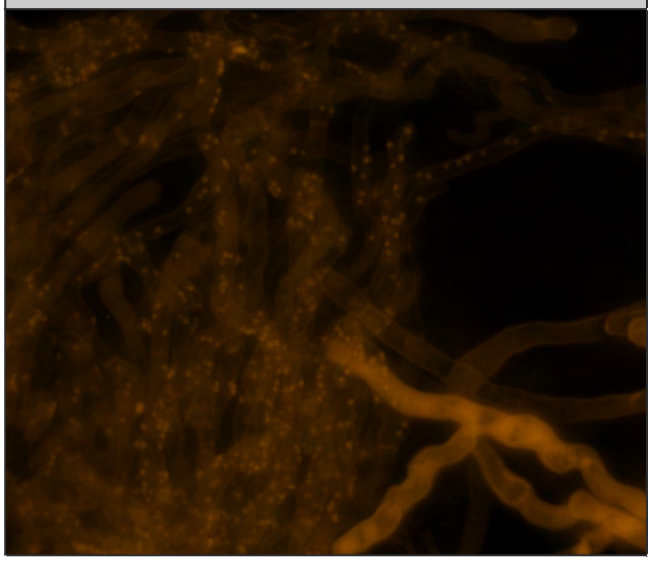	

CBS 591.93 - Microscopy Photographs

CBS 7243 - Culture Plates	
GYPA	**MEA**
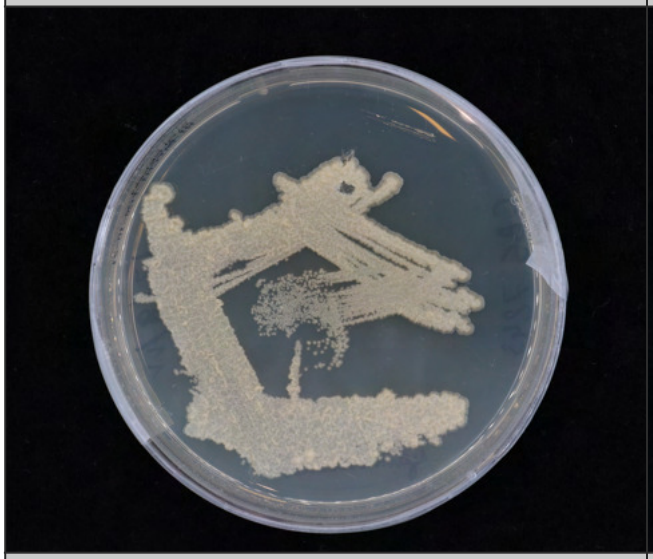	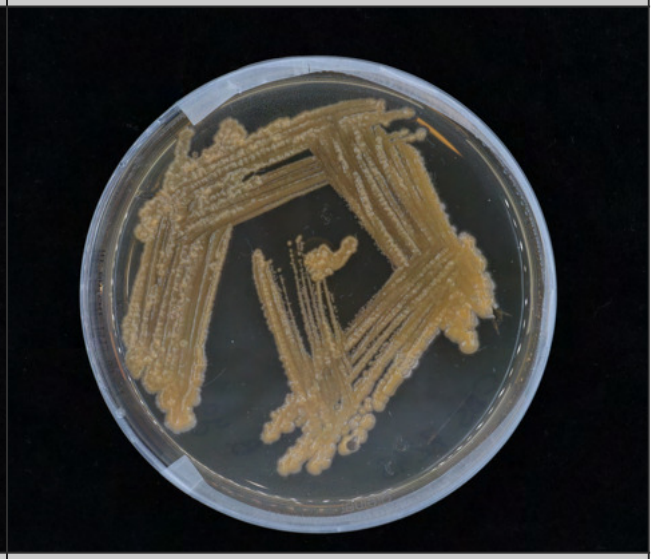
PDA	**X-AGAR**
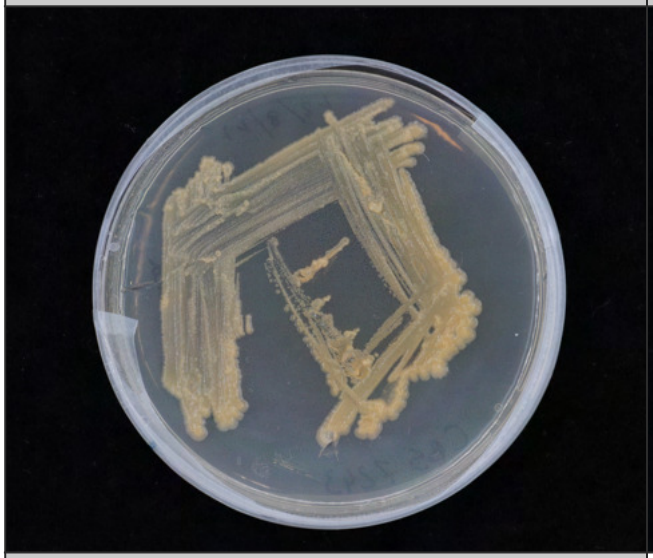	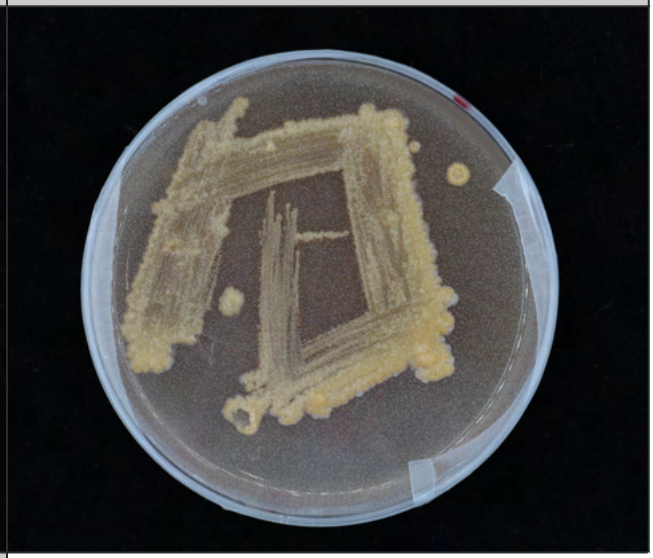
NITROGEN DEPLETED	
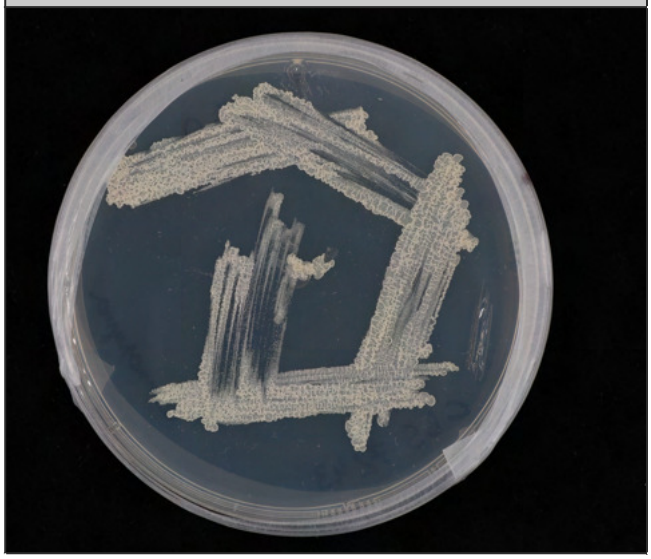	

CBS 7243 - Culture Plates

CBS 7243 - Microscopy Photographs	
GYPA	**MEA**
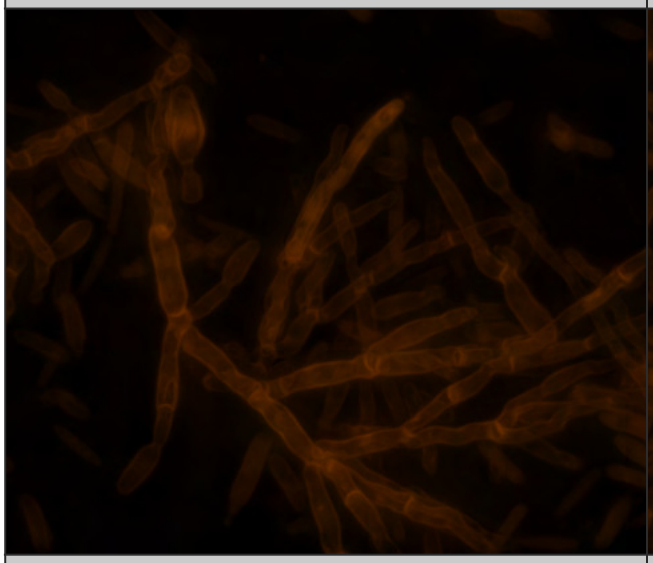	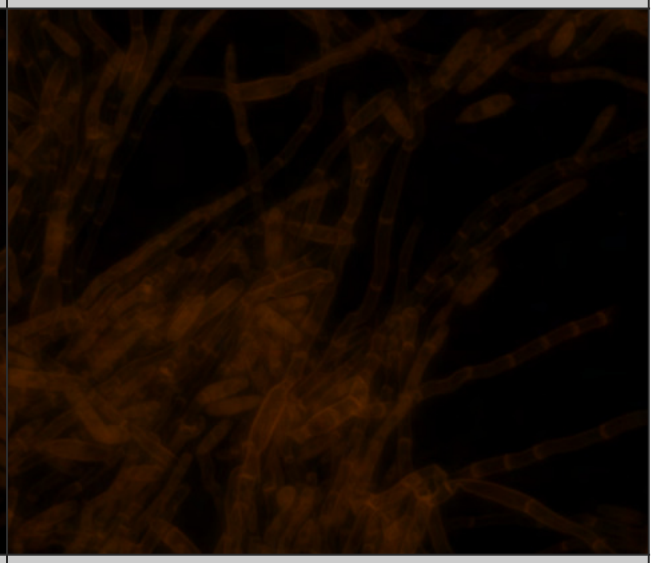
PDA	**X-AGAR**
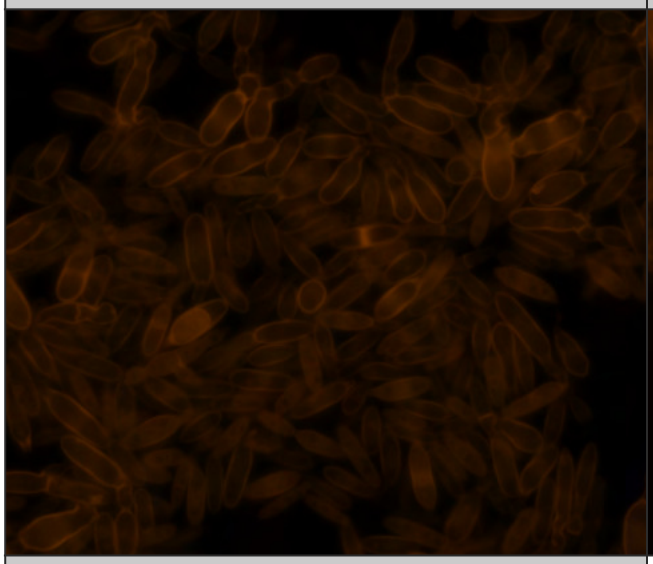	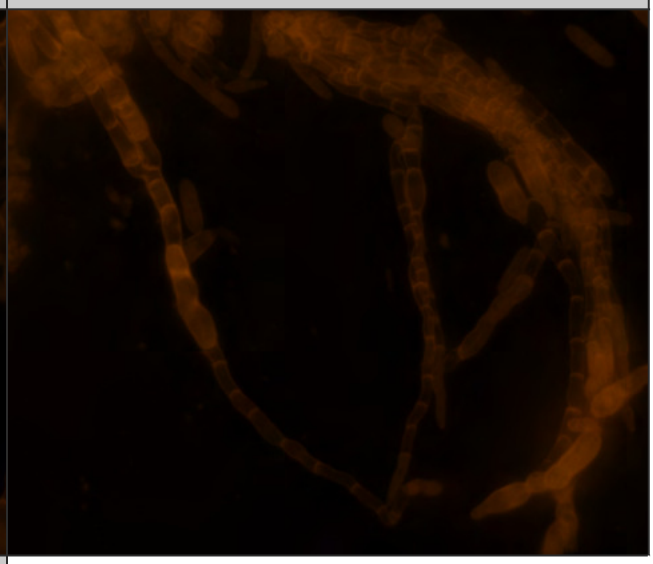
NITROGEN DEPLETED	
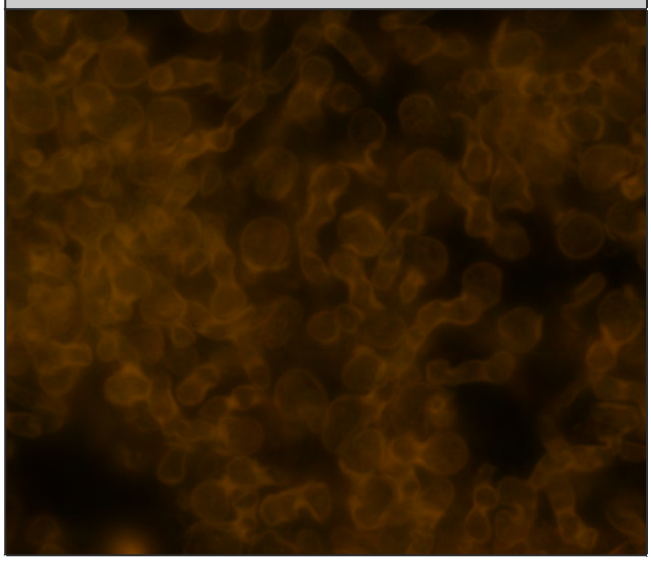	

CBS 7243 - Microscopy Photographs

CBS 497 - Culture Plates	
GYPA	**MEA**
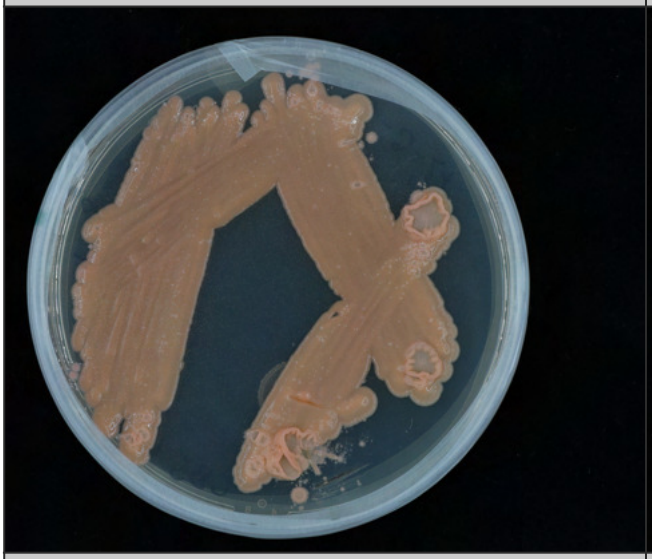	
PDA	**X-AGAR**
	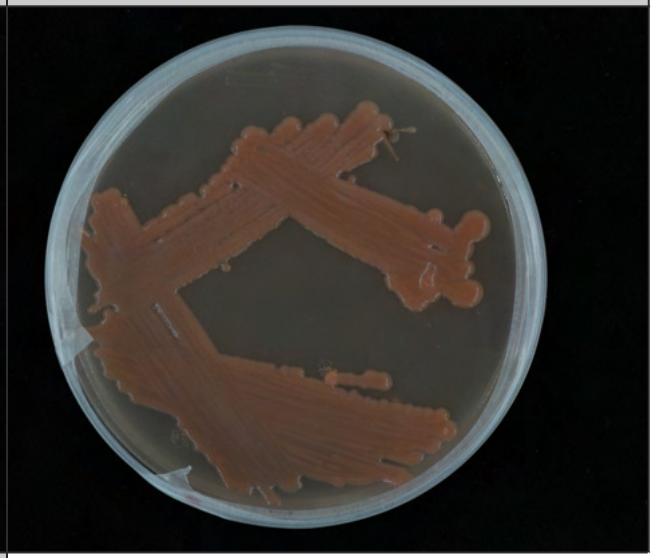
NITROGEN DEPLETED	
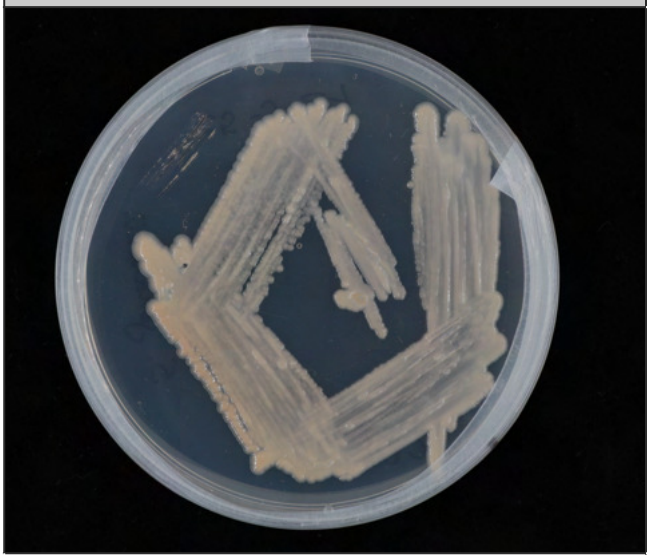	

CBS 497 - Culture Plates

CBS 497 - Microscopy Photographs	
GYPA	**MEA**
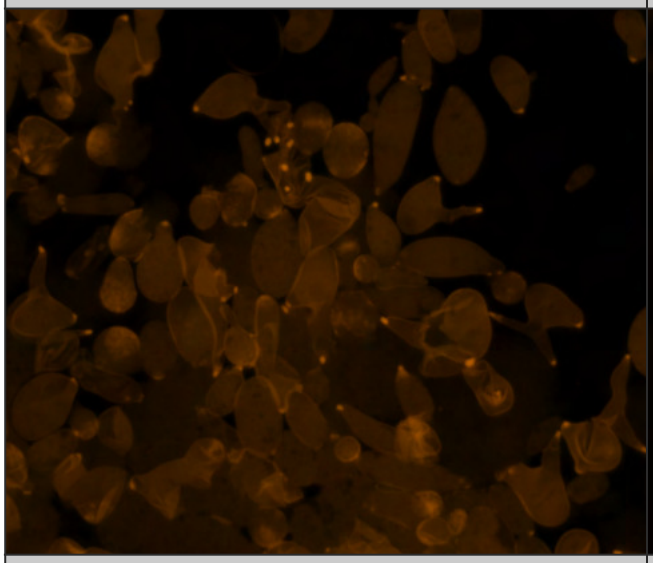	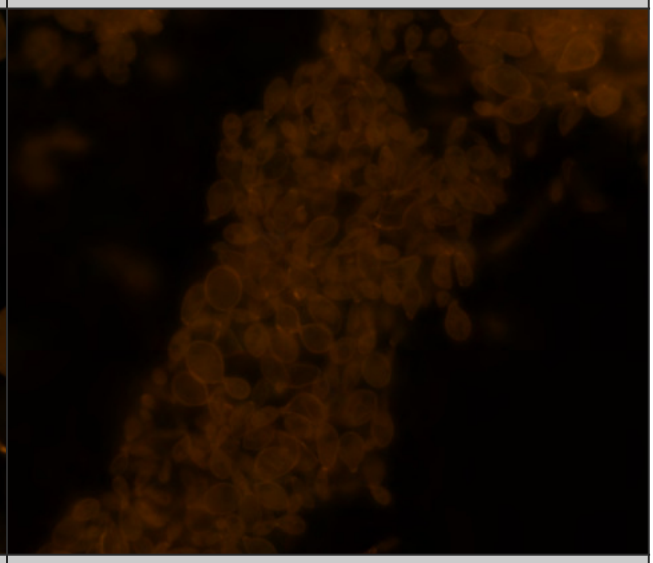
PDA	**X-AGAR**
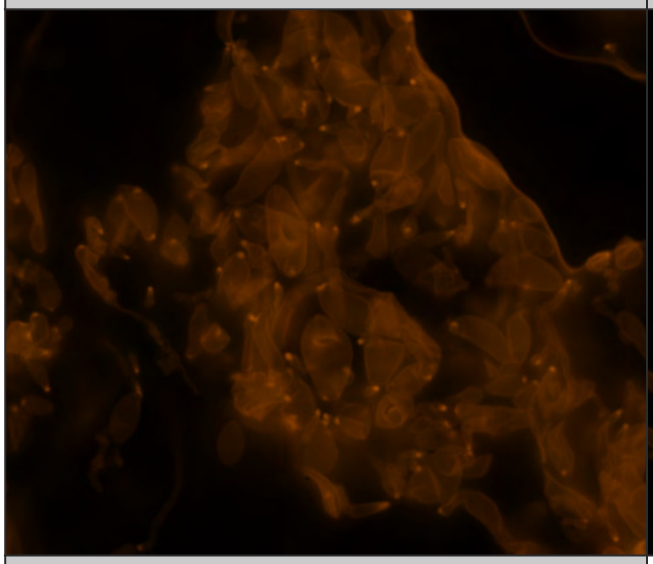	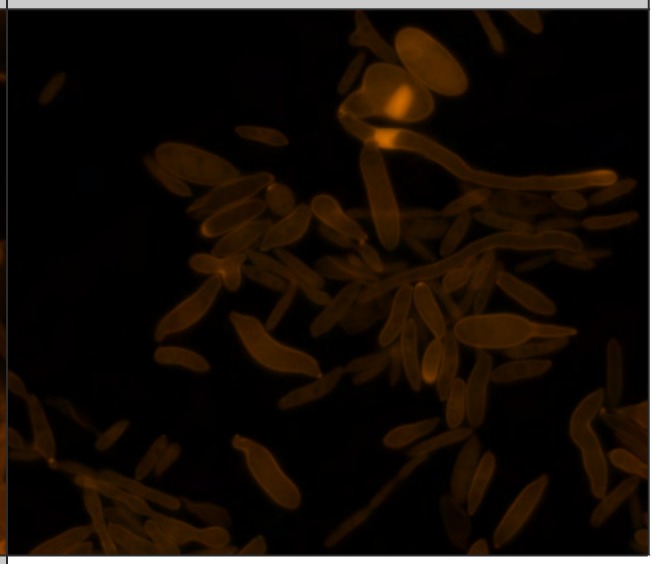
NITROGEN DEPLETED	
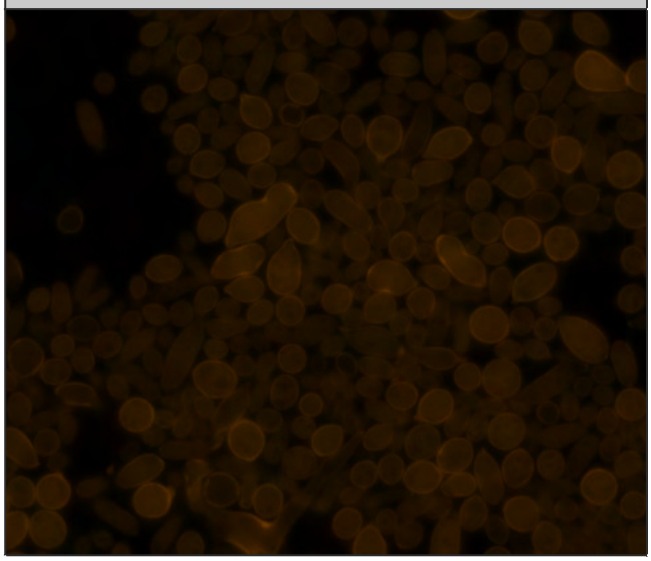	

CBS 497 - Microscopy Photographs

CBS 1522 - Culture Plates	
GYPA	**MEA**
	
PDA	**X-AGAR**
	
NITROGEN DEPLETED	
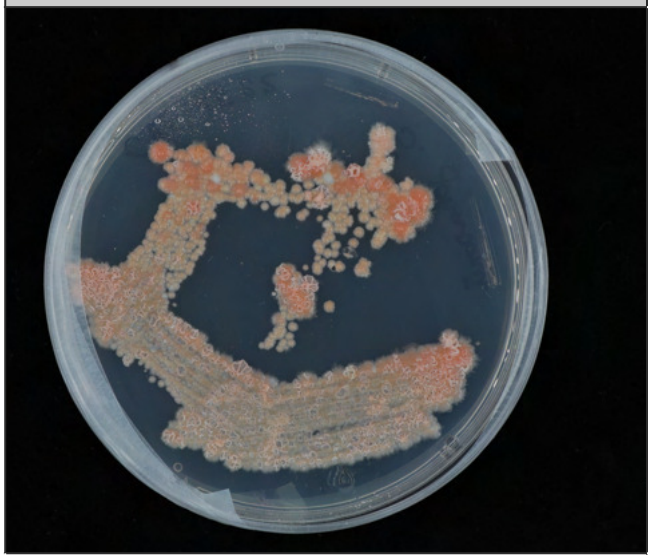	

CBS 1522 - Culture Plates

CBS 1522 - Microscopy Photographs	
GYPA	**MEA**
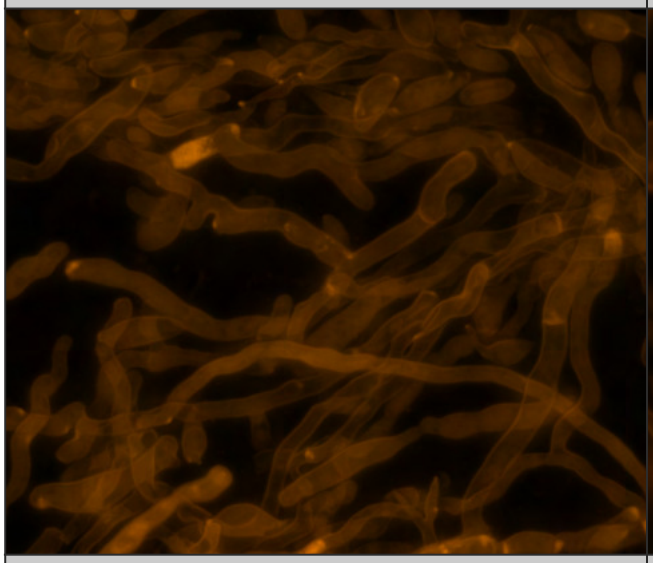	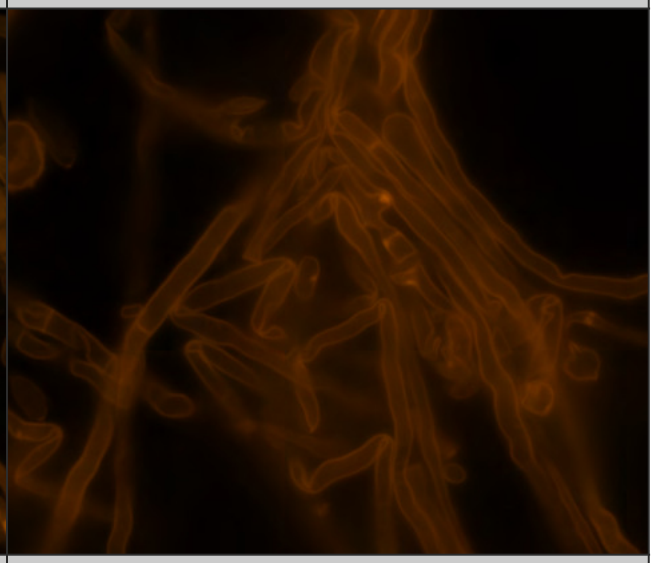
PDA	**X-AGAR**
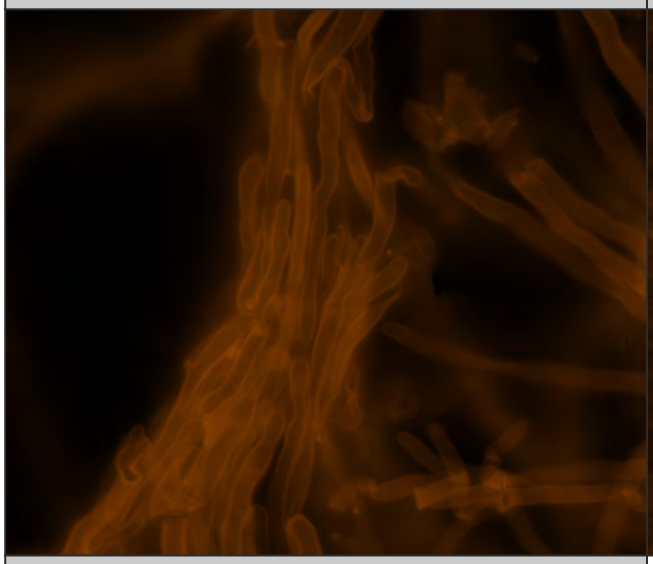	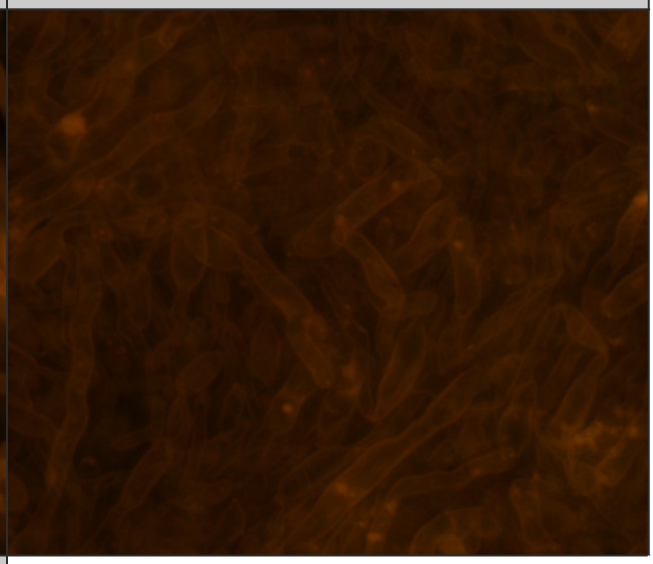
NITROGEN DEPLETED	
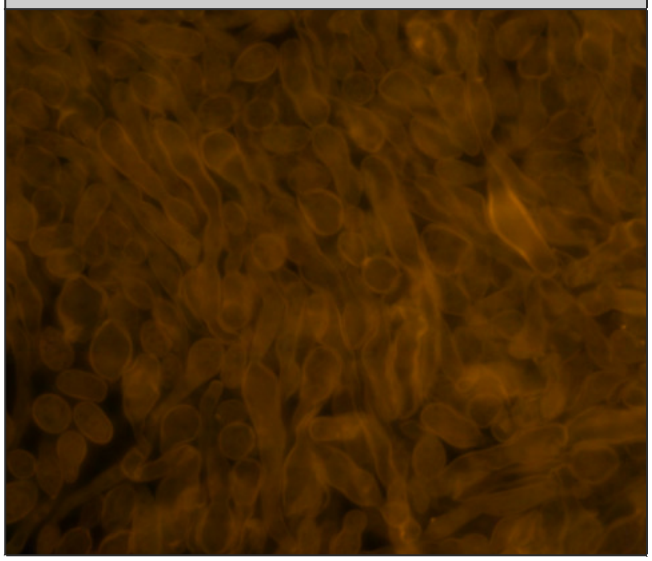	

CBS 1522 - Microscopy Photographs

CBS 5001 - Culture Plates	
GYPA	**MEA**
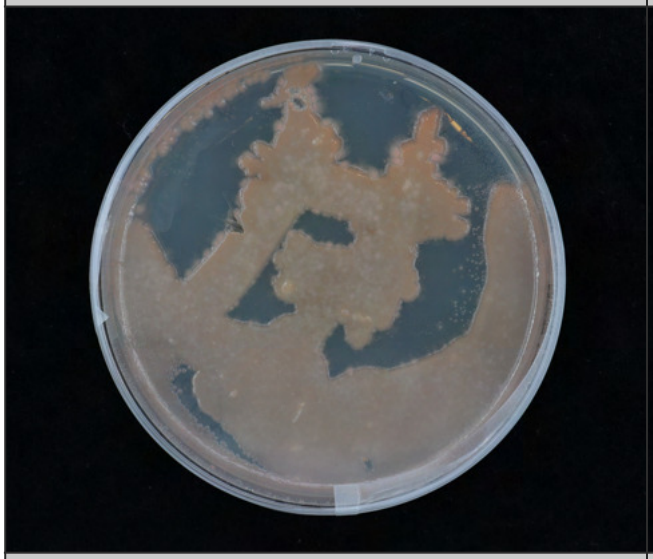	
PDA	**X-AGAR**
	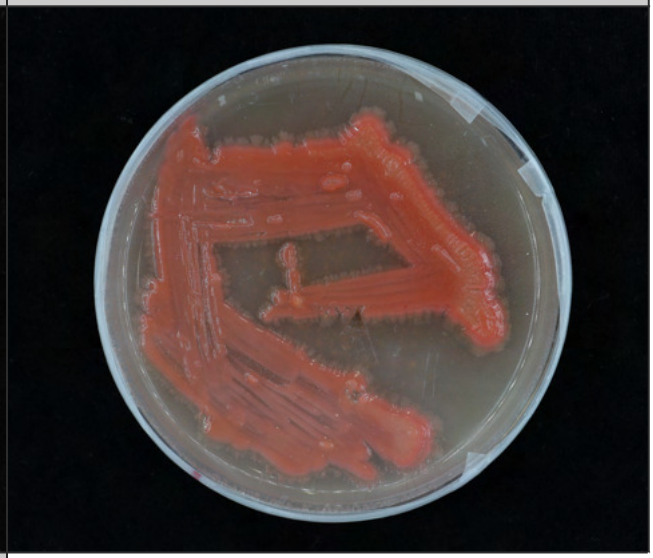
NITROGEN DEPLETED	
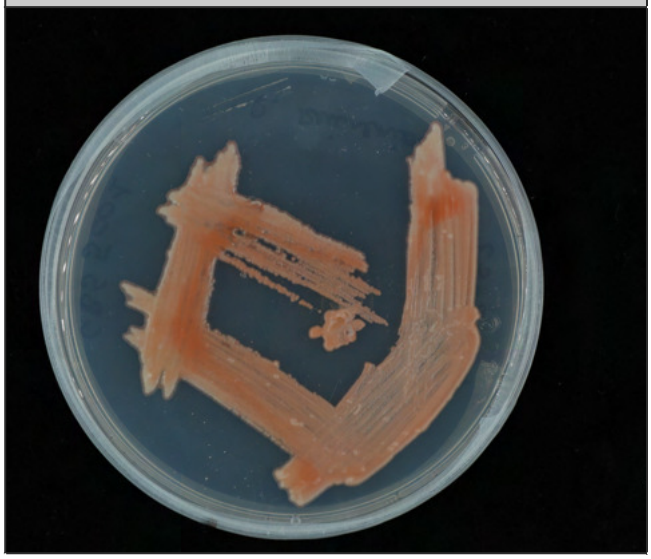	

CBS 5001 - Culture Plates

CBS 5001 - Microscopy Photographs	
GYPA	**MEA**
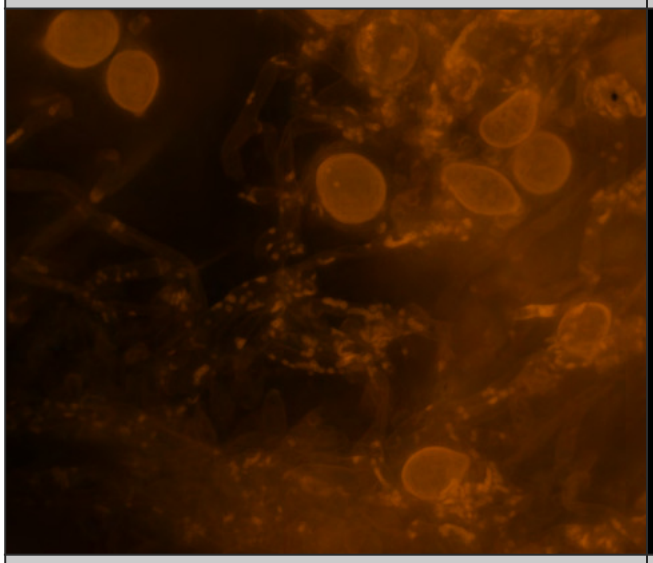	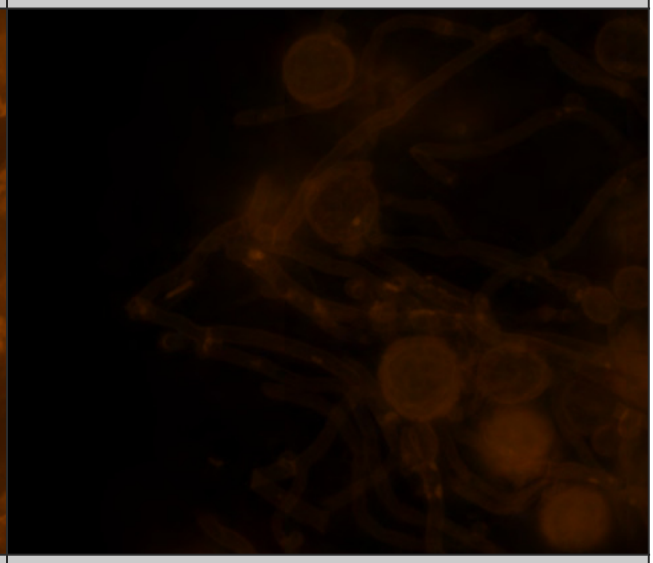
PDA	**X-AGAR**
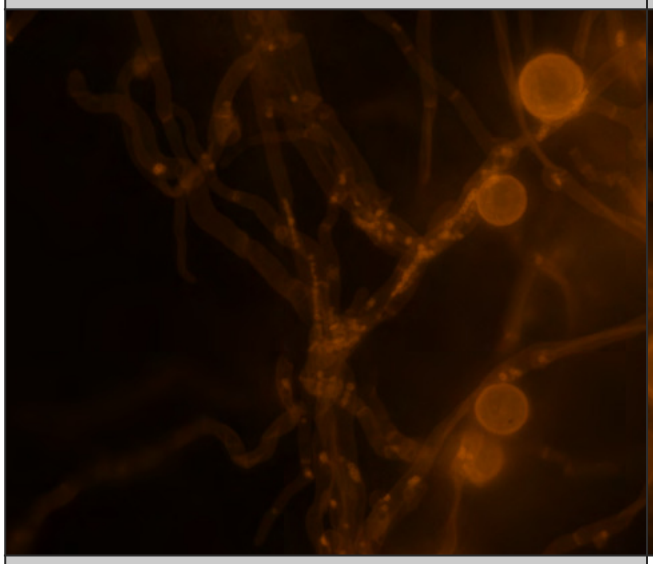	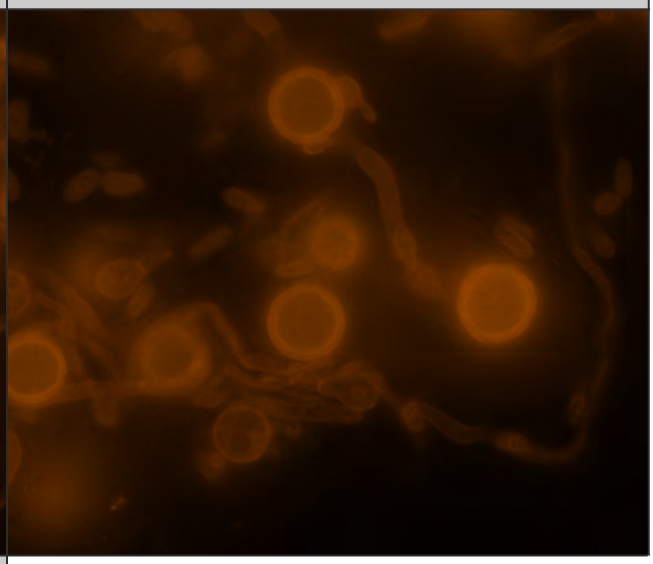
NITROGEN DEPLETED	
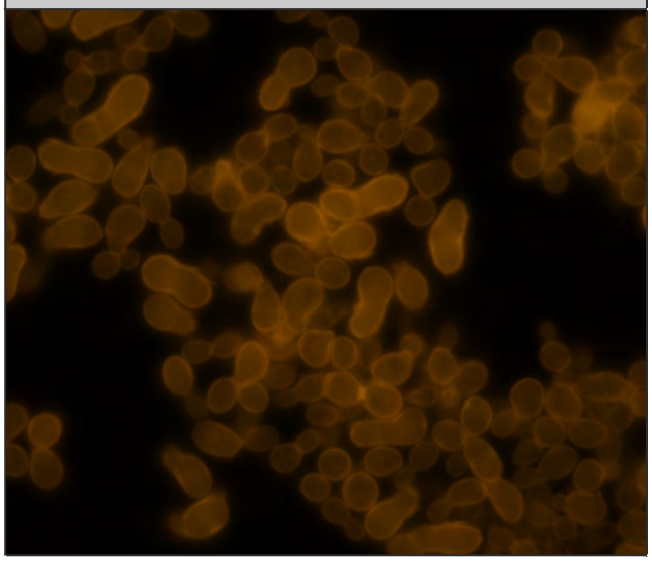	

CBS 5001 - Microscopy Photographs

CBS 9111 - Culture Plates	
GYPA	**MEA**
	
PDA	**X-AGAR**
	
NITROGEN DEPLETED	
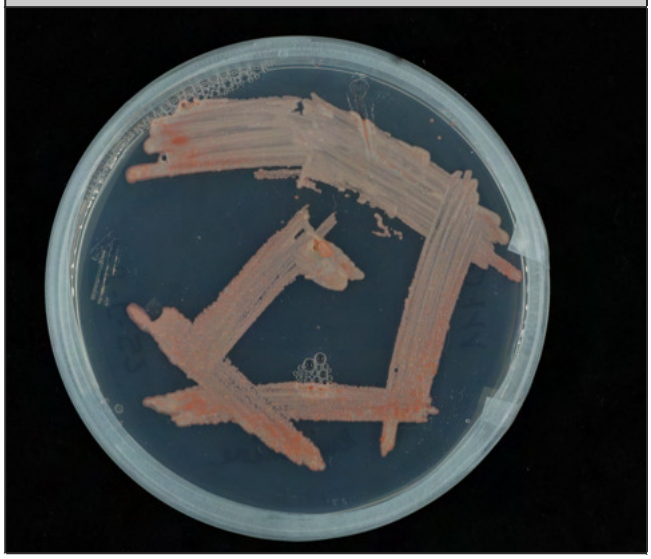	

CBS 9111 - Culture Plates

CBS 9111 - Microscopy Photographs	
GYPA	**MEA**
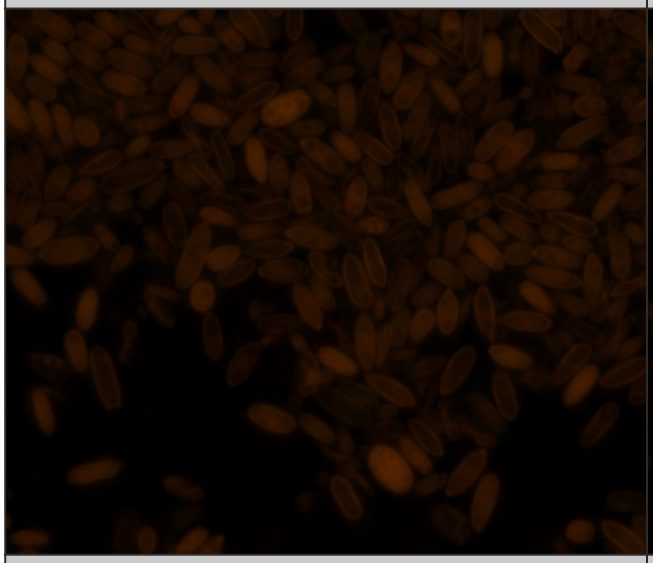	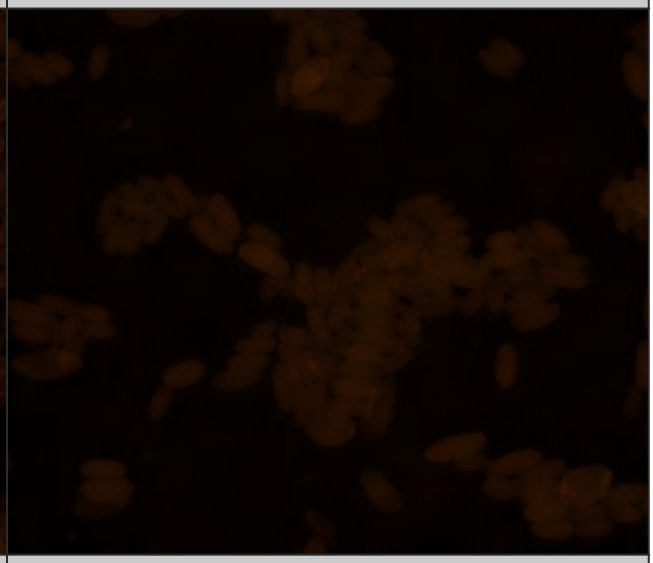
PDA	**X-AGAR**
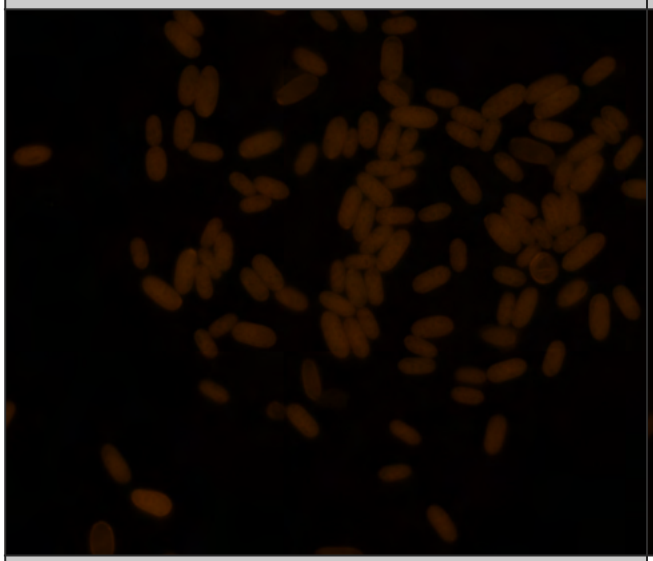	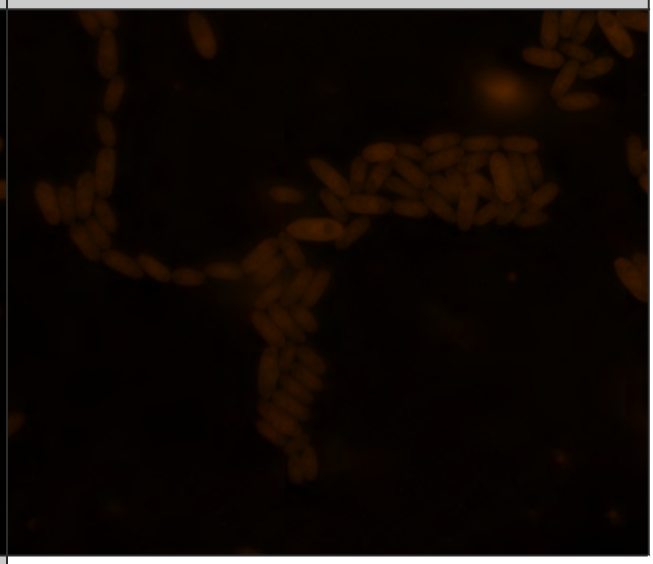
NITROGEN DEPLETED	
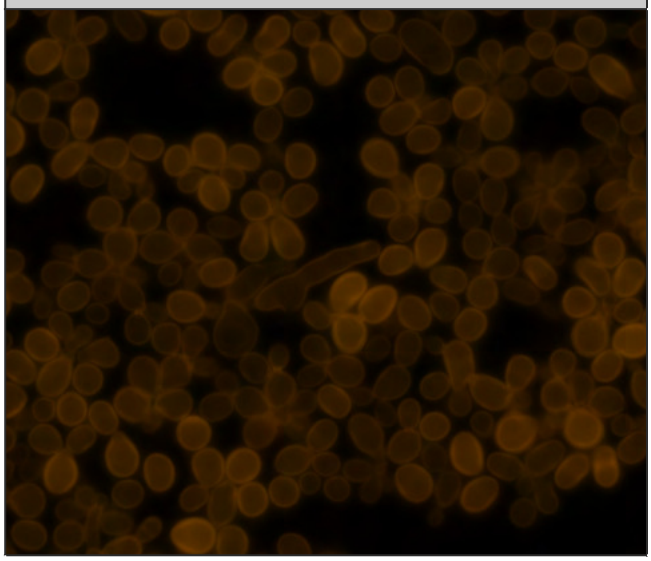	

CBS 9111 - Microscopy Photographs

CBS 483 - Culture Plates	
GYPA	**MEA**
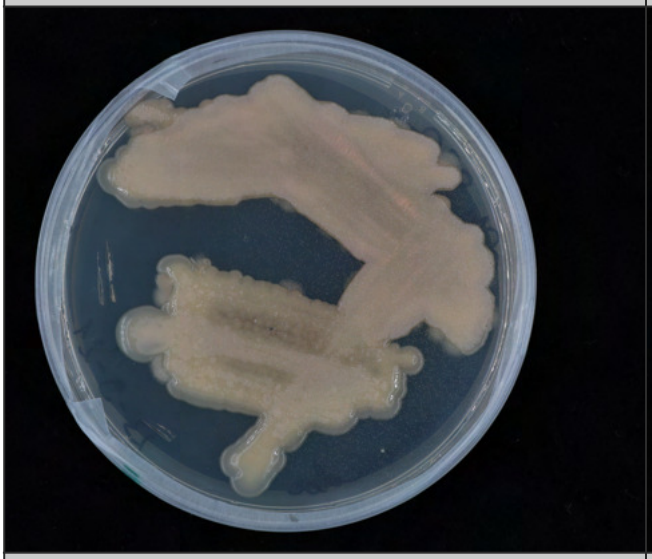	
PDA	**X-AGAR**
	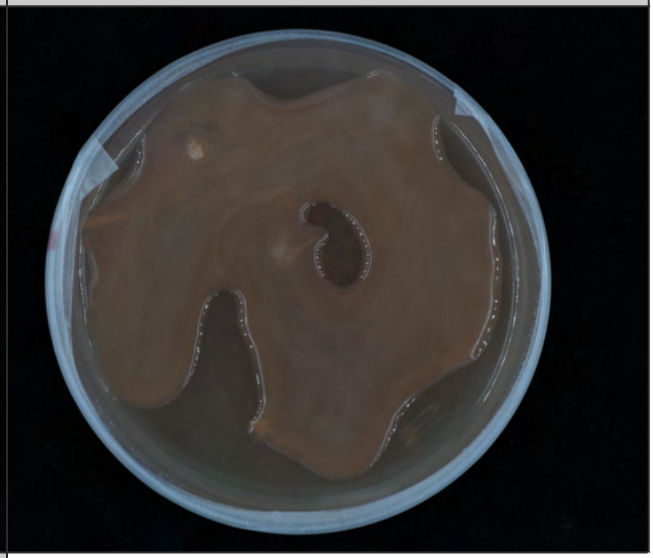
NITROGEN DEPLETED	
	

CBS 483 - Culture Plates

CBS 483 - Microscopy Photographs	
GYPA	**MEA**
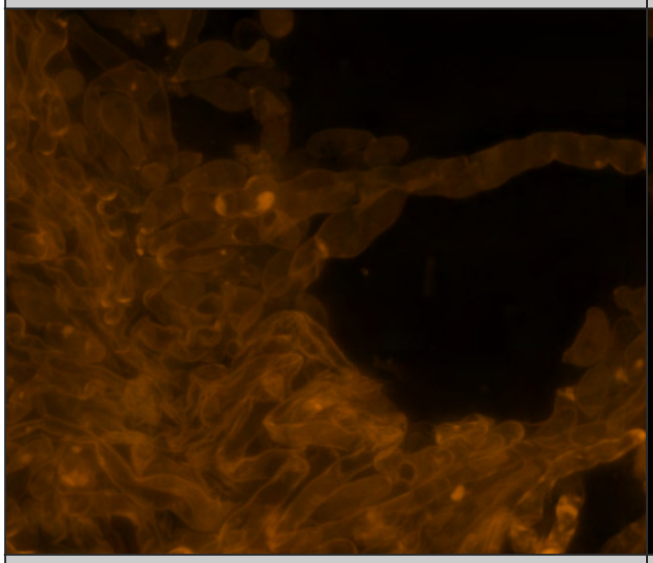	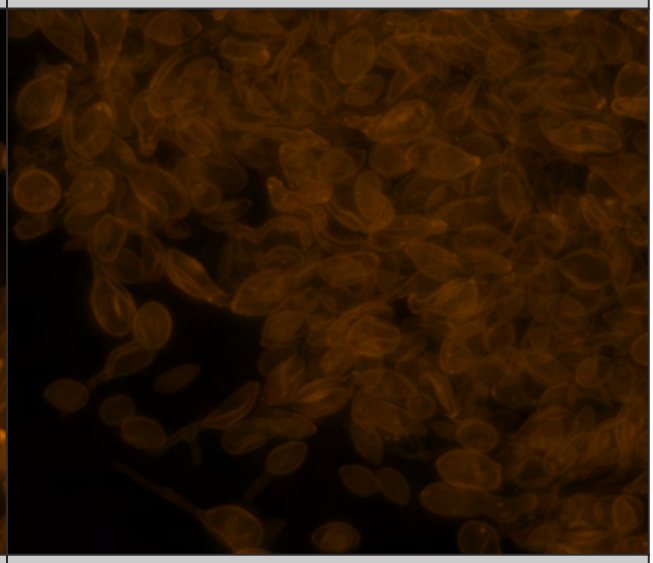
PDA	**X-AGAR**
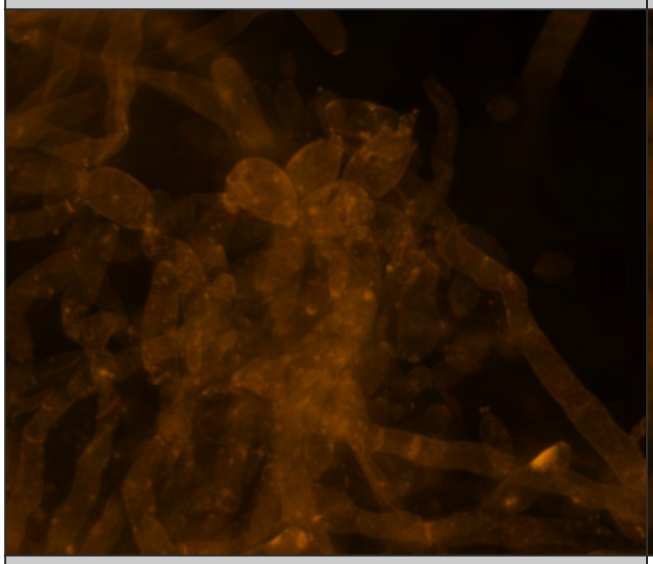	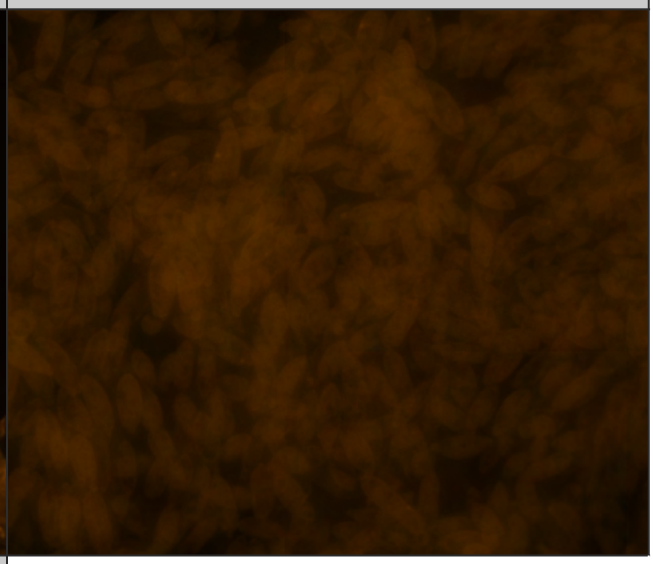
NITROGEN DEPLETED	
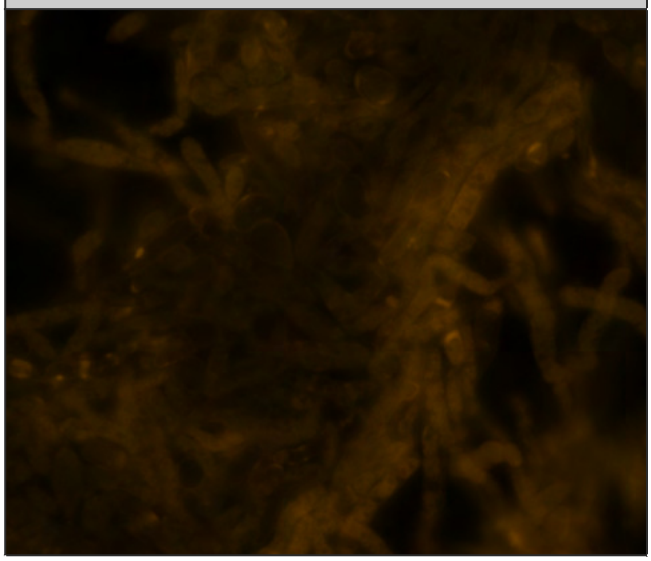	

CBS 483 - Microscopy Photographs

CBS 490 - Culture Plates	
GYPA	**MEA**
	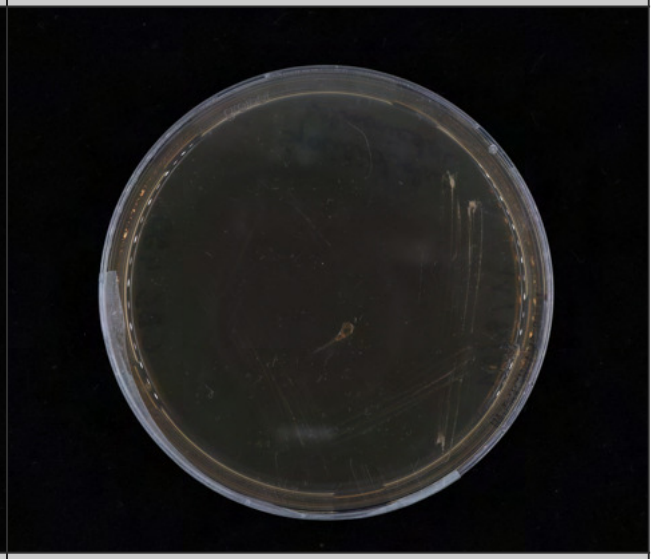
PDA	**X-AGAR**
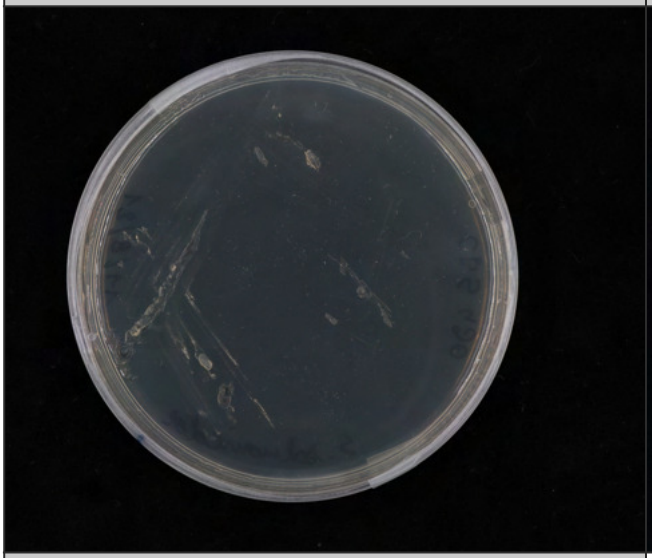	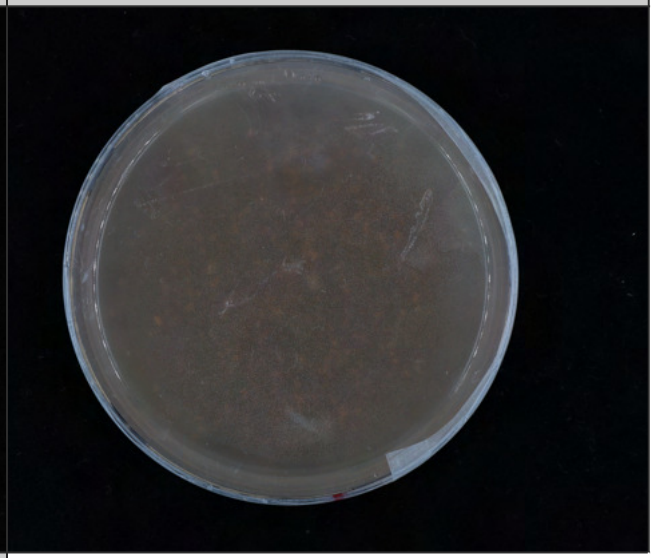
NITROGEN DEPLETED	
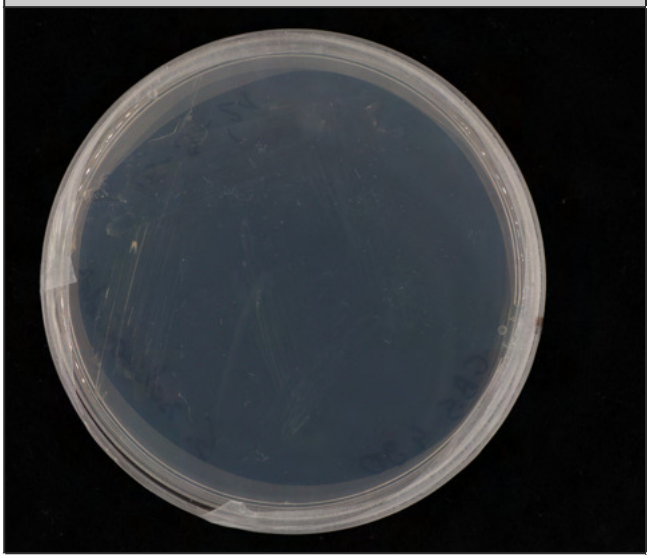	

CBS 490 - Culture Plates

CBS 490 - Microscopy Photographs	
GYPA	**MEA**
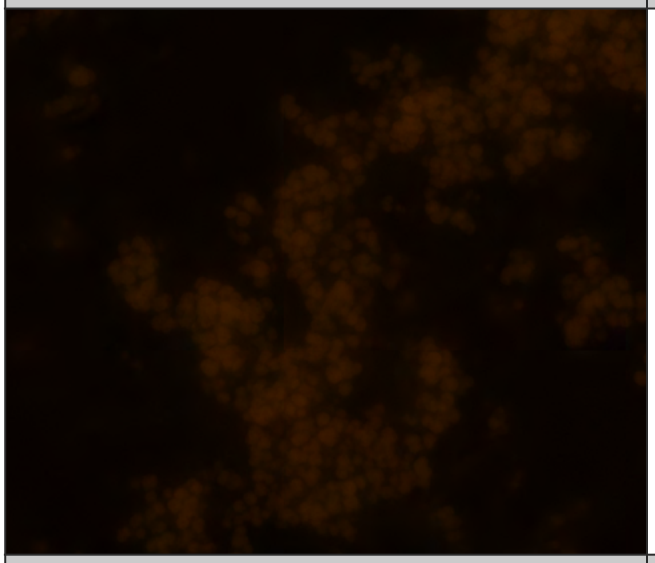	No growth detected.
PDA	**X-AGAR**
No growth detected.	No growth detected.
NITROGEN DEPLETED	
No growth detected.	

CBS 490 - Microscopy Photographs

CBS 1012 - Culture Plates	
GYPA	**MEA**
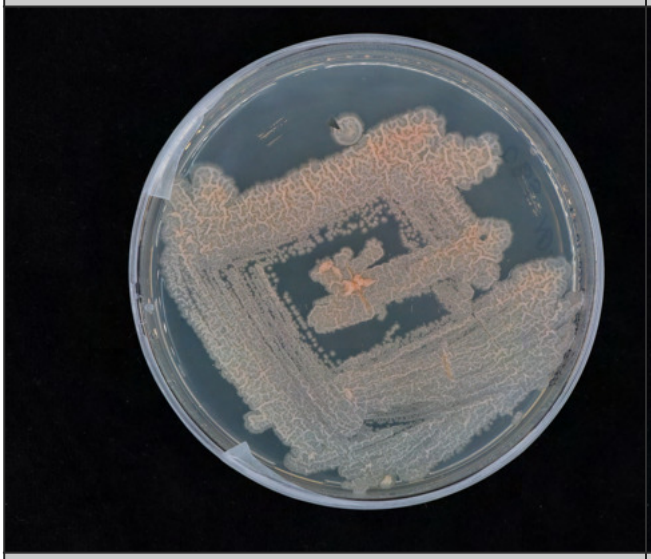	
PDA	**X-AGAR**
	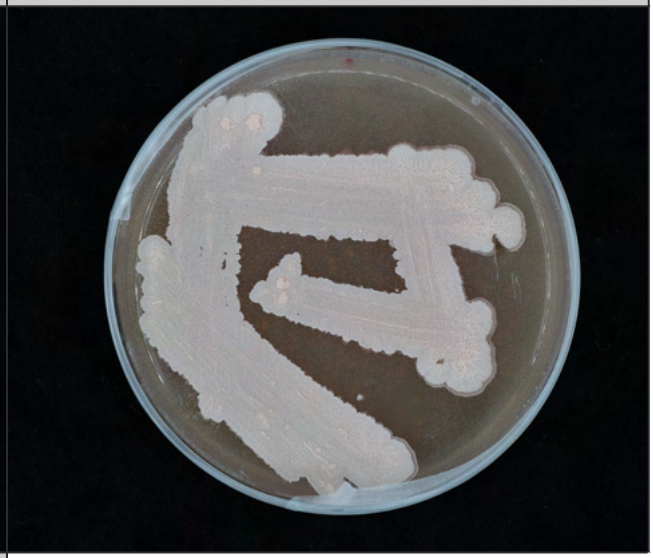
NITROGEN DEPLETED	
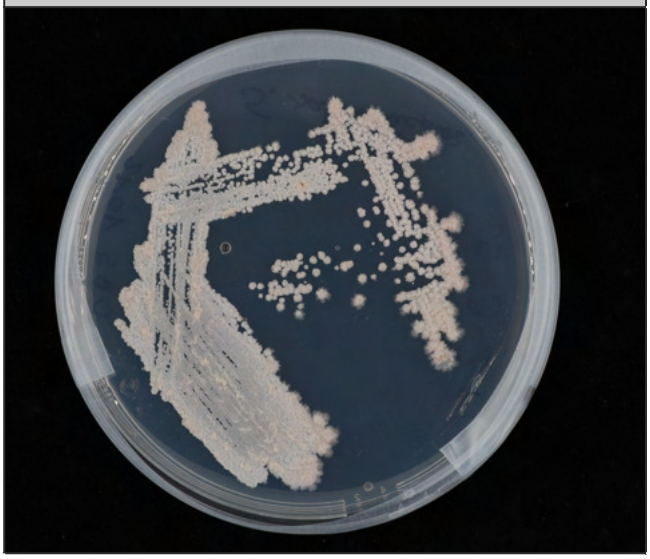	

CBS 1012 - Culture Plates

CBS 1012 - Microscopy Photographs	
GYPA	**MEA**
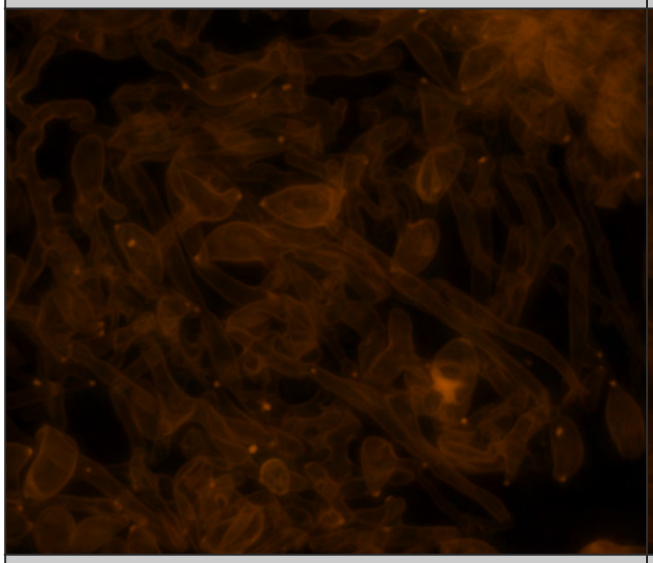	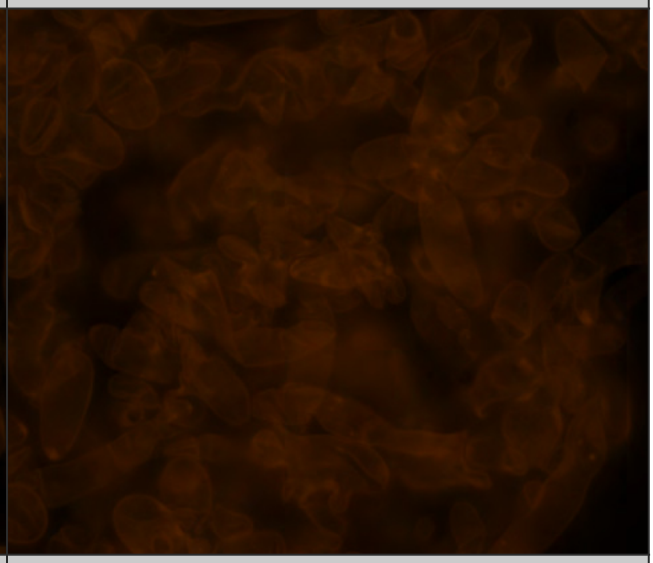
PDA	**X-AGAR**
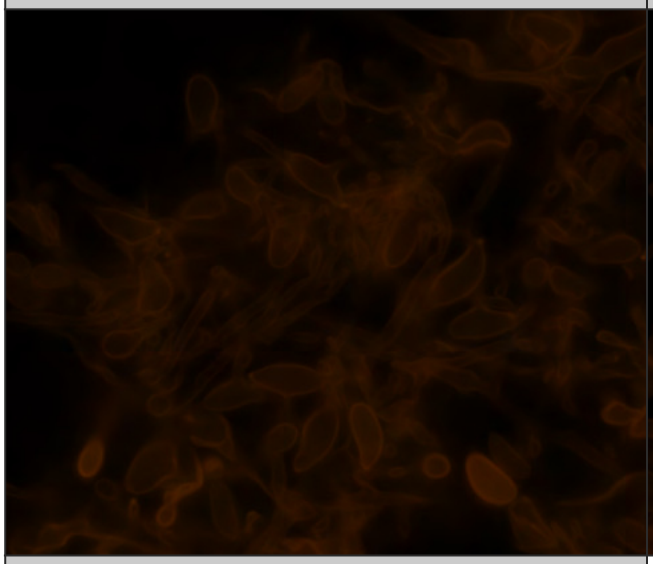	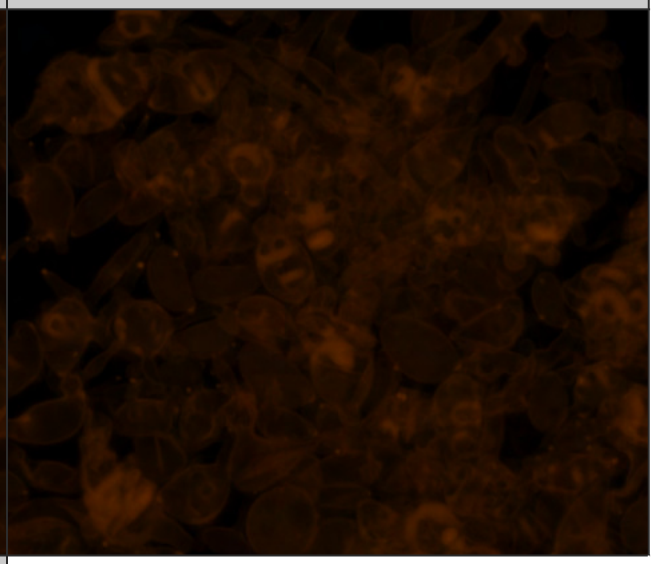
NITROGEN DEPLETED	
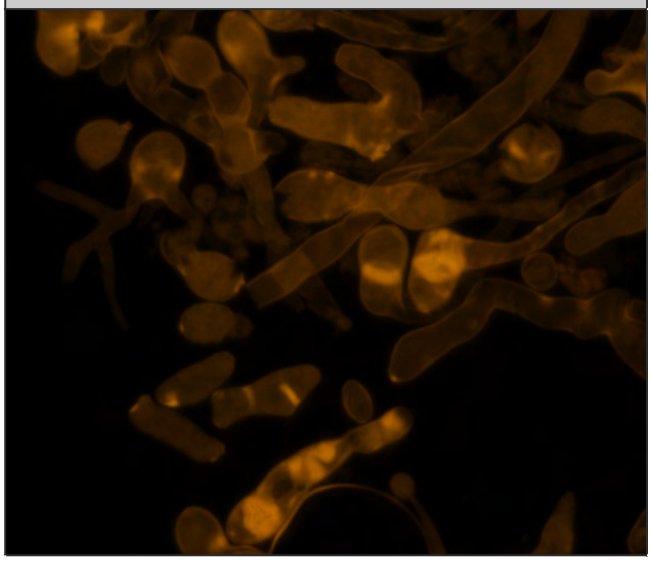	

CBS 1012 - Microscopy Photographs

CBS 2630 - Culture Plates	
GYPA	**MEA**
	
PDA	**X-AGAR**
	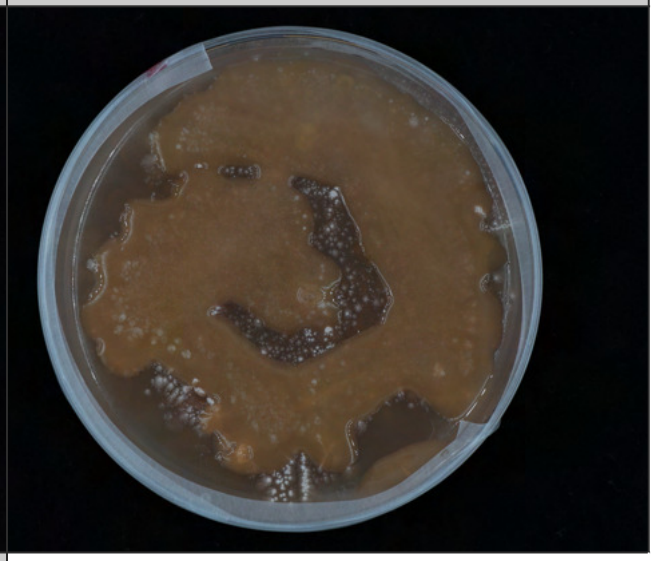
NITROGEN DEPLETED	
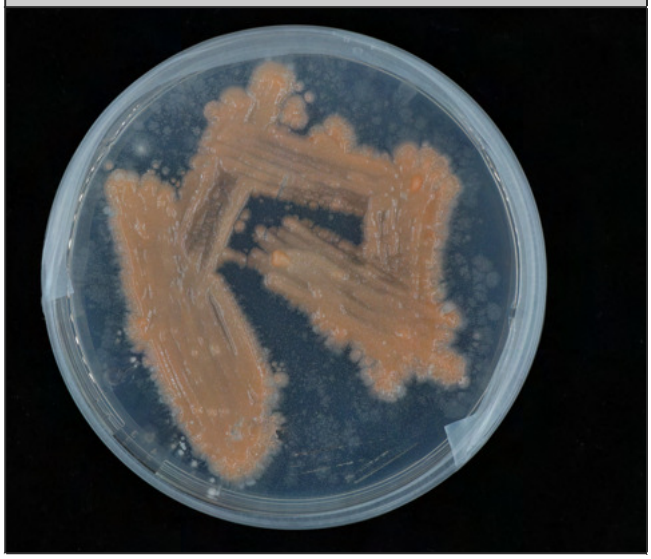	

CBS 2630 - Culture Plates

CBS 2630 - Microscopy Photographs	
GYPA	**MEA**
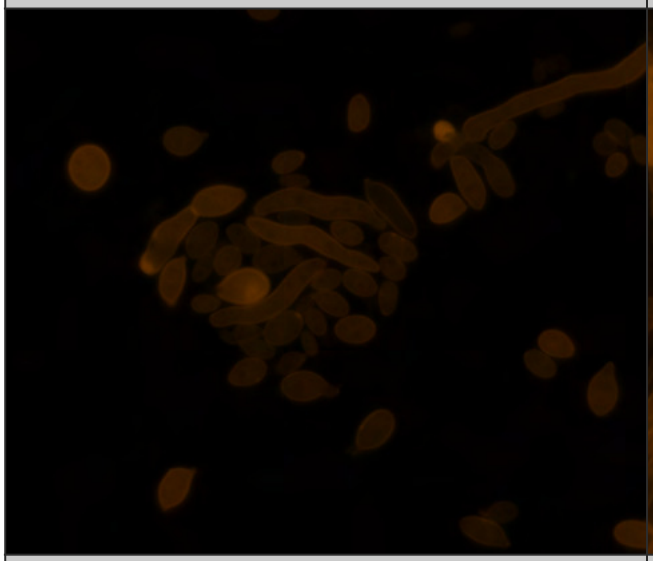	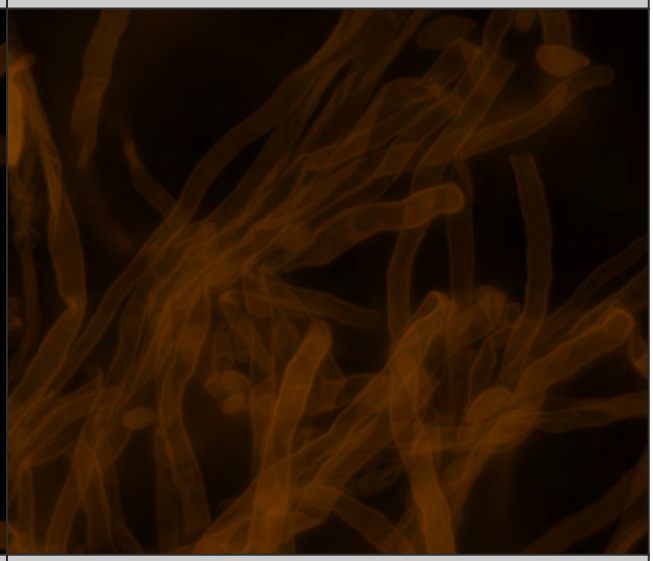
PDA	**X-AGAR**
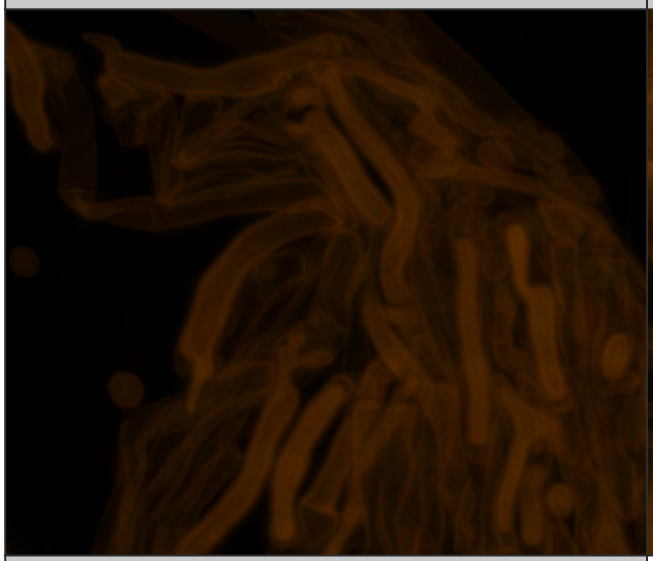	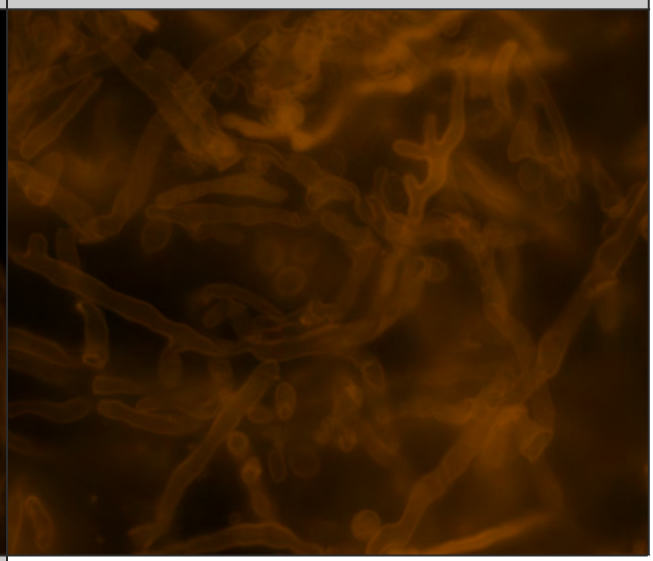
NITROGEN DEPLETED	
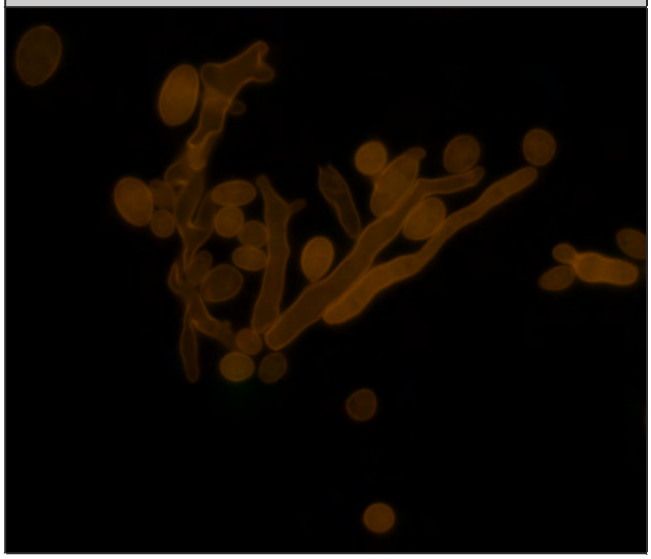	

CBS 2630 - Microscopy Photographs

CBS 6561 - Culture Plates	
GYPA	**MEA**
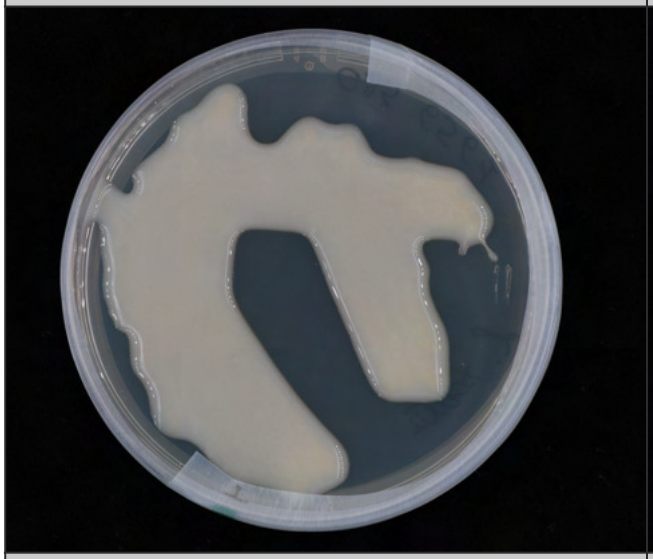	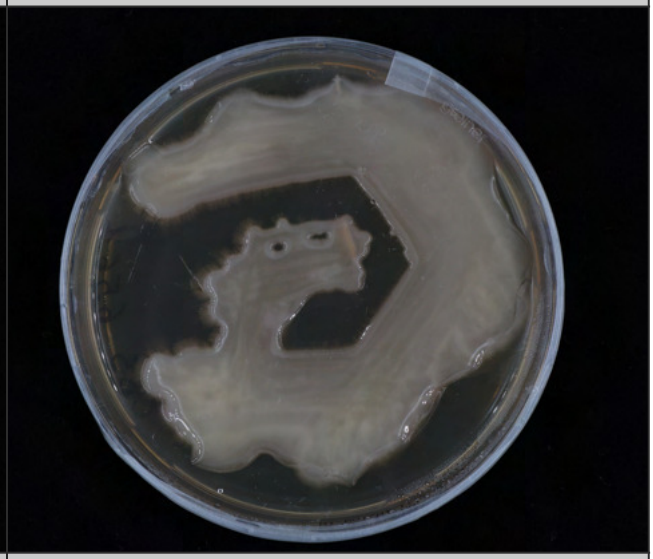
PDA	**X-AGAR**
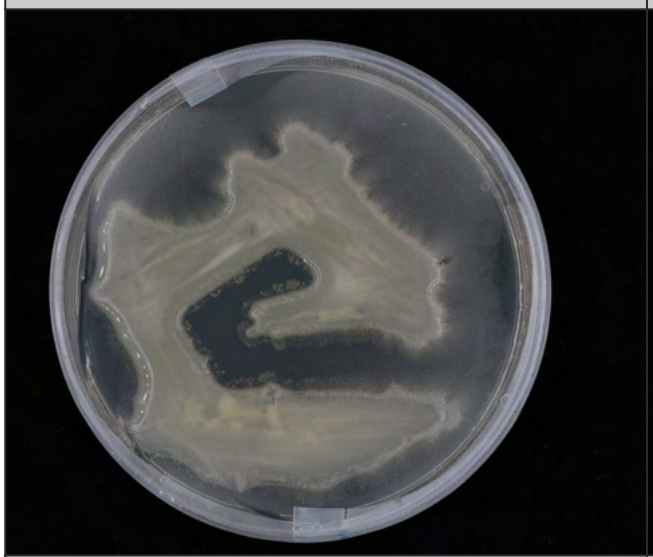	
NITROGEN DEPLETED	
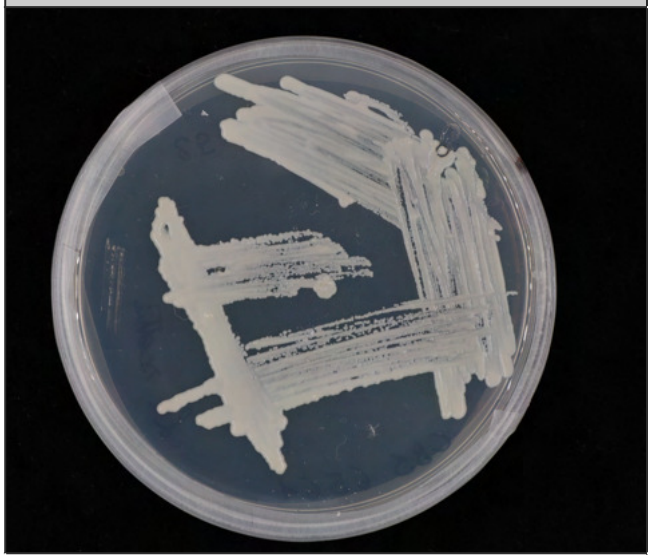	

CBS 6561 - Culture Plates

CBS 6561 - Microscopy Photographs	
GYPA	**MEA**
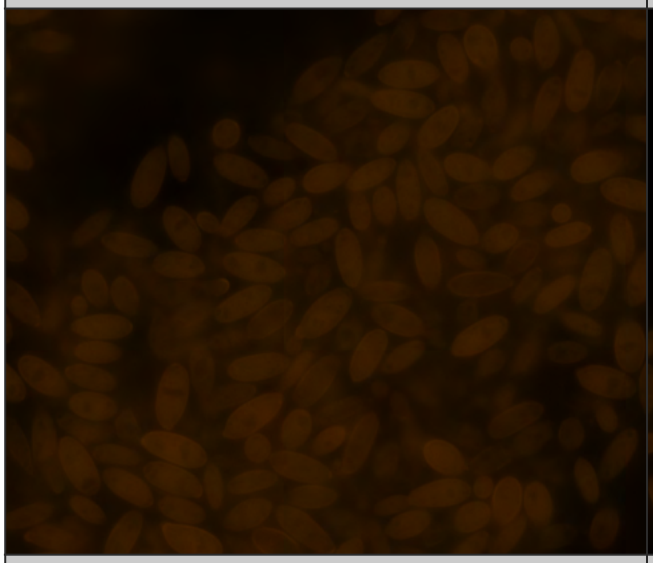	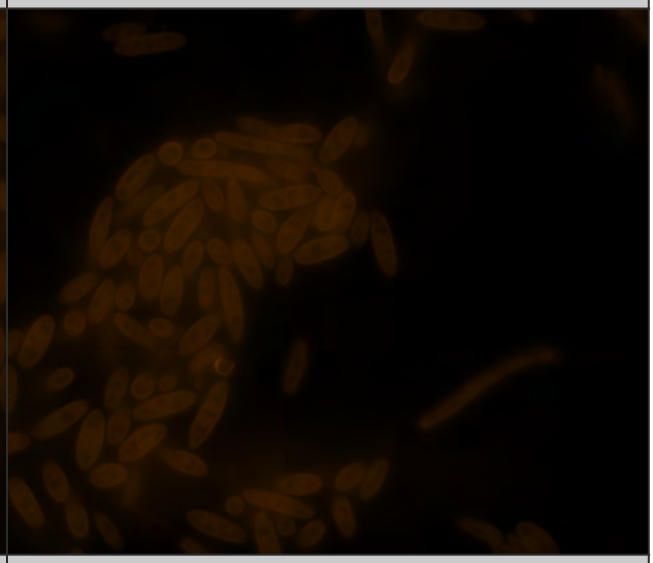
PDA	**X-AGAR**
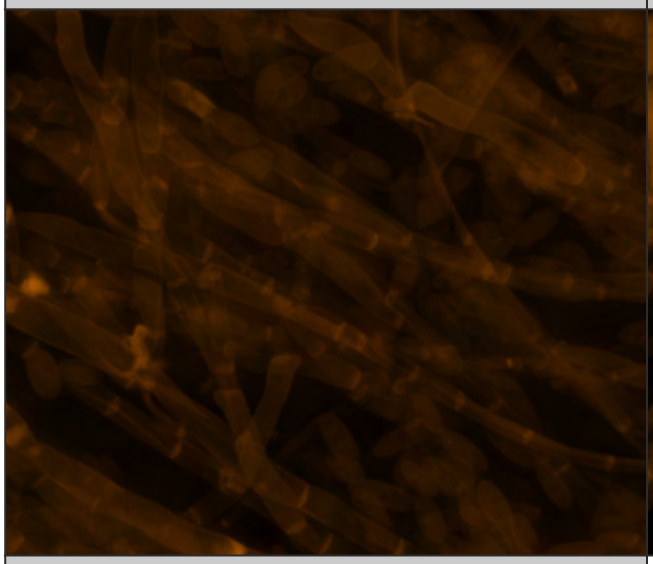	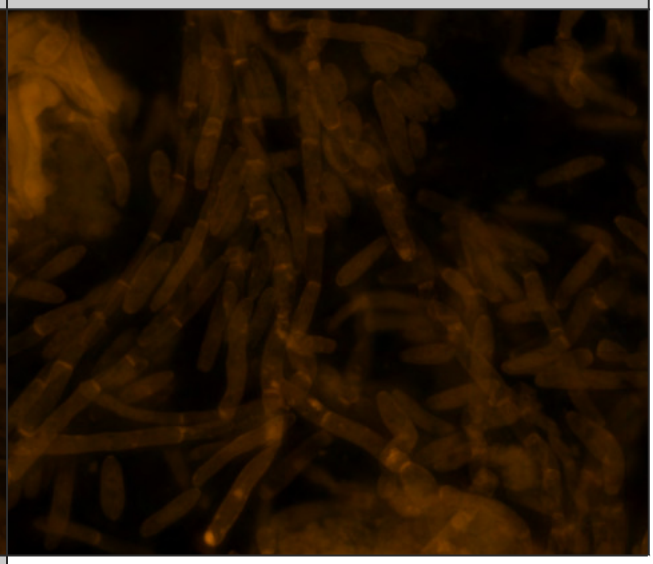
NITROGEN DEPLETED	
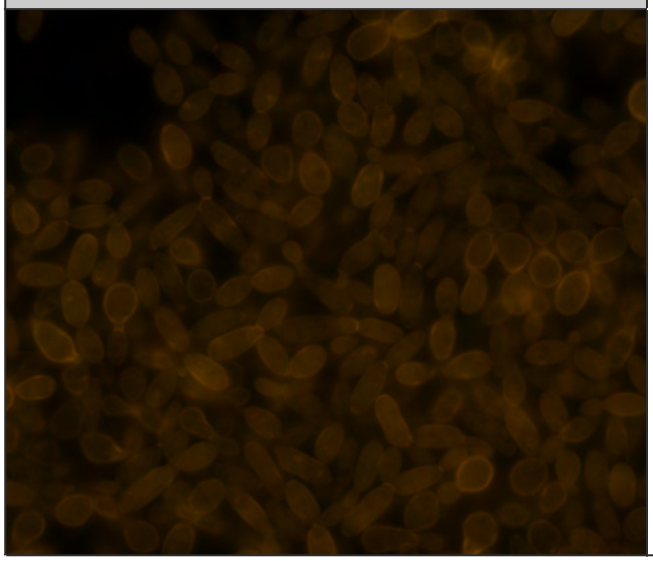	

CBS 6561 - Microscopy Photographs

CBS 7041 - Culture Plates	
GYPA	**MEA**
	
PDA	**X-AGAR**
	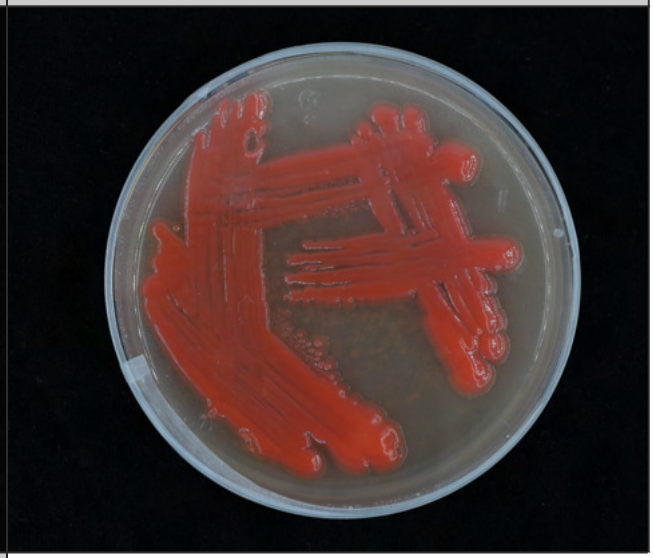
NITROGEN DEPLETED	
	

CBS 7041 - Culture Plates

CBS 7041 - Microscopy Photographs	
GYPA	**MEA**
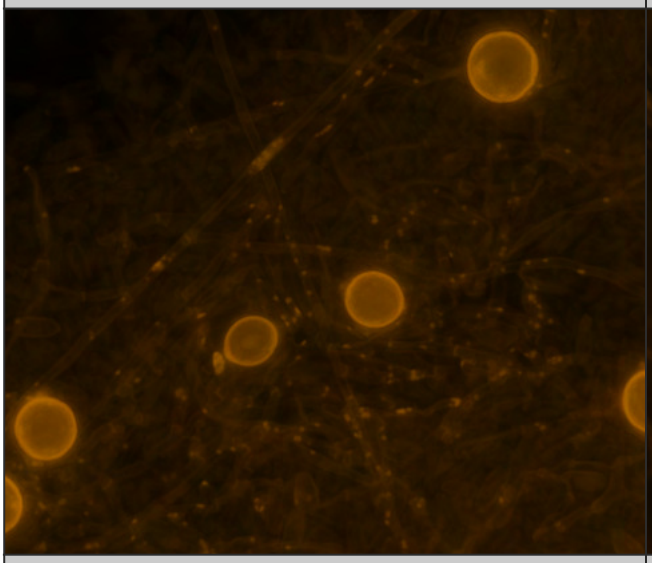	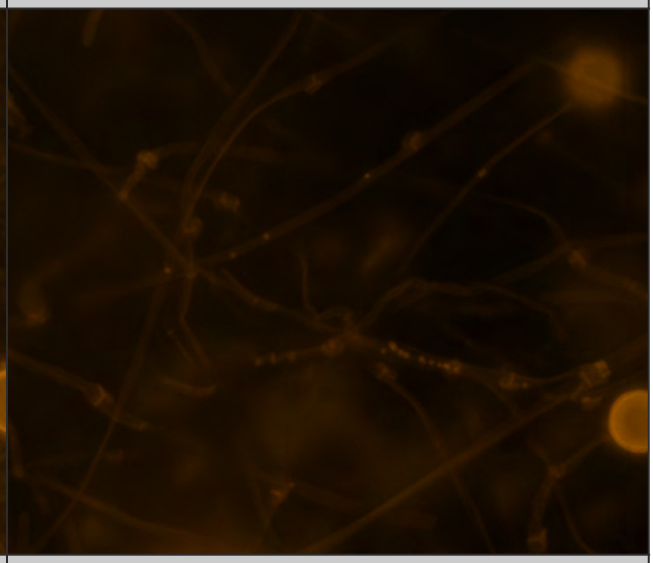
PDA	**X-AGAR**
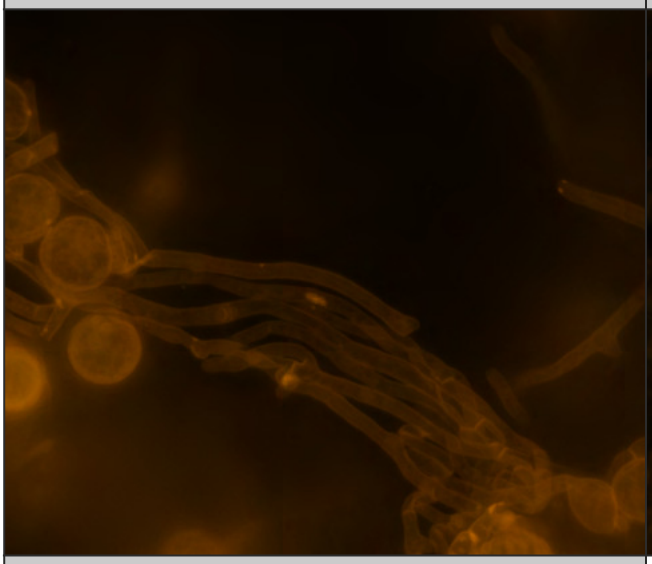	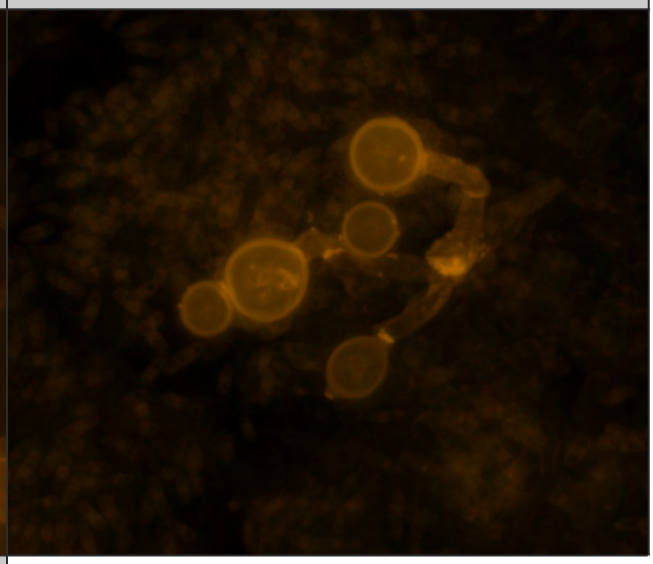
NITROGEN DEPLETED	
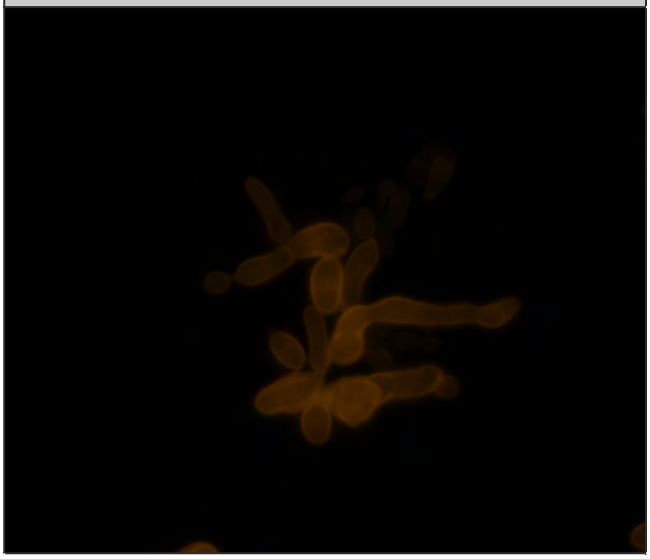	

CBS 7041 - Microscopy Photographs

CBS 14 - Culture Plates	
GYPA	**MEA**
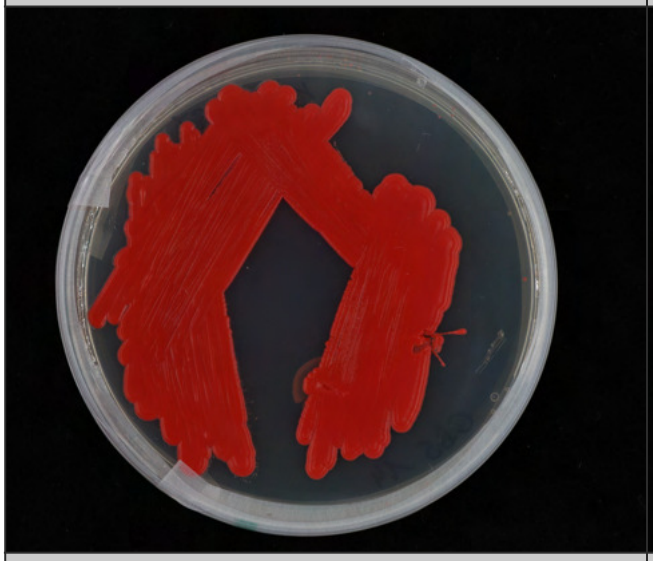	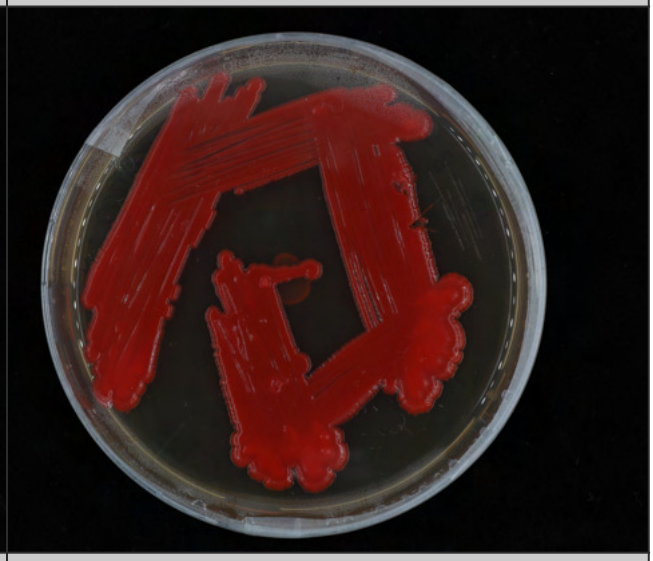
PDA	**X-AGAR**
	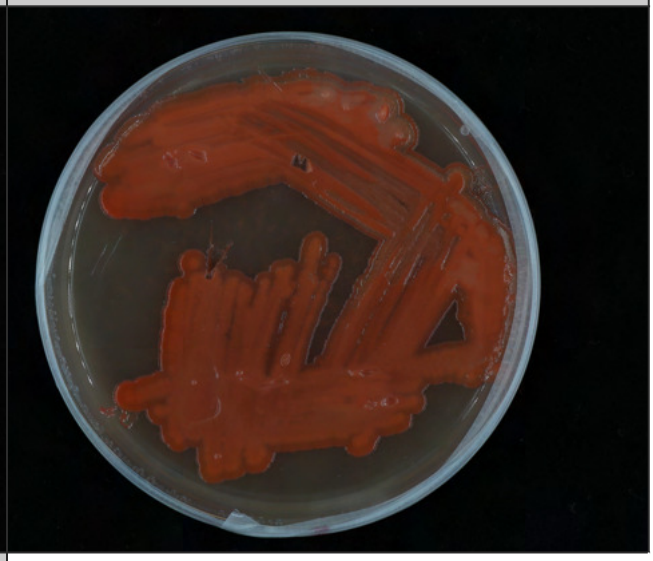
NITROGEN DEPLETED	
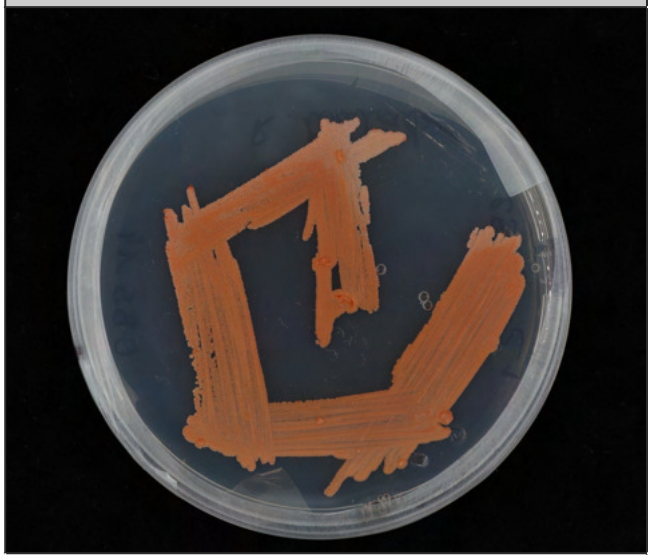	

CBS 14 - Culture Plates

CBS 14 - Microscopy Photographs	
GYPA	**MEA**
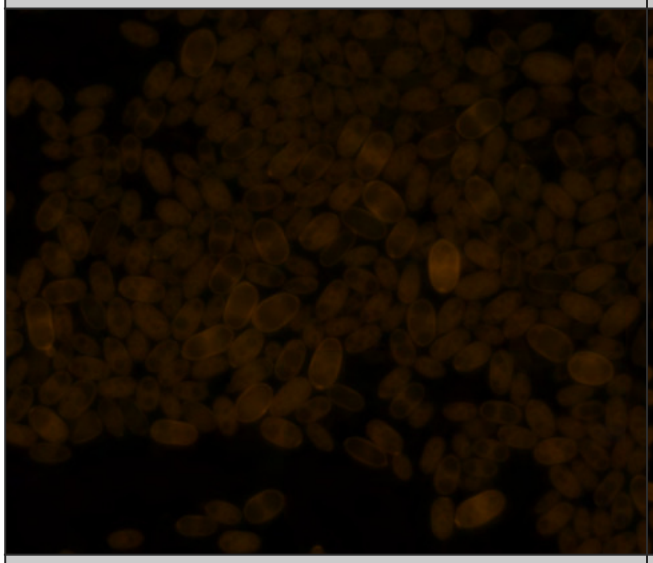	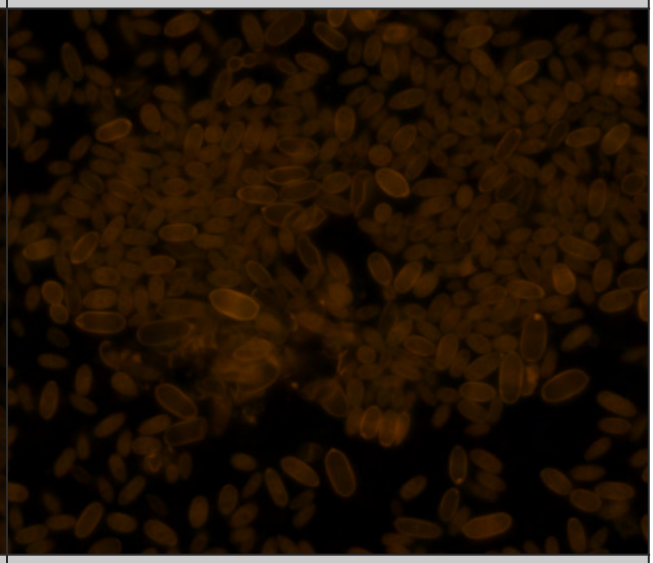
PDA	**X-AGAR**
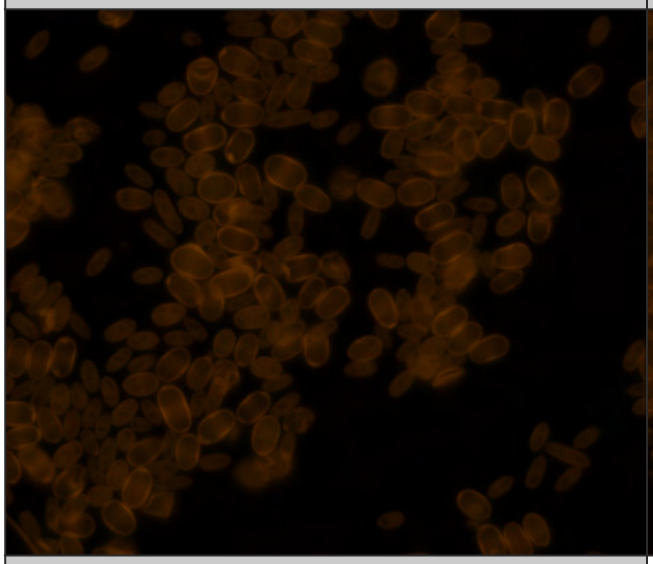	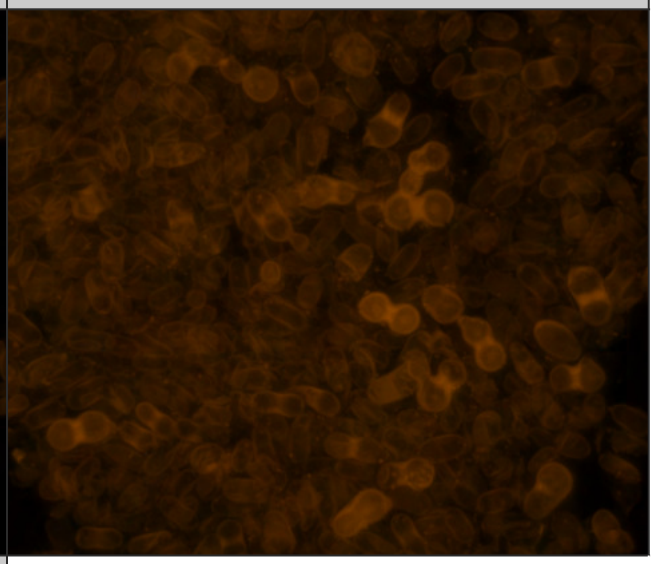
NITROGEN DEPLETED	
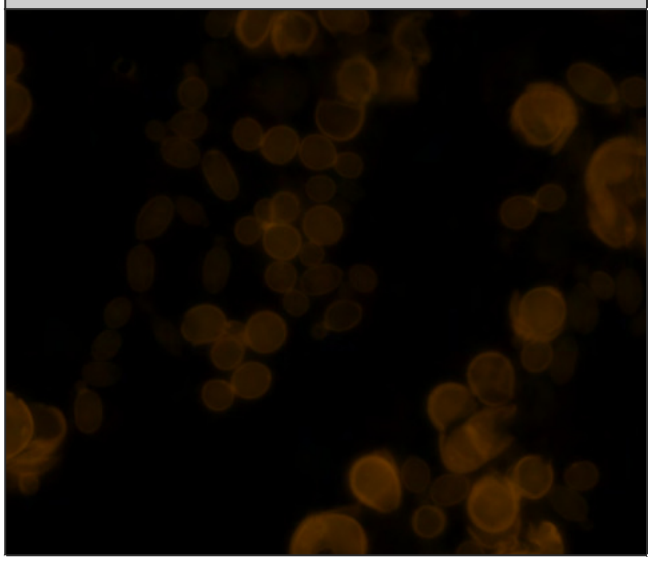	

CBS 14 - Microscopy Photographs

CBS 349 - Culture Plates	
GYPA	**MEA**
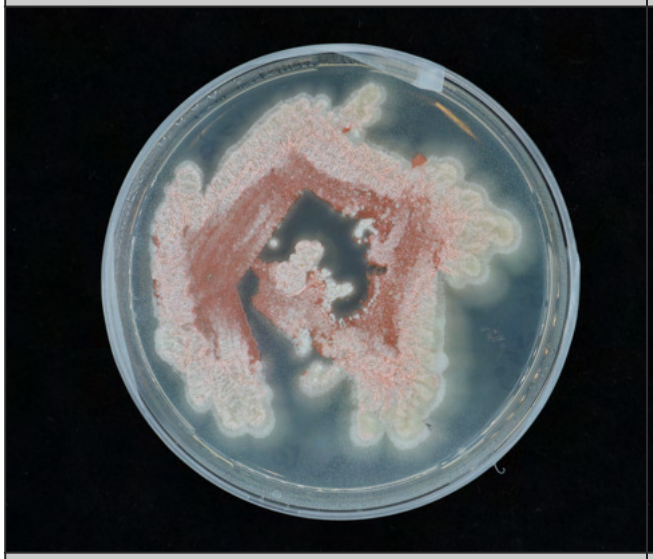	
PDA	**X-AGAR**
	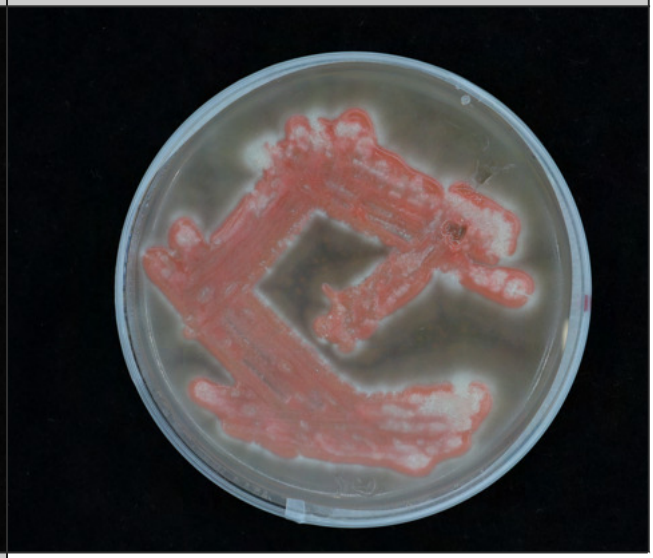
NITROGEN DEPLETED	
	

CBS 349 - Culture Plates

CBS 349 - Microscopy Photographs	
GYPA	**MEA**
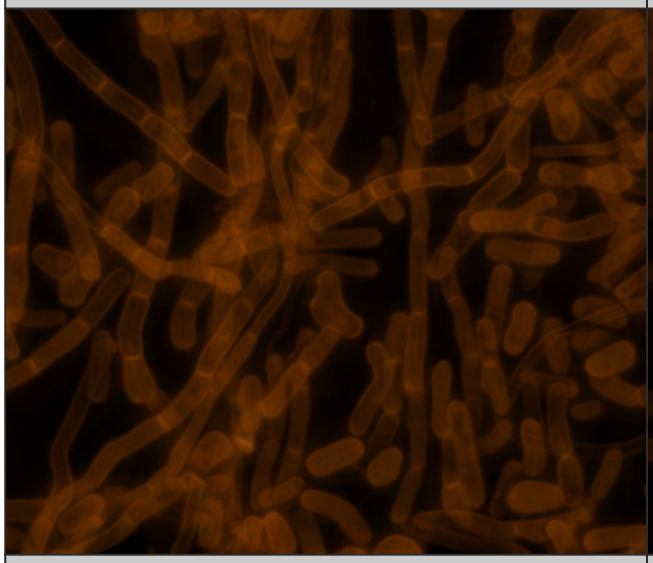	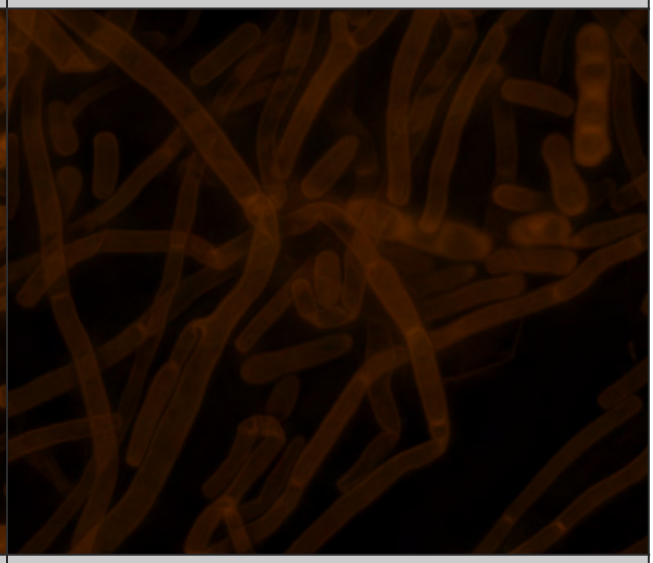
PDA	**X-AGAR**
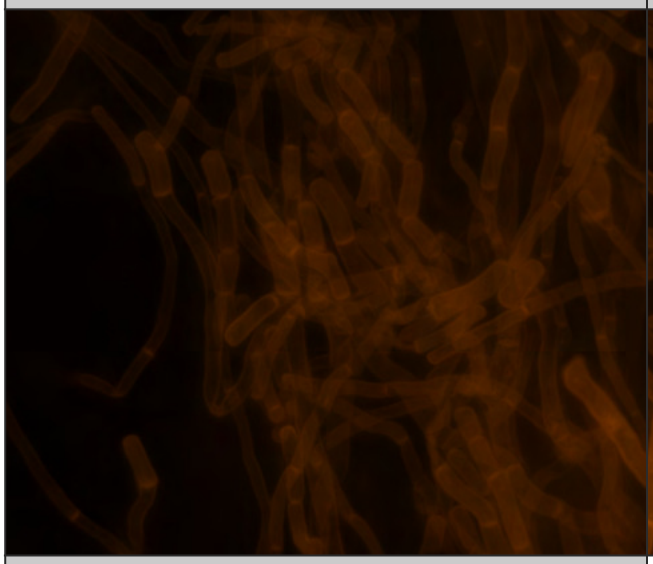	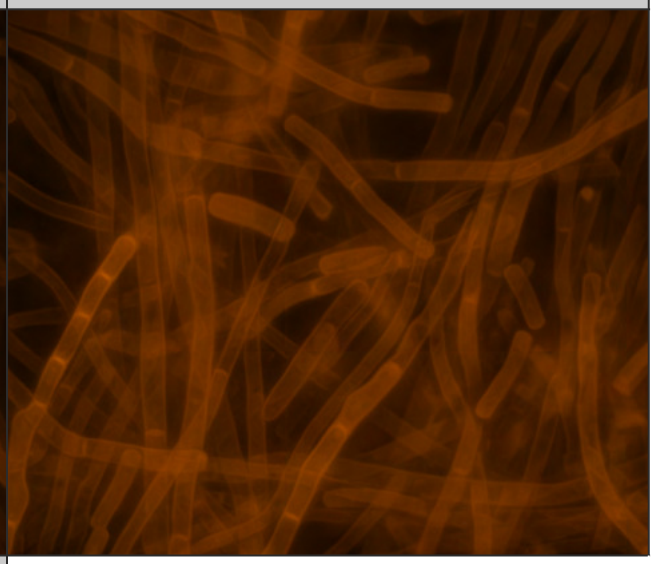
NITROGEN DEPLETED	
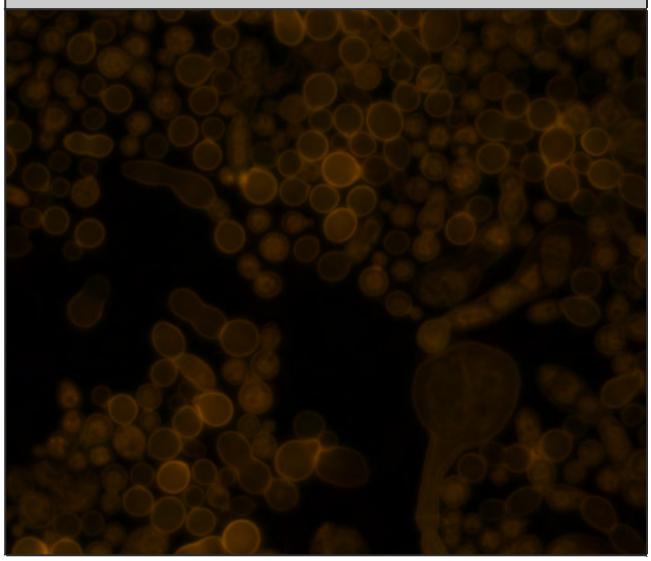	

CBS 349 - Microscopy Photographs

CBS 5940 - Culture Plates	
GYPA	**MEA**
	
PDA	**X-AGAR**
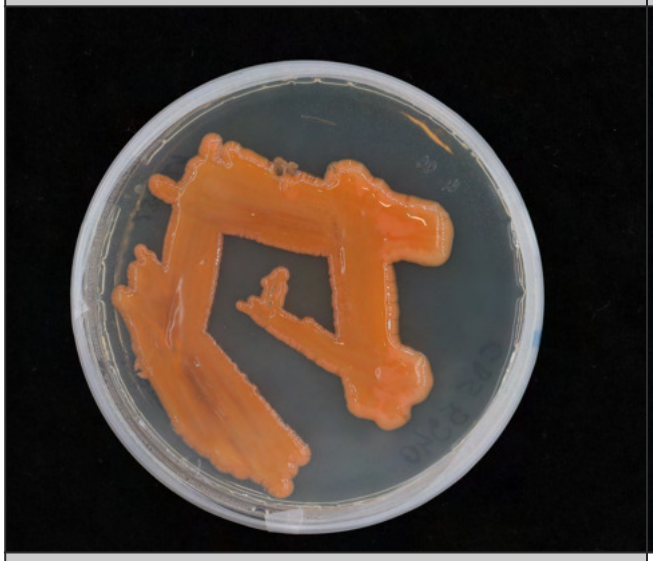	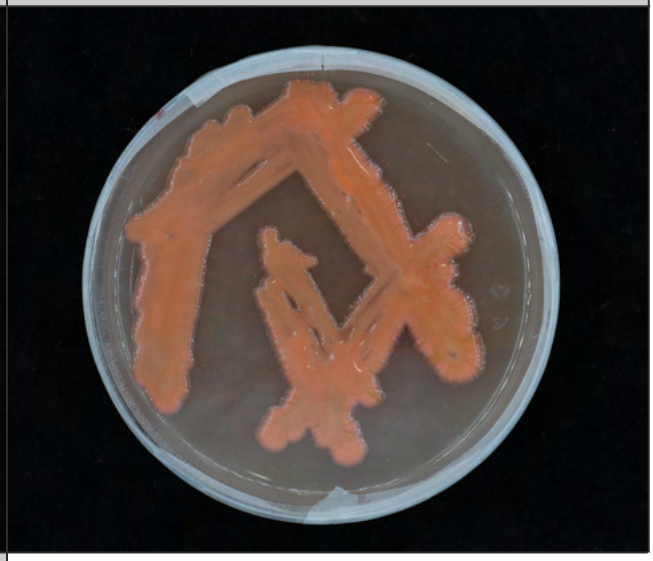
NITROGEN DEPLETED	
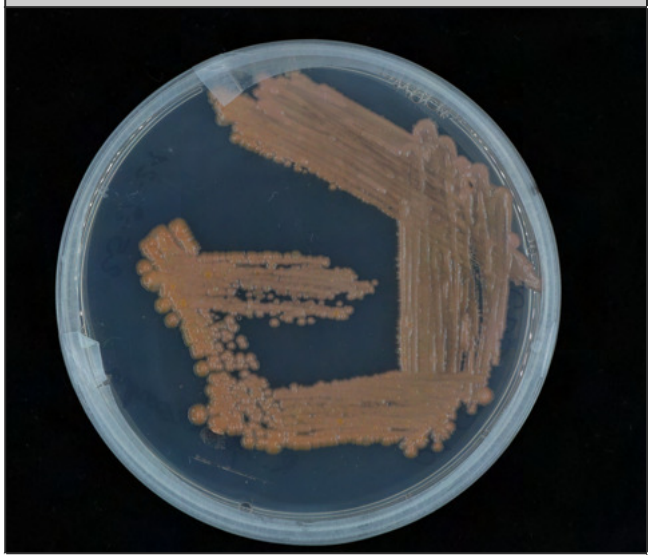	

CBS 5940 - Culture Plates

CBS 5940 - Microscopy Photographs	
GYPA	**MEA**
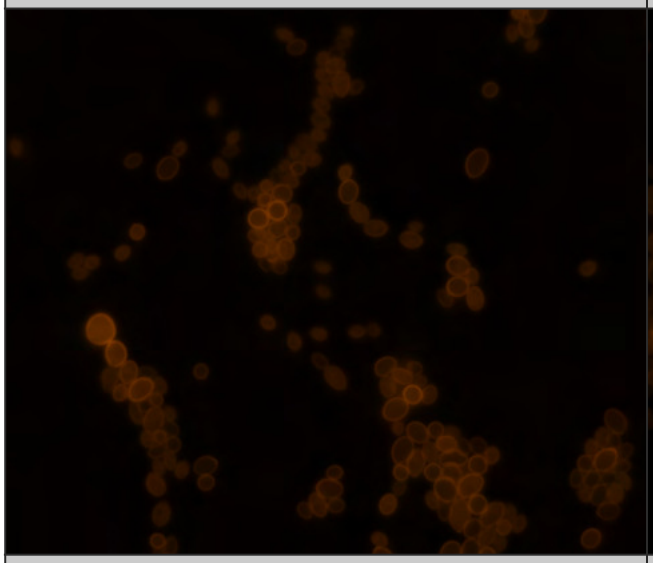	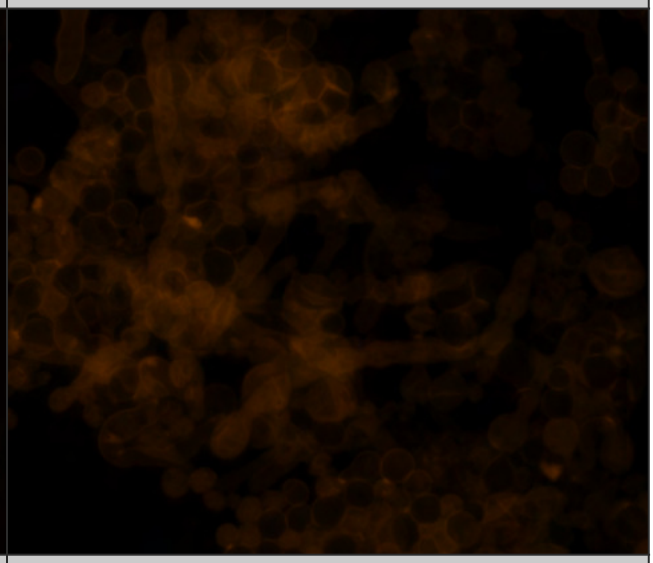
PDA	**X-AGAR**
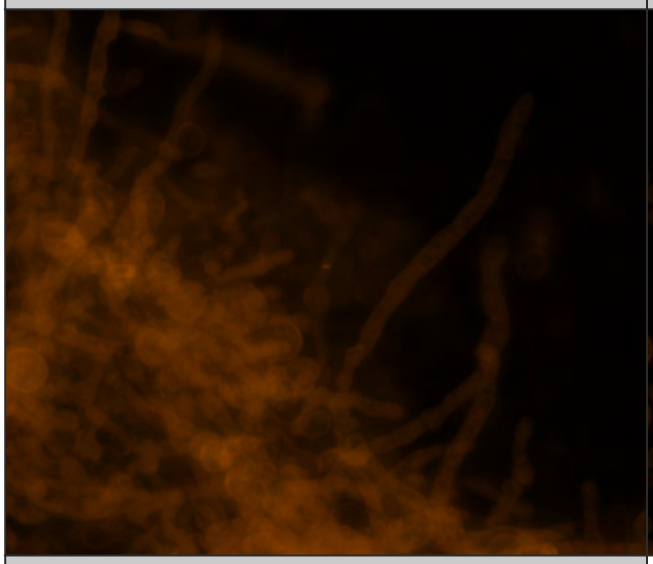	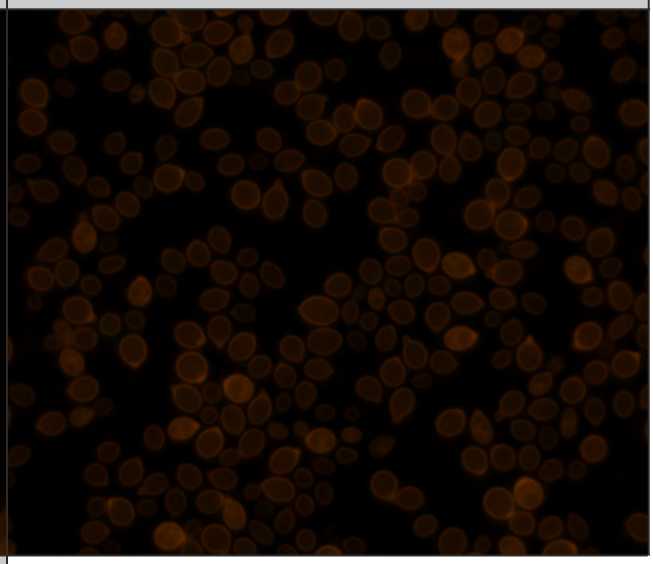
NITROGEN DEPLETED	
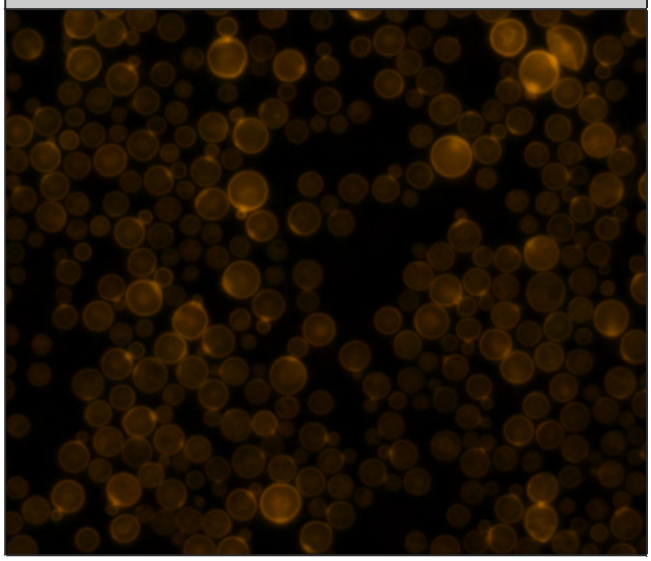	

CBS 5940 - Microscopy Photographs

CBS 5941 - Culture Plates	
GYPA	**MEA**
	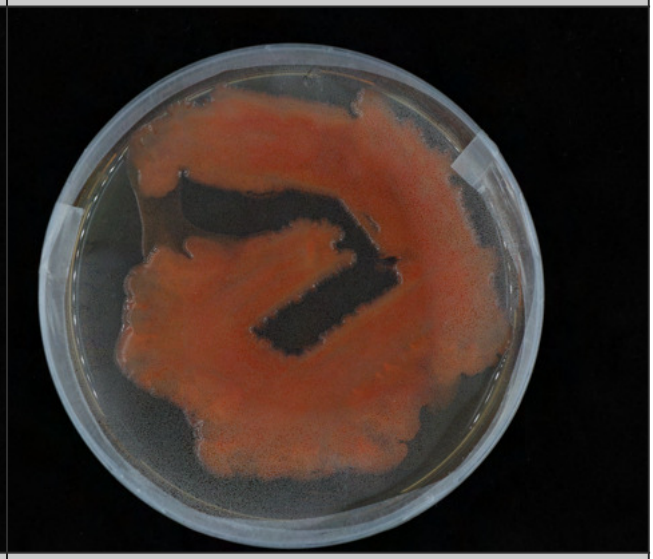
PDA	**X-AGAR**
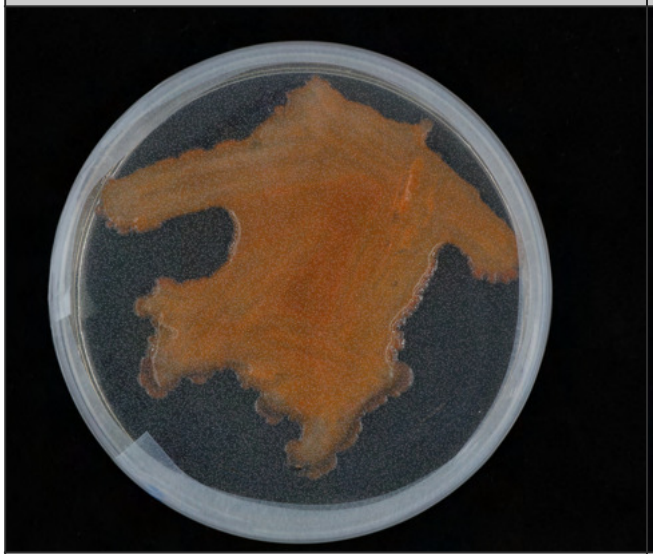	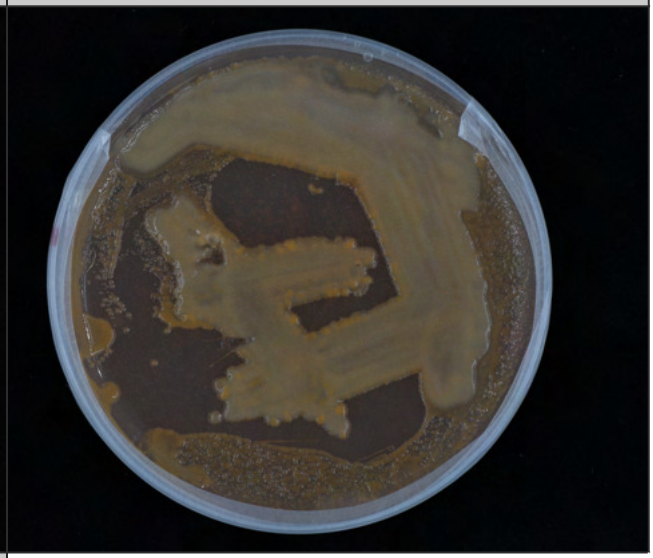
NITROGEN DEPLETED	
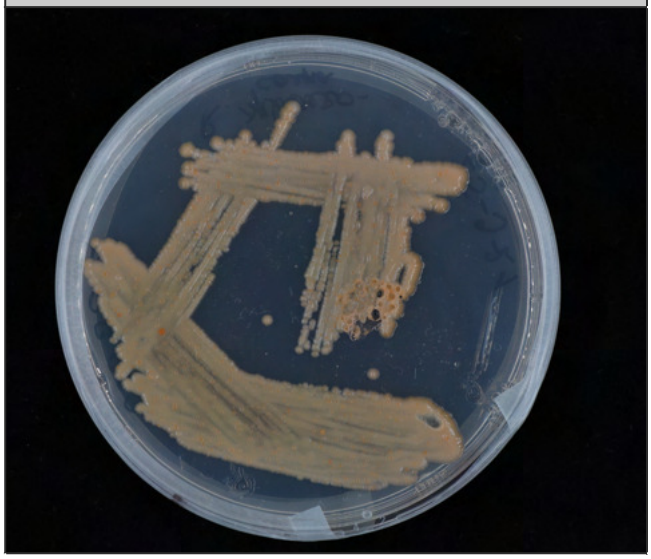	

CBS 5941 - Culture Plates

CBS 5941 - Microscopy Photographs	
GYPA	**MEA**
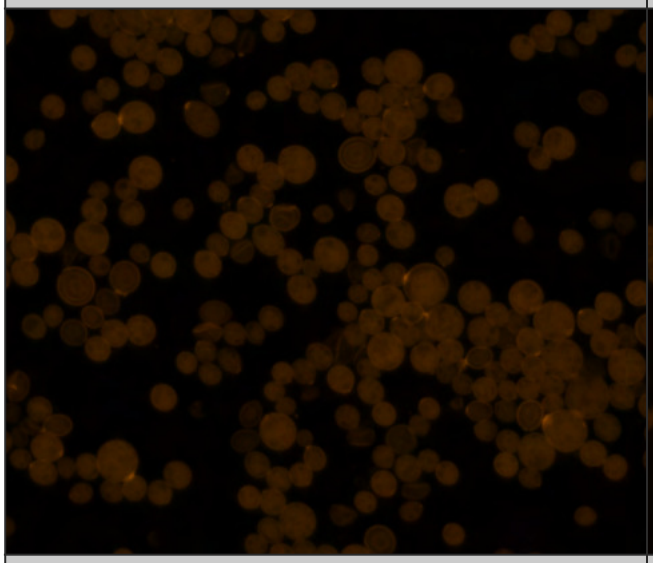	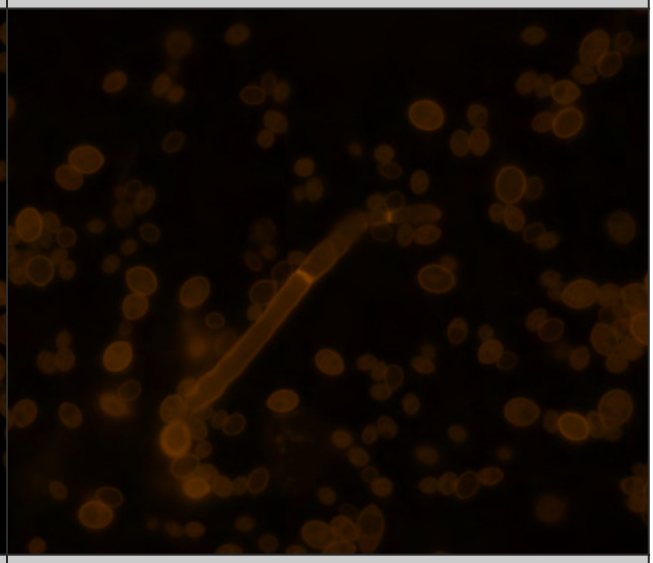
PDA	**X-AGAR**
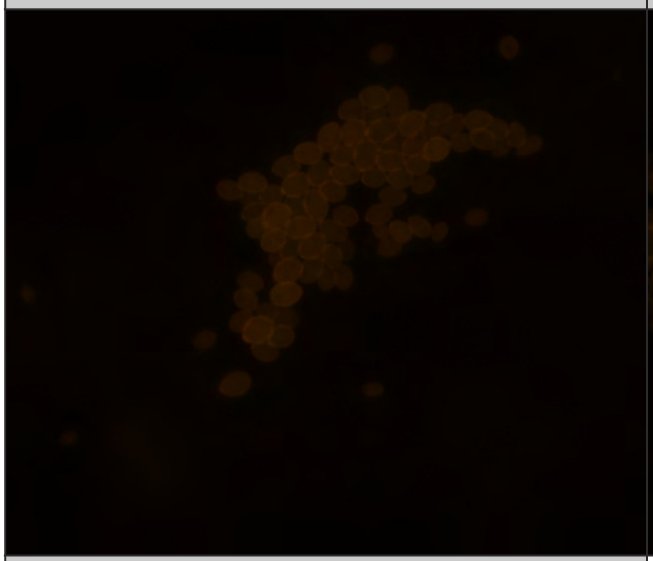	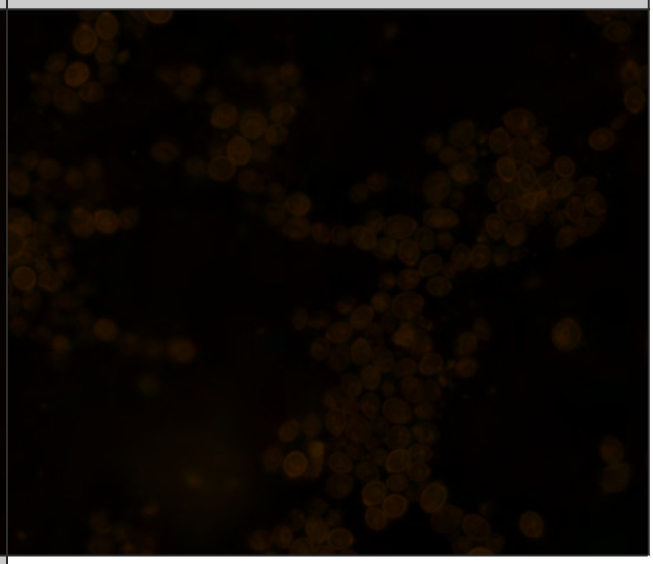
NITROGEN DEPLETED	
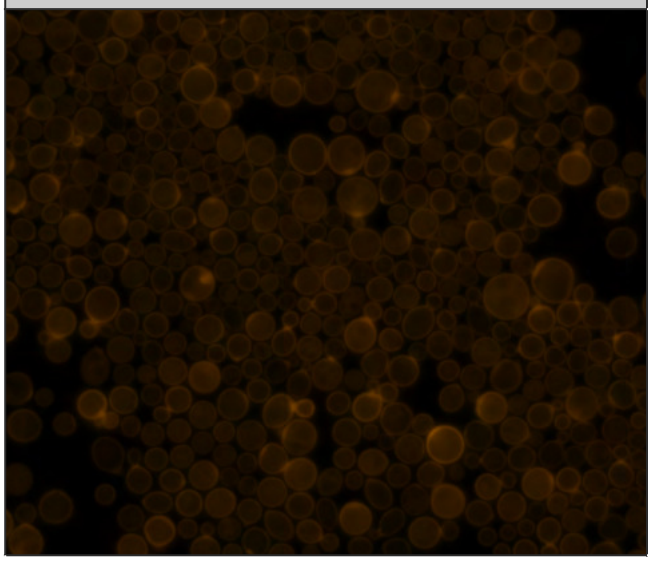	

CBS 5941 - Microscopy Photographs

CBS 5939 - Culture Plates	
GYPA	**MEA**
	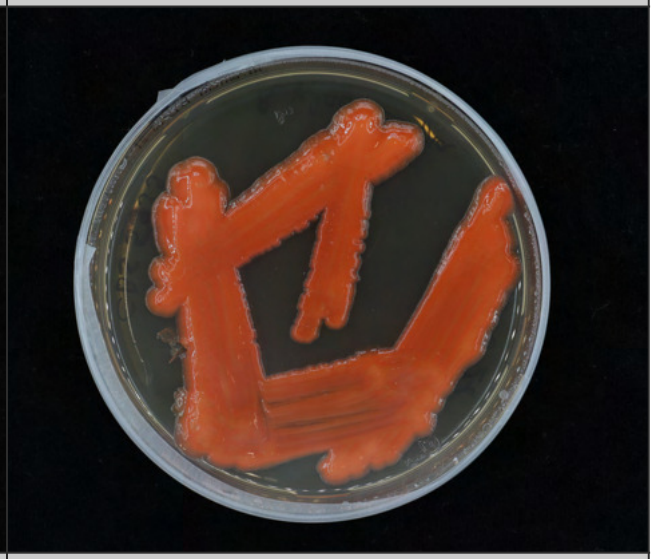
PDA	**X-AGAR**
	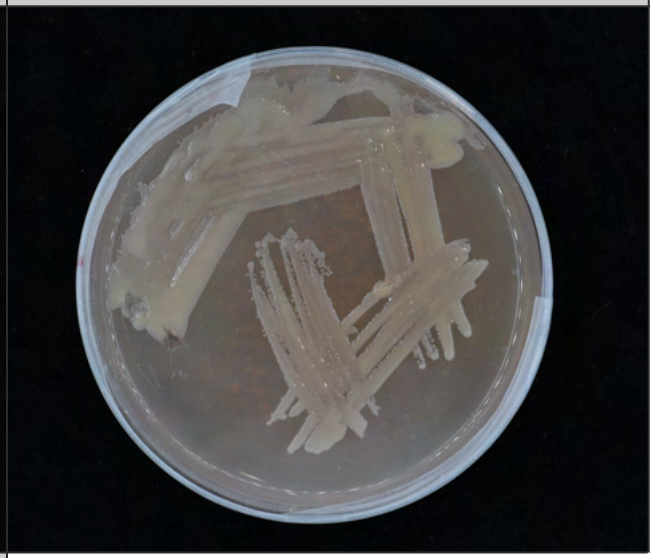
NITROGEN DEPLETED	
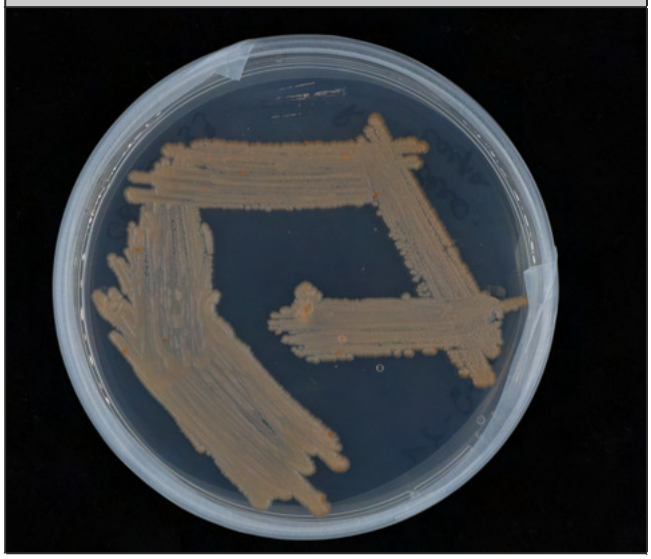	

CBS 5939 - Culture Plates

CBS 5939 - Microscopy Photographs	
GYPA	**MEA**
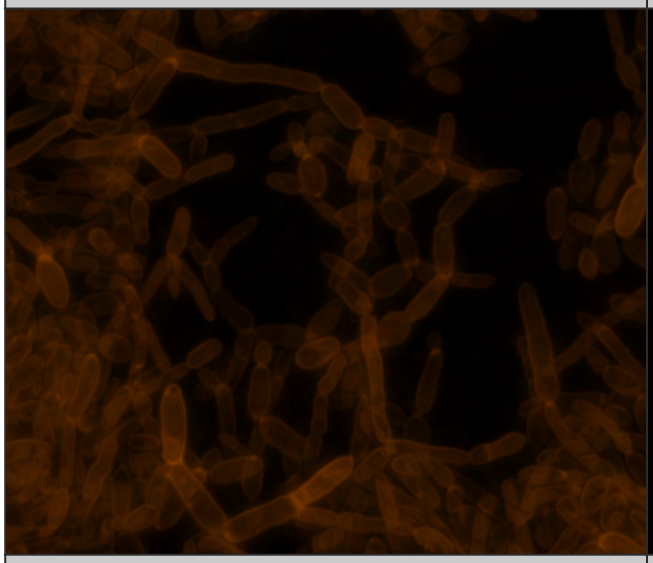	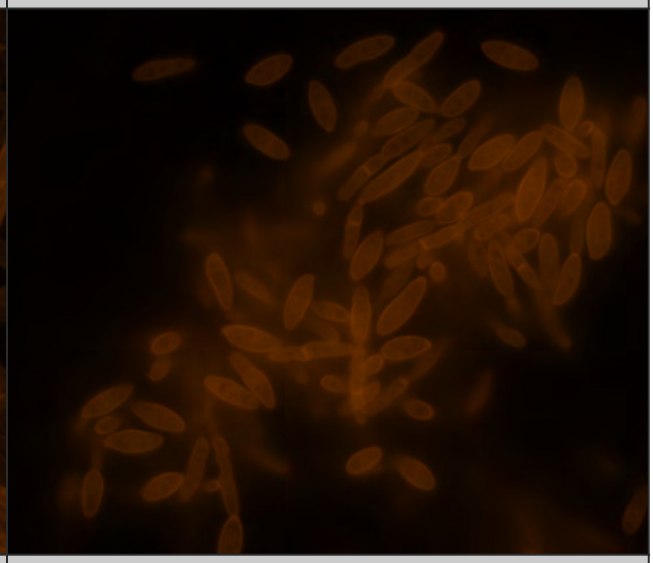
PDA	**X-AGAR**
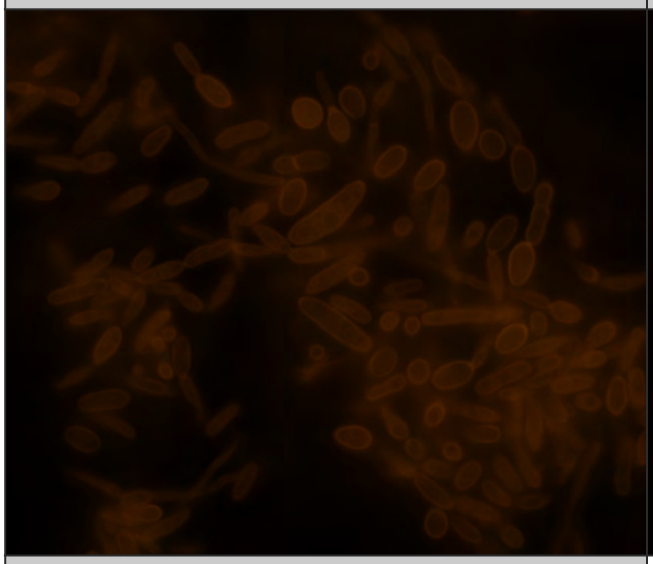	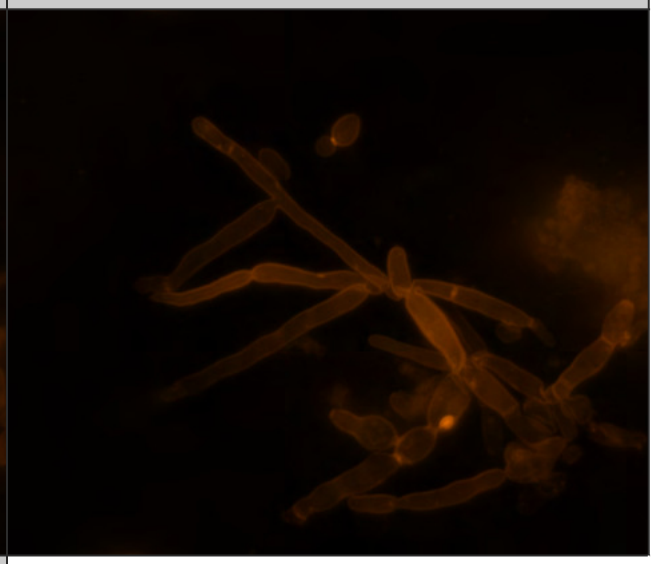
NITROGEN DEPLETED	
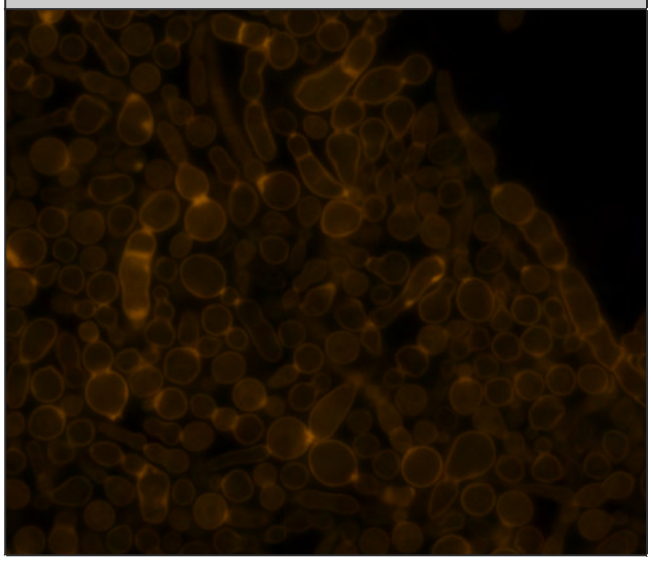	

CBS 5939 - Microscopy Photographs

Annexes - Protocols & Recipes

Media recipes

Cherry extract
- Cherries without stones and without petioles
- Tap water (1L)

Boil and simmer for 2 hours and filter.
Sterilize at 110˚C for 30 minutes.

GYPA

= Glucose-peptone-yeast extract agar
- Glucose (40g)
- Bactopeptone (5g)
- Yeast extract (5g)
- Water (1l)
- Spanish Agar (15g)

Prepare on hotplate stirrers to ensure complete dissolving of components.
Autoclaving at 110˚C for 15 minutes

MEA

= Malt extract agar
- Malt extract (30g) (Commercially at Oxoid CM59)
- Spanish Agar (15g)
- Water (1l)

Autoclaving at 121˚C for 15 minutes

Nitrogen-depleted (N-Dep)
- Bactopeptone (0,5g)
- yeast extract (1g)
- glucose (5g)
- sea salt (36g)
- agar (14g)
- water (1l)
- Spanish Agar (15g)

Additional centrifugation of the medium might also help deplete the medium of Nitrogen.
Autoclaving at 121˚C for 15 minutes

Oatmeal extract (600ml)
- Oatmeal (30g)
- Tap water (1l)

Wrap oatmeal flakes in cloth and hang in pan. Bring to boil and simmer for 2 hours. Filter through cloth.
Sterilize at 121˚C for 15 minutes

PDA

= Potato-dextrose extract agar
- Potato extract (0,23L)
- Glucose (20g)
- Water (0,77L)
- Spanish Agar (15g)

Autoclaving at 121˚C for 15 minutes

PEGS

= Peptone-Glucose-Sacharose
- Bactopeptone (5g)
- K_2HPO_4 (1g)
- $MgSO_4 \cdot 7H_2O$ (0,5g)
- $Ca(NO_3)_2$ (1g)
- Glucose (20g)
- Sacharose (10g)
- Water (1l)

Sterilize at 110˚C for 30 minutes

Potato extract

Wash and grind the desired amount of potatoes. Use 300ml tap water for 100g potatoes. Leave at 4˚C overnight & filter.
Sterilize at 121˚C for 15 minutes. Final pH = 6.6

X-Agar

= Glucose-peptone-yeast extract agar
- Cherry extract (110ml)
- PEGS (600ml)
- Oatmeal extract (600ml)
- Water (600ml)
- Spanish Agar (15g)

Mix all ingredients except cherry extract, heat and stir until dissolved. Add cherry extract & mix. Sterilize at 110˚C for 30 minutes final pH = 5.4

YPD

= Yeast-peptone-dextrose agar
- Bactopeptone (1g)
- yeast extract (1g)
- glucose (10g)
- sea salt (36g)
- agar (14g)
- water (1l)
- Spanish Agar (15g)

Autoclaving at 121˚C for 15 minutes

Protocol 1

1. Prepare two samples. Take 0,2g from the liquid culture for each sample and place them into a separate eppendorf containing 1 ml CTAB (100mM Tris-HCl, 1,4M NaCl, 20mM EDTA, 2% (w/v) CTAB, 1% (w/v) PVP).
2. Add 0,5 g glass beads.
3. Vortex 10 times for 30 seconds with 30 seconds of rest in between.
4. Split the samples into two treatments:
    1. Short treatments named “K”:

        Samples continue to the centrifugation procedure.

    2. Long treatment named “L”

        Vortex samples for 10 minutes and proceed to the centrifugation procedure afterwards.
5. Transfer the sample to a new eppendorf using a pipette while avoiding picking up too many glass beads.
6. Centrifugation procedure:

G	Time	Acquired fractions
2000	8 minutes	pellet
4000	8 minutes	pellet, floating mass
8000	8 minutes	pellet, floating mass
12000	10 minutes	pellet, floating mass, supernatans

    Between every centrifugation step, the supernatant is separated from the pellet and the supernatant is used in the next centrifugation step.
7. Evaluate the fractions through epi-fluorescence microscopy with a TRITC filter after staining the sample with Congo red.

Protocol 2

1. Prepare two samples. Take 0,2g from the liquid culture for each sample and place them into a separate eppendorf.
2. Stain each sample with 0,5 ml of Congo red.
3. Vortex the sample briefly to ensure a homogenized staining of the sample.
4. Transfer the stained samples into a new eppendorf.
5. Split the samples:
    1. Sample labeled “**CR-CTAB**”:

        Add 1ml of CTAB.

    2. Sample labeled “**CR-TRIS**”:

        Add 1ml of TRIS.
6. Add 0,5 g glass beads to each sample.
7. Vortex 10 times for 30 seconds with 30 seconds of rest in between.
8. Transfer the sample to a new eppendorf using a pipette while avoiding picking up too many glass beads.
9. Centrifugation procedure:

G	Time	Acquired fractions
8000	8 minutes	pellet, floating mass
12000	10 minutes	pellet, floating mass, supernatans

    Between every centrifugation step, the supernatant is separated from the pellet and the supernatant is used in the next centrifugation step.
10. Evaluate the fractions through epi-fluorescence microscopy with a TRITC filter.

Protocol 3

1. Prepare two samples. Take 0,2g from the liquid culture for each sample and place them into a separate eppendorf.
2. Stain each sample with 0,5 ml of Congo red.
3. Vortex the sample briefly to ensure a homogenized staining of the sample.
4. Remove the excess of Congo red with blotting paper.
5. Transfer the stained samples into a new eppendorf and add 1ml of CTAB to each.
6. Let the samples incubate for 48 hours at room temperature.
7. Split the samples:
    1. Sample labeled “**BB-B**” (Bead Beater - Buffer):

       Add 0,5 g glass beads to the eppendorf.
    2. Sample labeled “**BB-NB**” (Bead Beater - No Buffer):

       Remove the sample from the buffer and transfer it into a new eppendorf. Add 0,5 g glass beads to the eppendorf.
8. Put both samples into liquid nitrogen for a few seconds until completely frozen.
9. Bead beat the samples for 1 minute at a frequency of 30 Hz. Repeat this step once more.
10. Add 1ml of CTAB to the “**BB-NB**” sample.
11. Transfer the sample to a new eppendorf using a pipette while avoiding picking up too many glass beads.
12. Centrifugation procedure:

G	Time	Acquired fractions
8000	10 minutes	pellet
12000	10 minutes	pellet, floating mass, supernatans

    Between every centrifugation step, the supernatant is separated from the pellet and the supernatant is used in the next centrifugation step.
13. Evaluate the fractions through epi-fluorescence microscopy with a TRITC filter.

Protocol 4

1. Prepare three samples. Take 0,2g from the liquid culture for each sample and place them into a separate eppendorf.
2. Stain each sample with 0,5 ml of Congo red.
3. Vortex the sample briefly to ensure a homogenized staining of the sample.
4. Remove the excess of Congo red with blotting paper.
5. Transfer the stained samples into a new eppendorf and add 1ml of CTAB to each.
6. Let the samples incubate for 72 hours at room temperature.
7. Split the samples:
    1. Sample labeled "**CR-CT3-N2**" (Congo red - CTAB, 3 days - Liquid nitrogen):

       Remove the sample from the buffer and transfer it into a new eppendorf.
       Put the sample into liquid nitrogen for a few seconds until completely frozen.
       Add 0,5 g glass beads to the eppendorf.
    2. Sample labeled "**CR-CT3-N2B**" (Congo red - CTAB, 3 days - Liquid nitrogen - Buffer):

       Remove the sample from the buffer and transfer it into a new eppendorf.
       Put the sample into liquid nitrogen for a few seconds until completely frozen.
       Add 0,5 g glass beads to the eppendorf.
       Add 1ml of CTAB buffer.
    3. Sample labeled "**CR-CT3-BBB**" (Congo red - CTAB, 3 days - Bead Beater Buffer):

       Remove the sample from the buffer and transfer it into a new eppendorf.
       Add 0,5 g glass beads to the eppendorf.
       Add 1ml of CTAB buffer.
8. Bead beat the samples for 1 minute at a frequency of 30 Hz. Repeat this step once more.
9. Add 1ml of CTAB buffer to the "**CR-CT3-N2**" sample.
10. Transfer the sample to a new eppendorf using a pipette while avoiding picking up too many glass beads.
11. Centrifugation procedure:

G	Time	Acquired fractions
8000	10 minutes	pellet
12000	10 minutes	pellet, floating mass, supernatans

    Between every centrifugation step, the supernatant is separated from the pellet and the supernatant is used in the next centrifugation step.
12. Evaluate the fractions through epi-fluorescence microscopy with a TRITC filter.

Protocol 5

1. Prepare one sample. Take 0,2g from the liquid culture and place it into an eppendorf.
2. Stain the sample with 0,5 ml of Congo red.
3. Vortex the sample briefly to ensure a homogenized staining of the sample.
4. Remove the excess of Congo red with blotting paper.
5. Transfer the stained sample into a new eppendorf and add 1ml of TRIS buffer (0,375M, pH = 8,8).
6. Leave the samples for a moment. Remove the tissue from the buffer and put it into a new eppendorf.
7. Put the sample into liquid nitrogen for a few seconds until completely frozen.
8. Take a new eppendorf and add 0,5 g glass beads. Add the frozen tissue to this eppendorf.
9. Label the sample as "**CR-TR-N2**" (Congo red - TRIS - liquid nitrogen).
10. Bead beat the sample for 1 minute at a frequency of 30 Hz. Repeat this step once more.
11. Add 1ml of TRIS buffer to the sample.
12. Transfer the sample to a new eppendorf using a pipette while avoiding picking up too many glass beads.
13. Centrifugation procedure:

G	Time	Acquired fractions
4000	10 minutes	pellet
8000	10 minutes	pellet
12000	10 minutes	pellet, supernatans

    Between every centrifugation step, the supernatant is separated from the pellet and the supernatant is used in the next centrifugation step.

14. Evaluate the fractions through epi-fluorescence microscopy with a TRITC filter.

Protocol 6

1. Prepare one sample. Take 0,2g from the liquid culture and place it into an eppendorf.
2. Stain the sample with 0,5 ml of Congo red.
3. Vortex the sample briefly to ensure a homogenized staining of the sample.
4. Remove the excess of Congo red with blotting paper.
5. Transfer the stained sample into a new eppendorf and add 1ml of TRIS buffer (0,375M, pH = 8,8).
6. Leave the samples for a moment. Remove the tissue from the buffer and put it into a new eppendorf.
7. Put the tissue directly into liquid nitrogen (not in an ependorf) for a few seconds until completely frozen.
8. Take a new eppendorf and add 0,5 g glass beads. Add the frozen tissue to this eppendorf.
9. Label the sample as "**CR-TR-BB4**" (Congo red - TRIS - liquid nitrogen - Bead Beater).
10. Bead beat the sample for 1 minute at a frequency of 30 Hz. Repeat this step once more.
11. Add 1ml of TRIS buffer to the sample.
12. Transfer the sample to a new eppendorf using a pipette while avoiding picking up too many glass beads.
13. Centrifugation procedure:

G	Time	Acquired fractions
4000	10 minutes	pellet
8000	10 minutes	pellet
12000	10 minutes	pellet, supernatans

Between every centrifugation step, the supernatant is separated from the pellet and the supernatant is used in the next centrifugation step.

14. Evaluate the fractions through epi-fluorescence microscopy with a TRITC filter.

Protocol 7

1. Prepare one sample. Take 0,2g from the liquid culture and place it into an eppendorf.
2. Stain the sample with 0,5 ml of Congo red.
3. Vortex the sample briefly to ensure a homogenized staining of the sample.
4. Remove the excess of Congo red with blotting paper.
5. Transfer the stained sample into a new eppendorf and add 1ml of TRIS buffer (0,375M, pH = 8,8).
6. Leave the samples for a moment. Remove the tissue from the buffer and put it into a new eppendorf.
7. Put the tissue directly into liquid nitrogen (not in an ependorf) for a few seconds until completely frozen.
8. Refine the sample with a mortar and pestle.
9. Take a new eppendorf and add 0,5 g glass beads. Add the refined tissue to this eppendorf.
10. Bead beat the sample for 1 minute at a frequency of 30 Hz. Repeat this step once more.
11. Add 1ml of TRIS buffer to the sample.
12. Transfer the sample to a new eppendorf using a pipette while avoiding picking up too many glass beads.
13. Centrifugation procedure:

G	Time	Acquired fractions
4000	10 minutes	pellet
8000	10 minutes	pellet
12000	10 minutes	pellet, supernatans

Between every centrifugation step, the supernatant is separated from the pellet and the supernatant is used in the next centrifugation step.

14. Evaluate the fractions through epi-fluorescence microscopy with a TRITC filter.

Sequential Filter Protocol

1. Take 0,2g sample from the liquid culture and place it into an eppendorf.
2. Stain the sample with 0,5 ml of Congo red.
3. Vortex the sample briefly to ensure a homogenized staining of the sample.
4. Remove the tissue from the Congo red and remove the excess of Congo red from the tissue with blotting paper.
5. Transfer the stained sample into a new eppendorf and add 1ml of TRIS buffer (0,375M, pH = 8,8).
6. Leave the samples for a moment. Remove the tissue from the buffer and put it into a new eppendorf.
7. Put the tissue directly into liquid nitrogen (not in an ependorf) for a few seconds until completely frozen.
8. Take a new eppendorf and add 0,5 g glass beads. Add the frozen tissue to this eppendorf.
9. Bead beat the sample for 1 minute at a frequency of 30 Hz. Repeat this step once more.
10. Add 200µl of TRIS buffer to the sample and briefly vortex to homogenize the sample.
11. Take a new eppendorf and place a pluriStrainer Mini with mesh size **100µm** in it. Transfer the entire sample, including all glass beads onto the filter.
12. Centrifuge 10 minutes at 8000G.
13. Remove the filter and resuspend the pellet.
    1. Take a few microliters to make a microscopy slide to evaluate the fraction.
14. Transfer the filtrate onto a pluriStrainer Mini with mesh size **40µm** in a new eppendorf.
15. Centrifuge 10 minutes at 8000G.
16. Remove the filter and resuspend the pellet.
    1. Take a few microliters to make a microscopy slide to evaluate the fraction.
17. Transfer the filtrate onto a pluriStrainer Mini with mesh size **20µm** in a new eppendorf.
18. Centrifuge 10 minutes at 8000G.
19. Remove the filter and resuspend the pellet.
    1. Take a few microliters to make a microscopy slide to evaluate the fraction.
20. Transfer the filtrate onto a pluriStrainer Mini with mesh size **10µm** in a new eppendorf.
21. Centrifuge 10 minutes at 8000G. Resuspend the pellet.
    1. Take a few microliters to make a microscopy slide to evaluate the fraction.
22. Gently dry the slides on a heat plate and evaluate the slides through epi-fluorescence microscopy.

Annexes - Tables

Species (Basionym)	current name	Classification
Mastigobasidium intermedium Golubev	Leucosporidium intermedium (Nakase & M. Suzuki) M. Groenew. & Q.M. Wang	Microbotryomycetes
Leucosporidium fellii Gim.-Jurado & Uden	Leucosporidium fellii Gim.-Jurado & Uden	Microbotryomycetes
Leucosporidium golubevii Gadanho, J.P. Samp. & R. Bauer	Leucosporidium golubevii Gadanho, J.P. Samp. & R. Bauer	Microbotryomycetes
Leucosporidium scottii Fell, Statzell, I.L. Hunter & Phaff	Leucosporidium scottii Fell, Statzell, I.L. Hunter & Phaff	Microbotryomycetes
Sporidiobolus ruinenii Holzschu, Tredick & Phaff	Rhodosporidiobolus ruineniae (Holzschu, Tredick & Phaff) Q.M. Wang, F.Y. Bai, M. Groenew. & Boekhout	Microbotryomycetes
Sporidiobolus johnsonii Nyland	Sporobolomyces johnsonii (Nyland) Q.M. Wang, F.Y. Bai, M. Groenew. & Boekhout	Microbotryomycetes
Blastoderma salmonicolor B. Fisch. & Brebeck	Sporobolomyces salmonicolor (B. Fisch. & Brebeck) Kluyver & C.B. Niel	Microbotryomycetes
Rhodosporidium toruloides Banno	Rhodotorula toruloides (Banno) Q.M. Wang, F.Y. Bai, M. Groenew. & Boekhout	Microbotryomycetes
Rhodosporidium sphaerocarpum S.Y. Newell & Fell	Rhodotorula sphaerocarpa (S.Y. Newell & Fell) Q.M. Wang, F.Y. Bai, M. Groenew. & Boekhout	Microbotryomycetes
Sporobolomyces yamatoanus Nakase, M. Suzuki & Itoh	Bannozyma yamatoana (Nakase, M. Suzuki & Itoh) Q.M. Wang, F.Y. Bai, M. Groenew. & Boekhout	Microbotryomycetes
Heterogastridium pycnidioideum Oberw. & R. Bauer	Heterogastridium pycnidioideum Oberw. & R. Bauer	Microbotryomycetes
Atractocolax pulvinatus R. Kirschner, R. Bauer & Oberw.	Atractocolax pulvinatus R. Kirschner, R. Bauer & Oberw.	Microbotryomycetes
Platygloea effusa J. Schröt.	Colacogloea effusa (J. Schröt.) V. Malysheva, Schoutteten & Spirin	Microbotryomycetes
Colacogloea papilionacea R. Kirschner & Oberw.	Colacogloea papilionacea R. Kirschner & Oberw.	Microbotryomycetes
Colacosiphon filiformis R. Kirschner, R. Bauer & Oberw.	Colacosiphon filiformis R. Kirschner, R. Bauer & Oberw.	Cryptomycocolacomycetes
Cryptomycocolax abnormis Oberw. & R. Bauer	Cryptomycocolax abnormis Oberw. & R. Bauer	Cryptomycocolacomycetes
Krieglsteinera lasiosphaeriae Pouzar	Krieglsteinera lasiosphaeriae Pouzar	Basidiomycota incertae sedis

Platygloea bispora Hauerslev	Colacogloea bispora (Hauerslev) Oberw. & R. Bauer	Basidiomycota incertae sedis
Colacogloea allantospora Ginns & Bandoni	Colacogloea allantospora Ginns & Bandoni	Basidiomycota incertae sedis

Table 1: Species that were confirmed to contain colacosomes.

Species	Class	Order	Family
Achroomyces insignis (Sloofia sp.)	Pucciniomycetes	Platygloeales	Platygloeaceae
Achroomyces sp. nov.	Pucciniomycetes	Platygloeales	Platygloeaceae
Bannozyma yamatoana	Microbotryomycetes		Chrysozymaceae
Colacogloea effusa (= C. peniophorae)	Microbotryomycetes		Colacogloeaceae
Colacogloea sp. nov.	Microbotryomycetes		Colacogloeaceae
Hyalopycnis blepharistoma/ Heterogastridium	Microbotryomycetes	Heterogastridiales	Heterogastridiaceae
Leucosporidium scottii	Microbotryomycetes	Microbotryales	Leucosporidiaceae
Rhodosporidiobolus microsporus	Microbotryomycetes	Sporidiobolales	Sporidiobolaceae
Rhodosporidiobolus ruineniae	Microbotryomycetes	Sporidiobolales	Sporidiobolaceae
Rhodotorula sphaerocarpum	Microbotryomycetes	Sporidiobolales	Sporidiobolaceae
Rhodotorula toruloides	Microbotryomycetes	Sporidiobolales	Sporidiobolaceae
Sporobolomyces johnsonii	Microbotryomycetes	Sporidiobolales	Sporidiobolaceae
Sporobolomyces salmonicolor	Microbotryomycetes	Sporidiobolales	Sporidiobolaceae

Table 2: Available species.

Species	Strain	Host	Host strain	Collection origins
Colacogloea effusa (= C. peniophorae)	NS 20-141-C2	Peniophorella praetermissa	NS 20-141-C1	GENT
Colacogloea effusa (= C. peniophorae)	ENZ 20-052-C1	Peniophorella praetermissa	/	GENT
Colacogloea effusa (= C. peniophorae)	ID 7149-C1	Peniophorella praetermissa	/	GENT
Colacogloea effusa (= C. peniophorae)	OMC 2212-C2	Peniophorella praetermissa	OMC2212-C2	GENT
Colacogloea effusa (= C. peniophorae)	VS 12415-C1	Peniophorella praetermissa	/	GENT
Colacogloea sp. nov.	MG 407-C1	Peniophorella pubera	/	GENT
Colacogloea sp. nov.	MG 438-C2	Peniophorella pubera	/	GENT
Achroomyces insignis (Sloofia sp.)	IS 20-006-C1	Myxarium podlachicum	/	GENT
Achroomyces insignis (Sloofia sp.)	HW 347-C1	Myxarium podlachicum	/	GENT
Achroomyces sp. nov.	TR 04096-C1	Phlebiella tulasnelloidea	/	GENT
Hyalopycnis blepharistoma/ Heterogastridium	CBS 149.68	ex Tricholoma populinum		WI
Hyalopycnis blepharistoma/ Heterogastridium	CBS 953.73	ex Russula nigricans		WI
Hyalopycnis blepharistoma/ Heterogastridium	CBS 582.80	ex Hypomyces lactifluorum on old agaric		WI
Hyalopycnis blepharistoma/ Heterogastridium	CBS 587.93	ex decaying skin of walnut		WI
Hyalopycnis blepharistoma/ Heterogastridium	CBS 590.93	ex bulb of Iris hollandica		WI
Hyalopycnis blepharistoma/ Heterogastridium	CBS 591.93	ex bulb of Iris hollandica		WI
Bannozyma yamatoana	CBS 7243			WI
Sporobolomyces johnsonii	CBS 497			WI
Sporobolomyces johnsonii	CBS 1522	ex fodder yeast		WI
Rhodosporidiobolus ruineniae	CBS 5001	ex foliage Chinese holly, Malphigia coccigera		WI

Rhodosporidiobolus ruineniae	CBS 9111	ex garden soil		WI
Sporobolomyces salmonicolor	CBS 483	ex rusted leaf of orange tree		WI
Sporobolomyces salmonicolor	CBS 490	culture contaminant		WI
Sporobolomyces salmonicolor	CBS 1012	ex leaf of Aristolochea		WI
Sporobolomyces salmonicolor	CBS 2630	ex air		WI
Leucosporidium scottii	CBS 6561	progeny CBS 5930 x CBS 5931		WI
Rhodosporidiobolus microsporus	CBS 7041	ex herbaceous culm		WI
Rhodotorula toruloides	CBS 14	ex wood pulp of conifer		WI
Rhodotorula toruloides	CBS 349	ex soil		WI
Rhodotorula sphaerocarpum	CBS 5940	ex seawater		WI
Rhodotorula sphaerocarpum	CBS 5941	ex seawater		WI
Rhodotorula sphaerocarpum	CBS 5939	ex seawater		WI

Table 3: Available strains.

Species	Strain	GYPA	MEA	PDA	X-AGAR	N-DEP
Colacogloea effusa (= C. peniophorae)	NS 20-141-C2	NO	NO	NO	NO	NO
Colacogloea effusa (= C. peniophorae)	ENZ 20-052-C1	NO	NO	NO	NO	NO
Colacogloea effusa (= C. peniophorae)	ID 7149-C1	NO	NO	NO	NO	NO
Colacogloea effusa (= C. peniophorae)	OMC2212-C1	No Growth	No Growth	No Growth	No Growth	No Growth
Colacogloea effusa (= C. peniophorae)	VS 12415-C1	NO	NO	NO	NO	NO
Colacogloea sp. nov.	MG 407-C1	NO	NO	NO	NO	NO
Colacogloea sp. nov.	MG 438-C2	No Growth	No Growth	No Growth	No Growth	No Growth
Achroomyces insignis (Sloofia sp.)	IS 20-006-C1	NO	NO	NO	NO	NO
Achroomyces insignis (Sloofia sp.)	HW 347-C1	NO	NO	NO	NO	NO
Achroomyces sp. nov.	TR 04096-C1	No Growth	No Growth	No Growth	No Growth	No Growth
Hyalopycnis blepharistoma/ Heterogastridium	CBS 149.68	YES	YES	NO	YES	NO
Hyalopycnis blepharistoma/ Heterogastridium	CBS 953.73	YES	NO	NO	NO	NO
Hyalopycnis blepharistoma/ Heterogastridium	CBS 582.80	YES	NO	YES	NO	YES
Hyalopycnis blepharistoma/ Heterogastridium	CBS 587.93	NO	NO	NO	NO	NO
Hyalopycnis blepharistoma/ Heterogastridium	CBS 590.93	Not Ideal	NO	NO	NO	NO
Hyalopycnis blepharistoma/ Heterogastridium	CBS 591.93	YES	NO	YES	YES	YES
Bannozyma yamatoana	CBS 7243	NO	NO	NO	NO	NO
Sporobolomyces johnsonii	CBS 497	NO	NO	NO	NO	NO
Sporobolomyces johnsonii	CBS 1522	NO	NO	NO	NO	NO

Species	Strain	GYPA	MEA	PDA	X-AGAR	N-DEP
Rhodosporidiobolus ruineniae	CBS 5001	YES	NO	YES	NO	NO
Rhodosporidiobolus ruineniae	CBS 9111	NO	NO	NO	NO	NO
Sporobolomyces salmonicolor	CBS 483	NO	NO	NO	NO	NO
Sporobolomyces salmonicolor	CBS 490	NO	No Growth	No Growth	No Growth	No Growth
Sporobolomyces salmonicolor	CBS 1012	NO	NO	NO	NO	NO
Sporobolomyces salmonicolor	CBS 2630	NO	NO	NO	NO	NO
Leucosporidium scottii	CBS 6561	NO	NO	NO	NO	NO
Sporobolomyces microsporus	CBS 7041	NO	NO	NO	NO	NO
Rhodotorula toruloides	CBS 14	NO	NO	NO	NO	NO
Rhodotorula toruloides	CBS 349	NO	NO	NO	NO	NO
Rhodotorula sphaerocarpum	CBS 5940	NO	NO	NO	NO	NO
Rhodotorula sphaerocarpum	CBS 5941	NO	NO	NO	NO	NO
Rhodotorula sphaerocarpum	CBS 5939	NO	NO	NO	NO	NO

Table 6: Full screening results for the presence of colacosomes on solid medium.

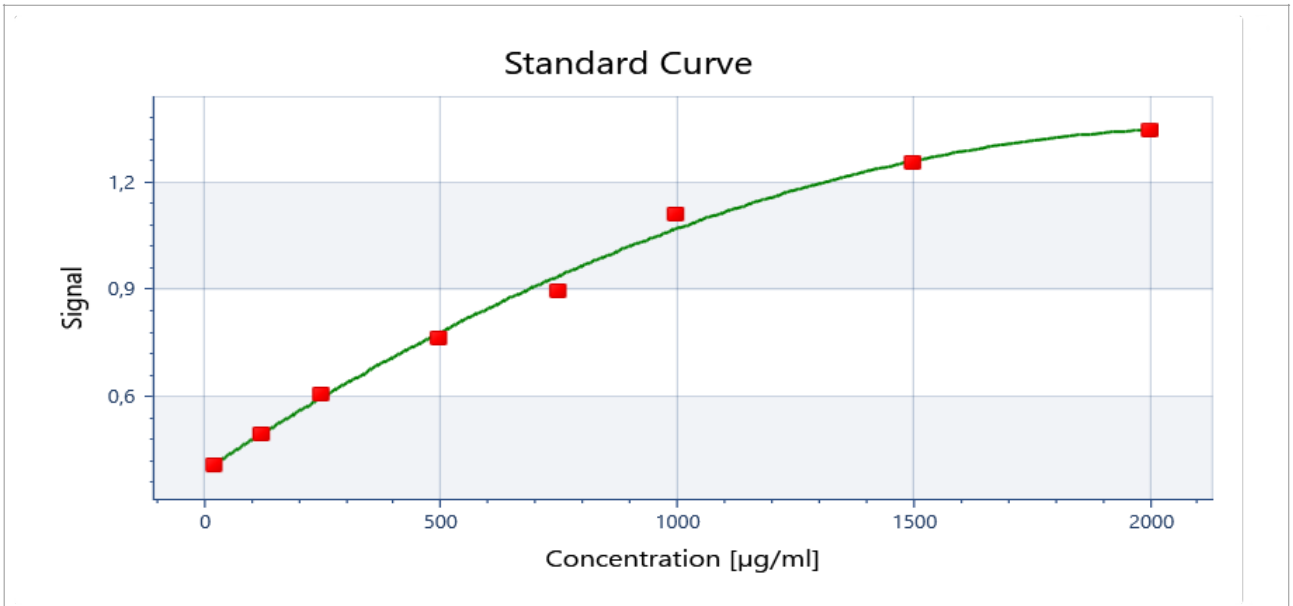

y = -2,01142E-07x^2 + 0,000882785x + 0,383589	
y = ax^2 + bx + c	
Where:	
a =	-0,000000201141574279404
b =	0,000882785118564241
c =	0,383589420304014
R^2: 0,996	

Table 9: Details of the standard curve of the Bradford analysis.

Plate 1										
Signal	1	2	3	4	5	6	7	8	9	10
A	1,318	1,257	1,097	0,8941	0,7577	0,6075	0,4961	0,3958		
B	1,382	1,246	1,102	0,8897	0,7852	0,6117	0,4942	0,4112		
C	1,325	1,253	1,126	0,8923	0,7444	0,5950	0,4894	0,4096		
D	1,217	1,431	1,149	1,305	1,245	0,5010	0,5482	0,4810	0,5307	0,5130
E	1,221	1,423	1,157	1,280	1,247	0,5077	0,5559	0,4871	0,5361	0,5062
F	1,190	1,385	1,217	1,294	1,187	0,4986	0,5402	0,4863	0,5335	0,5292
Conc. [µg/ml]	1	2	3	4	5	6	7	8	9	10
A	1783	1508	1068	685,3	475,2	270,3	131,4	NaN		
B	NaN	1468	1079	678,1	515,5	275,7	129,1	31,50		
C	1828	1492	1134	682,3	456,1	254,2	123,3	29,66		
D	1373	NaN	1190	1711	1465	137,3	195,1	113,3	173,5	151,8
E	1387	NaN	1209	1594	1472	145,4	204,7	120,6	180,2	143,6
F	1298	NaN	1376	1656	1289	134,4	185,2	119,6	176,9	171,7
Sample	1	2	3	4	5	6	7	8	9	10
A	Std0001	Std0002	Std0003	Std0004	Std0005	Std0006	Std0007	Std0008		
B	Std0001	Std0002	Std0003	Std0004	Std0005	Std0006	Std0007	Std0008		
C	Std0001	Std0002	Std0003	Std0004	Std0005	Std0006	Std0007	Std0008		
D	Unfiltered measurement 1	100 µm	40µm	20µm	10µm	Unfiltered measurement 1 (1:10dil)	100 µm 1:10 dil	40µm 1:10 dil	20 µm 1:10 dil	10 µm 1:10 dil
E	Unfiltered measurement 2	100 µm	40µm	20µm	10µm	Unfiltered measurement 2 (1:10dil)	100 µm 1:10 dil	40µm 1:10 dil	20 µm 1:10 dil	10 µm 1:10 dil
F	Unfiltered measurement 3	100 µm	40µm	20µm	10µm	Unfiltered measurement 3 (1:10dil)	100 µm 1:10 dil	40µm 1:10 dil	20 µm 1:10 dil	10 µm 1:10 dil

Table 10: Complete results of Bradford analysis.